VIBRATION SERVICEABILITY ASSESSMENT OF A STEEL MODULAR FLOOR SYSTEM

Maria Angelica Mercado Celin

Thesis submitted to the faculty of the Virginia Polytechnic Institute and State University in partial fulfillment of the requirements for the degree of

Master of Science
In
Civil Engineering

Matthew R. Eatherton, Chair
Onur Avci
Rodrigo Sarlo

June 22, 2023
Blacksburg, Virginia

Keywords: Floor Vibrations, Natural Frequency, Accelerations, Vibration Tests, Modular Construction, Modular Steel Floor System, Frequency Response Functions, Modal Assurance Criterion.

VIBRATION SERVICEABILITY ASSESSMENT OF A STEEL MODULAR FLOOR SYSTEM

Maria Angelica Mercado Celin

ABSTRACT

A new modular steel floor system, named FastFloor, is proposed for commercial buildings. The system is conceptualized to be prefabricated at the shop and ready to be installed on a previously erected skeleton frame structure consisting of girders and columns or connected to core shear walls. The system configuration aims to increase the speed of design, fabrication, and erection of a steel project by eliminating concrete pouring and curing times. Other advantages include reducing the weight of the building and its carbon footprint.

Several module configurations were considered and evaluated based on a series of interviews with experts in steel fabrication and erection engineering. The selection relied not only on addressing the issues related to fabrication, transportation, and erection but also on satisfying floor vibrations, as it was determined to be the governing limit state of the plate thickness, section sizes, and beam spacing due to the presence of an unstiffened bare plate acting as a slab. Observations were performed regarding fabrication sequence and transportation on the chosen configuration.

The dynamic properties of the module are particularly important because DG11 was developed for composite concrete-steel floor systems, and its applicability to all steel-floor systems needs to be evaluated. In parallel, a vibration testing program was conducted to determine the dynamic properties of the module, including natural frequencies and mode shapes. Lastly, the acceptability of the modular system for floor vibrations was evaluated

by both a calculation method and a modeling approach. The analysis results suggest that the module will not satisfy floor vibrations criteria, but a modified module with added stiffeners is shown to be acceptable. Upcoming tests, by others, on specimens with a raised access floor will be necessary to refine the predictions and determine if the stiffeners are actually required.

VIBRATION SERVICEABILITY ASSESSMENT OF A STEEL MODULAR FLOOR SYSTEM

Maria Angelica Mercado Celin

GENERAL AUDIENCE ABSTRACT

FastFloor is an innovative modular all-steel floor system that aims to revolutionize the construction of commercial buildings, with benefits including enhanced efficiency in design, fabrication, and erection, as well as reduced environmental impact, by eliminating the need for concrete pouring and curing and full prefabrication in shops.

Several module configurations were evaluated based on insights from industry experts in steel fabrication and erection engineering. It was observed that the main challenge in the early phases was to address issues related to fabrication, transportation, and erection while ensuring optimal performance in terms of floor vibrations.

This thesis project focused on a preliminary assessment of the vibration behavior of the system by conducting dynamic tests and evaluating the compatibility with the analytical and computational procedures in Design Guide 11, which is not calibrated for an all-steel system like FastFloor.

Based on the results, it was concluded that the initial configuration did not fully satisfy the floor vibrations criteria. However, through further computational evaluation, a modified module, based on the initial configuration with added stiffeners, was predicted to be satisfactory. Thus, future research will continue to refine the system behavior and predictions and evaluate the contributions of Raised Access Floor to the vibration performance.

ACKNOWLEDGEMENTS

FastFloor is a collaborative research project with participating universities: Northeastern, Johns Hopkins University, Iowa State University, West Virginia University, and Virginia Tech. This research is supported by the Charles Pankow Foundation, Magnusson Klemencic Associates Foundation (MKA Foundation), the American Institute of Steel Construction (AISC), and Nucor Corporation. Cooper Steel of Shelbyville, TN, Nucor Corporation, Atlas Tube, Clark Construction, and Hensel Phelps provided in-kind funding. The team appreciates the contributions of the fabricators, erectors, and advisory panel members. Any opinions, findings, conclusions, or recommendations expressed in this material are those of the authors and do not necessarily reflect the views of the sponsors.

Getting more personal, I would like to dedicate a few paragraphs to express my gratitude after fulfilling what I refer to as my "International dream." Back in 2018, when I applied to the SEM program, I thought that my only concern would be to work hard and get good grades. Little did I know that grades would only account for a portion of my journey. God knew better and took care of everything else, allowing me to meet awesome people.

Academically speaking, just after college, I had the blessing of working with Rene Jacir, my first ever boss, who was patient enough for months, where I was being paid to learn, and when I was becoming to be more "useful" didn't hesitate to help me pursue my master's degree. At Virginia Tech, I was honored to meet two people that gave me what I needed at the beginning of the master's: A chance to prove my eagerness to learn and contribute. Dr. Murray and Dr. Eatherton trusted me by involving me in multiple projects in these two short years. I will be forever grateful for their guidance, comprehension, and

support. I also want to thank my committee members, who were involved during the thesis development. Dr. Avci and Dr. Sarlo helped tremendously week after week in brainstorming ways to enhance the research and get ready, given the time constraints.

Now focusing on my personal life, after a first hard year (and the very first away from home), I had the best two roommates one could ever ask for. Donlee Drive felt like a portion of Colombia thanks to the love and care of Carolina and Nestor. The first year I attended almost every event with free food…That changed in the second year. I think I was longing, not for the free food, but for the warmth of sharing with good friends. Thanks for "La abundancia" of a true friendship. Special mention to the Latin association LAIGSA and my friends during the master's, who made the student life better.

Truly, all this experience wouldn't have been possible without the constant support of my parents, Eduardo and Margarita, and my sister, Maria Jose, my family, and friends from high school and undergrad, who were rooting for me from the distance. There were always words of wisdom and encouragement during difficult times and laughs to celebrate every small achievement. My beloved husband, Leonardo, eased the challenges I faced and magnified the happy moments; I cannot think of a moment when he wasn't there with me. My biggest fan, as he calls himself, patiently dealt with the perks of being a student with a hectic schedule.

As I mentioned, God took care of everything and allowed me to get to this point, to Him all Honor and Glory.

Table of Contents

List of Figures

List of Tables

Chapter 1. Introduction

1.1. Motivation

A new modular steel floor system is proposed for commercial buildings, able to act as floor framing and diaphragm even in high seismic zones. The system is conceptualized to be fully prefabricated at the shop and ready to be installed on a previously erected skeleton frame structure consisting of girders and columns or connected to core shear walls. A raised-access floor, placed on top of the modules, is also considered for Mechanical Electrical Plumbing (MEP) applications.

The system configuration aims to increase the speed of design, fabrication, and erection of a steel project by eliminating concrete pouring and curing times and reducing the weight of the building and the carbon footprint. Other advantages related to modular construction include reducing waste, minimizing delays, flexibility of use, and quality of construction.

Several options regarding geometry and material were evaluated in the early phases of the project, as will be further discussed in Chapter 3. The chosen configuration considered feedback from seven experts in fabrication and erection engineering to determine issues related to fabrication, transportation, and erection to be considered during design, as summarized in Chapter 4.

The module utilizes a simple configuration to preserve fast fabrication times. Each specimen consists of 10 ft x 40 ft modules with two wide-flange beams and a bare plate with thicknesses between 3/8 in. and 1/2 in. These dimensions allow the system to fit on a flatbed truck and to be safely picked up by a medium-sized crane.

In the literature, this configuration has not been assessed, which implies there may be challenges associated with the overall structural design; for instance, there are research questions regarding plate local buckling, diaphragm action, gravity strength, acoustics, fire resistance, vibration performance, and others. Floor vibration performance has been determined to be the governing limit state of the section sizes, plate thickness, and beam spacing due to the use of an unstiffened bare plate.

The criteria contained in the AISC Design Guide 11 – Vibrations of Steel-Framed Structural Systems Due to Human Activity (hereafter referred to as DG11), including analytical and computational simulation approaches, is used to analyze the modular floor system. The applicability of the equations developed for composite slabs in DG11 Chapters 2 through 6, and the procedures recommended for FE Modelling in DG11 Chapter 7, needs to be evaluated and will be investigated as part of this work for application to systems without composite slabs.

Dynamic testing of full-scale specimens will be used to determine the dynamic properties of the system, including natural frequencies and mode shapes, and will be compared to the predicted values from DG11 equations and FE models. Both the calculation method and modeling approach will be used to judge the acceptability of the modular floor system for floor vibrations.

1.2. Overview

This research aims to answer the following research questions:

- Do the analytical and computational procedures in DG11 provide a reasonable approximation of the modular floor system's vibration behavior regarding natural frequencies?

- Is the proposed module geometry suitable for vibrations behavior for walking in commercial buildings according to the limits in DG11?
- What configurations of modules are most appropriate for considering the challenges of fabrication, transportation, and erection?

To answer these research questions, a research project was conducted with the following scope of work:

1. Explore different alternatives for the module configuration. Six all-steel configurations were considered, with variations on the beam spacing, plate seam locations, stiffening, and use of technology such as sandwich panels.
2. Investigate construction, transportation, and erection issues by interviewing seven experts in fabrication and erection engineering.
3. Evaluate module configurations for floor vibrations using the analytical method of Chapters 2 through 6 of DG11. Many assumptions were made based on scenarios for the worst case, best case, and best guess were determined by selecting ranges for the variables based on optimistic predictions, DG11 guidelines, and the expected service conditions, which will be evaluated later with vibration tests.
4. Evaluate module configurations for floor vibrations using the computational simulation method in Chapter 7 of DG11. A set of finite element (FE) models was developed to compare to the tests using a single-module configuration and models of a full-bay to evaluate vibration acceptability. Additionally, the effect of plate tension due to gravity loads action is investigated.

5. Conduct vibration testing of two full-scale 10 ft x 40 ft modules. The two specimens include a heavier and lighter version of the module steel design without raised access floor. Tests will be used to determine natural frequencies and mode shapes and compared to predicted values from equations and FE models to understand their limitations.

This thesis is organized as follows:

Chapter 1 discusses the motivation behind the present research and the overall organization of how it was conducted.

Chapter 2 contains the literature review regarding alternate floor systems, DG11 analytical and computational procedures, SCI P354 approach for lightweight floors, methods for dynamic testing, and modular systems found.

Chapter 3 presents the specimens' alternatives and summarizes each configuration's advantages and challenges.

Chapter 4 describes the interviews conducted with the experts in fabrication and erection engineering.

Chapter 5 focuses on the vibration performance predictions for both analytical and computational simulations of the chosen alternatives. The assumptions made are identified.

Chapter 6 describes the test setup for dynamic testing.

Chapter 7 describes the results of the experimental tests.

Finally, the conclusions and recommendations are discussed in Chapter 8.

Chapter 2. Literature Review

2.1. Analytical Procedure for Vibrations Assessment in DG11

The second edition of the AISC Steel Design Guide 11: Vibrations of Steel-Framed Structural Systems Due to Human Activity (Murray et al., 2016), hereafter referred to as DG11, contains the most frequently used criterion and procedures for vibration assessment in the US. It includes analytical methods focused on steel-framed structural systems consisting of W-Shaped sections with concrete-filled steel deck slabs and Finite Element Modelling techniques for unique systems and geometries, for instance, monumental stairs, pedestrian bridges, large balconies, and cantilevers.

The analytical procedures allow calculating values for the system's natural frequency and maximum acceleration due to walking excitation. Acceleration is compared to limiting values to evaluate the acceptability for human comfort according to the use of the structure. Specifically, the scenario of interest for this research is commercial buildings subjected to walking. Given that DG11 is calibrated for use with typical steel-framed structural systems with concrete-filled steel deck over steel beams, it is necessary to make assumptions about how to adapt DG11 to an all-steel modular floor system, to which currently there are no provisions and verify these assumptions using dynamic testing.

This section describes some critical parameters in DG11 as they pertain to a floor system with a concrete-filled steel deck on steel beams. The assumptions and modifications made to these parameters will be described in Chapter 4.

Panel Modes in DG11

The natural frequency of the system's fundamental mode is estimated by considering a beam panel mode and a girder panel mode separately. These are defined as

a rectangular area of the floor equal to the beam or joist span times an effective width derived from the structural characteristics of the floor system.

Boundary Conditions

In DG11, the midspan deflections of girders and beams, Δ, are calculated using Equation (2-1). This equation implies that the support conditions of the elements are taken as simply supported regardless of the connection type, e.g., shear tabs or moment connections.

$$\Delta = \frac{5wL^4}{384E_sI} \qquad (2\text{-}1)$$

Where

w = supported weight per unit length, plf

L = member span, ft

E_s = modulus of elasticity of steel = 29,000 ksi.

I = Transformed moment of inertia per unit width, $in.^4/ft$

Composite Properties

When determining the moment of inertia of the beam and girder panels used for deflection calculations, it is assumed that the elements and the deck slab act as composite members, even if shear studs are absent. This assumption is made since the shear forces due to human activity are small enough to be resisted by deck-to-member welding or friction.

Effective Concrete Slab Width

The transformed moment of inertia of beams and joists is calculated by including an effective concrete slab width governed by the minimum of Equation (2-2) for beams, and Equation (2-3), for girders.

$$min\left(0.4L_j,\ s\right) \tag{2-2}$$

$$min\left(0.2L_g,\ 0.4L_{j,left}\right) + min\left(0.2L_g,\ 0.4L_{j,right}\right) \tag{2-3}$$

Where

L_j= joist or beam span, ft.

$L_{j,left}$= joist or beam span at the left of the girder under analysis, ft.

$L_{j,right}$= joist or beam span at the right of the girder under analysis, ft.

L_g=girder span, ft.

s= joist or beam spacing, ft.

Effective Panel Width

The effective panel width is an important parameter to determine the effective panel weights required for the peak acceleration calculation of the system.

For the beam panel, the effective width is:

$$B_j = C_j\left(\frac{D_s}{D_j}\right)^{1/4} L_j \le \left(\frac{2}{3}\right) floor\ width \tag{2-4}$$

Where

C_j = 1.0 for beams parallel to a free edge, 2.0 for beams in other areas.

D_j = beam transformed moment of inertia per unit width, in.^{4}/ft

D_s = slab transformed moment of inertia per unit width, in.^{4}/ft

L_j = beam span, ft

Floor width = distance perpendicular to the span of the beams where adjacent bays are identical or nearly identical.

For the girder panel, the effective width is:

$$B_g = C_g\left(\frac{D_j}{D_g}\right)^{1/4} L_g \le \left(\frac{2}{3}\right) floor\ length \tag{2-5}$$

Where

C_g = 1.6 for girders supporting joists connected to the girder flange and 1.8 for girders supporting beams connected to the girder web.

D_g = girder transformed moment of inertia per unit width, in.^{4}/ft

L_g = girder span, ft

Floor length = distance perpendicular to the span of the girders where adjacent bays are identical or nearly identical.

Damping Ratio, β

Damping is a parameter that depends heavily on non-structural elements. The value must be determined experimentally. DG11 gives recommended cumulative values, in Table 4-2, based on experience, that can be used by building owners if no experimental tests are performed. For instance, the damping value for an electronic office (i.e., widely spaced workstations, few desks, and few demountable partitions) would consist of the following components:

$$\beta = 0.01\ (structural\ system) + 0.01\ (ceiling\ and\ ductwork) + 0.005\ (Electronic\ office\ fit\ out) = 0.025 \quad (2\text{-}6)$$

Loads

Unlike the design for strength, overestimating the superimposed loads is not a conservative approach. More vibrations are observed in lightly loaded floors, for instance, an empty classroom. DG11 recommends strictly including the elements permanently attached to the structure in the superimposed dead loads. A value of 4 psf is the recommended value for standard mechanical and ceiling installations. Regarding live loads, the value can be taken from 6 to 8 psf for electronic offices.

Effective Panel Weight, W

The individual panel weights for the beam and girder panel modes are calculated using Equation (2-7(a)) and Equation (2-7(a)), respectively. The system effective panel weight, W, is a function of the panel weights and their relative stiffnesses and is given by Equation (2-9).

$$W_j = w_j B_j L_j \qquad \textit{(2-7(a))}$$

$$W_g = w_g B_g L_g \qquad \textit{(2-8(b))}$$

$$W = \frac{\Delta_j}{\Delta_j + \Delta_g} W_j + \frac{\Delta_g}{\Delta_j + \Delta_g} W_g \qquad \textit{(2-9)}$$

Where

Δ_j = Midspan deflection of the beam

Δ_g = Midspan deflection of the girder

B_j = Effective beam panel width

B_g = Effective girder panel width

w_j = beam supported weight per unit area, psf

w_g = girder supported weight per unit area, psf

W_j = Effective panel weight for the beam

W_g = Effective panel weight for the girder

Fundamental Frequencies, f_n

If the beam and girders are assumed to be simply supported, the system frequency can be estimated based on the Dunkerley relationship and the fundamental natural frequency for simply supported beams with uniform mass, resulting in Equation (2-10). It can be observed that only the contribution from the beam and girder panels are included. Since the deck slab has significantly greater stiffness, its contribution to the overall system

is typically neglected. The Dunkerley relationship represents that the girder and beam panel masses are connected in series with springs.

$$f_n = 0.18\sqrt{\frac{g}{\Delta_j + \Delta_g}} \qquad (2\text{-}10)$$

Tolerance Limits for Human Comfort

For the intended use of the proposed modular system corresponding to offices, DG11 recommends a peak acceleration limit of 0.5%g to avoid the discomfort of humans due to floor motion of low-frequency floors with vibrations between 3 and 10 Hz. This limit value is obtained from Figure 2-1 for offices, residences, and quiet areas.

The acceptability limit is compared to the accelerations specific to the structure using the inequality in Equation (2-11)

$$\frac{a_p}{g} = \frac{P_o e^{-0.35 f_n}}{\beta W} \leq \frac{a_o}{g} \qquad (2\text{-}11)$$

Where

a_p/g= ratio of peak floor acceleration to gravity acceleration

a_o/g= vibration tolerance limit=0.5%g for offices

P_o= amplitude of the driving force = 65 lb. for floors

f_n= system fundamental natural frequency

W= effective weight of the floor

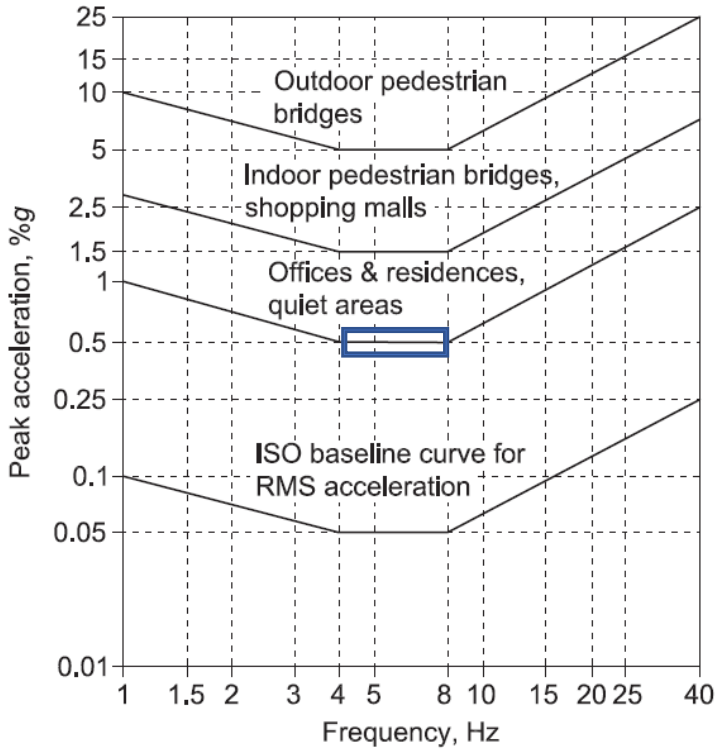

Figure 2-1. Recommended tolerance limits for human comfort. From [DG11, (2016)]

2.2. Finite Element Analysis Methods in DG11

DG11 includes a chapter addressing Finite Element Analysis for structures outside the scope of the analytical calculations presented in Chapters 2 through 6 of the guide. The recommended procedure consists of creating a three-dimensional model containing the evaluated bay and adjacent bays, considering that responsive modes shouldn't extend over four or five bays. This limit obeys the fact that experimental data has shown that floor motion is limited to several bays around the bay under analysis due to energy loss over the length and time. Including large areas of the floor could result in an underprediction of the acceleration response, given an unrealistic excitement of the contributing mass. A three-by-three grid of bays is recommended for an interior bay. The general procedure is listed below, including some notes on how to apply this procedure in SAP2000 (CSI, 2023).

Material Definition and Mass

The masses are computed by adding the self-weight of the slab, the superimposed dead load (e.g., MEP, Raised Access Floor), and live load. The loads, in psf, are converted to area masses, in psf-s^2/ft, by dividing by the acceleration of gravity, g =32.2 ft/s^2, and are assigned directly to the shell area section representing the floor slab. Masses related to cladding are applied directly to the members as linear masses.

To avoid double counting the slab self-weight, its material density is set to zero. On the other hand, the self-weight from the steel framing is calculated by the software (e.g., SAP2000); therefore, its material is defined, keeping the appropriate density for steel.

Slab Definition

DG11 is designed for steel-framed structural systems and concrete-filled steel deck slabs. The different stiffnesses in both directions must be considered to predict the natural frequency and mode shapes better. The slabs are modeled as shell elements with thin plate formulation, with the appropriate property modifiers for orthotropic properties in concrete-filled steel deck slabs.

Steel Members

The framing members are used with properties that are modified for transformed section properties. Shear deformations can be neglected (Barrett, 2006), meaning that flexibility is not considered, resulting in stiffer framing members and slightly greater frequencies.

Damping and Frequency Response Function (FRF) Magnitude Prediction

The Frequency Response Function (FRF) Magnitude plots are obtained by defining a steady-state function with a constant value of 1.0 for all frequencies. Then, a steady-state

load case and a unit load Case are created that corresponds to a 1 lb. load applied at a location of interest, for instance, at mid-bay, to evaluate the accelerations at this location. In SAP 2000, a scale factor of 100/g = 100/386 in/s^2 = 0.2591 can be specified to the load case to obtain the results in %g/lb., the units of interest.

The steady-state load case requires the hysteretic damping value. Specifically in SAP2000, the hysteretic damping type corresponds to "Constant Hysteretic Damping for all Frequencies"; the mass proportional coefficient is set to zero, while the stiffness proportional coefficient is set to twice the viscous damping. According to (Computers and Structures, Inc., n.d.), this is how to input the desired damping ratio in SAP.

Human Comfort Evaluation

The maximum response of a low-frequency floor, which has at least one natural frequency below 9 Hz, is due to a multiple-footstep resonant build-up. On the other hand, the maximum response of a high-frequency floor is due to individual footstep impulse response. Therefore, the evaluation methods for low frequencies are different from high-frequencies. The procedure is divided into two parts: first, the modes with low frequencies (< 9 Hz), if any, are analyzed individually, and second, the total response is calculated, including all the frequencies from 1 Hz to 20 Hz.

Low-Frequency Floor Procedure

The FRF method can be used at low frequencies to predict the resonant response. The expected peak sinusoidal acceleration is the product of the maximum FRF magnitude, the force harmonic amplitude, and a partial resonant build-up factor (Equation (2-12)). The latter is a factor that accounts for the inability of the steady state to be reached when the walking path is short (Catbas, 2014).

$$a_p = FRF_{Max} \alpha Q \rho \quad (2\text{-}12)$$

Where

FRF_{Max} = maximum FRF magnitude at frequencies below 9 Hz, %g/lb

Q = bodyweight = 168 lb

α = dynamic coefficient

ρ = resonant build-up factor

The dynamic coefficient, α, and resonant build-up factor, ρ, are calculated using Equations (2-13) and (2-14*(a)*), respectively.

$$\alpha = 0.09 e^{-0.075 f n} \quad (2\text{-}13)$$

$$\rho = 50\beta + 0.25 \text{ if } \beta < 0.01 \quad (2\text{-}14(a))$$

$$\rho = 12.5\beta + 0.625 \text{ if } 0.01 \leq \beta < 0.03 \quad (2\text{-}14(b))$$

$$\rho = 1.0 \text{ if } \beta \geq 0.03 \quad (2\text{-}14(c))$$

For the estimation of FRFs, the analysis location must be carefully selected. If an architectural layout has been determined, the midlength of an unobstructed walking path close to the maximum mode shape value should be chosen to apply the unit load. Otherwise, the analysis points should be those where the ultimate mode shapes are observed.

High-Frequency Floor Procedure

To evaluate the system for individual footstep responses. First, the highest FRF magnitude must be identified, which will control the step frequency, in Hz, given by:

$$f_{step} = \frac{f_{n,dominant}}{h} \quad (2\text{-}15)$$

Where

$f_{n,dominant}$= Natural frequency of the higher FRF Magnitude for modes up to 20 Hz

h= harmonic that can be matched by the dominant natural frequency, taken from Table 2-1

Table 2-1. Harmonic Selection for High-Frequency Floors. From [DG11 (2016)]

Dominant Frequency, Hz	*h*
9–11	5
11–13.2	6
13.2–15.4	7
15.4–17.6	8
17.6–20	9

The response of each mode is then calculated for all modes up to 20 Hz. The effective impulse, in lb-s, is calculated from Equation (2-16), and the peak acceleration from Equation (2-17).

$$I_{eff,k} = \left(\frac{f_{step}^{1.43}}{f_{n,k}^{1.30}}\right)\left(\frac{Q}{17.8}\right) \quad (2\text{-}16)$$

$$a_{p,k} = 2\pi f_{n,k}\phi_{i,k}\phi_{j,k}I_{eff,k} \quad (2\text{-}17)$$

Where

$f_{n,k}$ = natural frequency of mode k, Hz

$\phi i,k$ = kth mode mass-normalized shape value at the footstep

$\phi j,k$ = kth mode mass-normalized shape value at the affected occupant

The acceleration waveform for all modes is calculated per Equation (2-19) for all mode shapes. The function is evaluated for t=0 up to t=T_{step} (Equation (2-18)) in 0.005 s increments.

$$T_{step} = \frac{1}{f_{step}} \quad (2\text{-}18)$$

$$a_k(t) = a_{p,k}e^{-2\pi f_{n,k}\beta t}\sin\left(2\pi f_{n,k}t\right) \quad (2\text{-}19)$$

The total response between footsteps is estimated using Equation (2-20):

$$a(t) = \sum_{k=1}^{Nmodes} a_k(t) \qquad (2\text{-}20)$$

Lastly, as the peak acceleration from Equation (2-20) is not comparable to the limit based on the sinusoidal accelerations, an equivalent sinusoidal peak acceleration is calculated from Equation (2-21). This will be compared to the applicable DG11 limit.

$$a_{ESPA} = \sqrt{\frac{2}{N}\sum_{k=1}^{N} a_k^2} \qquad (2\text{-}21)$$

2.3. SCI Approach for Lightweight

The Steel Construction Institute (SCI) released Publication P354 (Smith et al., 2009), which contains the European guidelines for vibration design of all steel-framed floors. Like DG11, the procedure assumes that the floor is excited by a single harmonic force and a fundamental mode of vibration dominates the response; in other words, the structure is idealized as a Single Degree of Freedom (SDOF) system.

The SCI P354 specifically describes a procedure for Light Steel Frame Floors, which are defined as those consisting of support members, usually standard C or Z-shaped sections, with moments of inertia up to 450 cm^4, and slab materials such as timber boards, chipboard, plywood, or cement particle board. In addition, the floor must lie in the high-frequency range, greater than 8 Hz, so that the floor vibration response is dominated by impulsive excitation from walking forces.

The approach for lightweight floors is similar to DG11 in the initial steps. The mass properties are determined from the self-weight of the floor and any additional dead loads,

such as ceiling, services, and 10% of the imposed load, which accounts for the permanent loading on the floor. On the other hand, the stiffness properties are calculated from the elastic modulus and the composite moments of inertia of the floor members.

In turn, the natural frequencies are estimated from the mass and stiffness properties of the floor system. It is important to mention that only the mode of vibration associated with the motion of the joists is considered, given the orthotropic nature of lightweight floors, where the direction of the span of the beams is more flexible.

Stiffness Approach

The procedure for lightweight floors has a stiffness/frequency criterion that limits the system's frequency to be greater than or equal to 8 Hz within dwellings by setting a maximum deflection of floors based on the span. This is checked through the following equation:

$$I_b \geq \frac{L_y{}^3 \times 10.16}{N_{eff} \times \delta_j} \qquad (2\text{-}22)$$

Where

L_y = joist span (m)

N_{eff} = number of effective joists acting with single point load

δ_j = limiting defection (mm)

The values of N_{eff} and δ_j are prescribed in tables based on the flooring configurations and spans, respectively.

If the calculated value from Equation (2-22) is less than the beam moment of inertia, and the frequency is greater than 8 Hz, the floor is acceptable for its given occupancy use.

Response Factor Analysis

The Response Factor Analysis can be used to perform a response acceleration analysis. Initially, the modal mass is calculated based on the effective floor area that contributes to the motion of the system, per Equation (2-23)

$$M = mL_{eff}S \tag{2-23}$$

Where

m = floor mass per unit area, including dead load and imposed load during service

L_{eff} = Effective floor length

S = Effective floor width

Equations (2-24) and (2-25) define the effective length and width, respectively.

$$L_{eff} = n_y\left[0.2{L_y}^2 - 2.1L_y + 7.5\right] \times \sqrt{\frac{I_b}{5.3\times 10^{-6}}} \tag{2-24}$$

$$S = 0.75\left(L_x + 1\right) \times \sqrt{\frac{I_b}{5.3\times 10^{-6}}} + 5.9\left(0.6 - s_j\right) \le n_x L_x \tag{2-25}$$

Where

n_y= Number of consecutive floor spans in the direction of the floor joists

n_x = Number of consecutive floor widths assumed to be acting continuously ($n_x \le 4$)

I_b = Second moment of inertia of the floor joist per unit width, which can be taken as composite with the toping if suitable fixings are provided (m^4/m)

s_j = spacing of floor support members (m)

The following equation is then used to determine the root-mean-square (rms) acceleration:

$$a_{w,rms} = 2\pi\mu_e\mu_r \frac{185}{M{f_0}^{0.3}} \frac{Q}{700} \frac{1}{\sqrt{2}} W \tag{2-26}$$

Where

μ_e = mode shape factor at the point of excitation, normalized to the anti-node

μ_r = mode shape factor at the point of response, normalized to the anti-node

f_0 = fundamental frequency (Hz)

M = modal mass (kg)

Q = static force exerted by an average person, generally taken as 746 N.

W = appropriate weighting factor for human perception of vibrations, based on the fundamental frequency, f_0.

It is recommended to take μ_e and μ_r as 1.0 for the initial design, meaning that the response will be at a point on the floor where there is maximum vibration amplitude, and the excitation force will be applied simultaneously.

The weighting factor, *W*, for z-axis vibrations, is given by curves included in Chapter 5 of SCI P354, and it is based on the room type, e.g., critical working areas, residential, circulation spaces, etc. Conversely, given that the weighting factor is lower than one, a factor of 1.0 can be taken for preliminary designs.

Finally, the response factor for z-axis vibrations, R, can be calculated once the acceleration has been estimated through the following equation:

$$R = \frac{a_{w,rms}}{0.005} \qquad (2\text{-}27)$$

Acceptability Criteria

Based on measurements on several lightweight floors, the SCI set the acceptable limit for the response factor to be 16 for continuous vibrations (Figure 2-2). If the response factor lies within the limit, the floor is proper for continuous vibrations, and intermittent vibrations don't have to be considered. At this point, it can be observed that damping is not a variable involved in the calculations, unlike DG11.

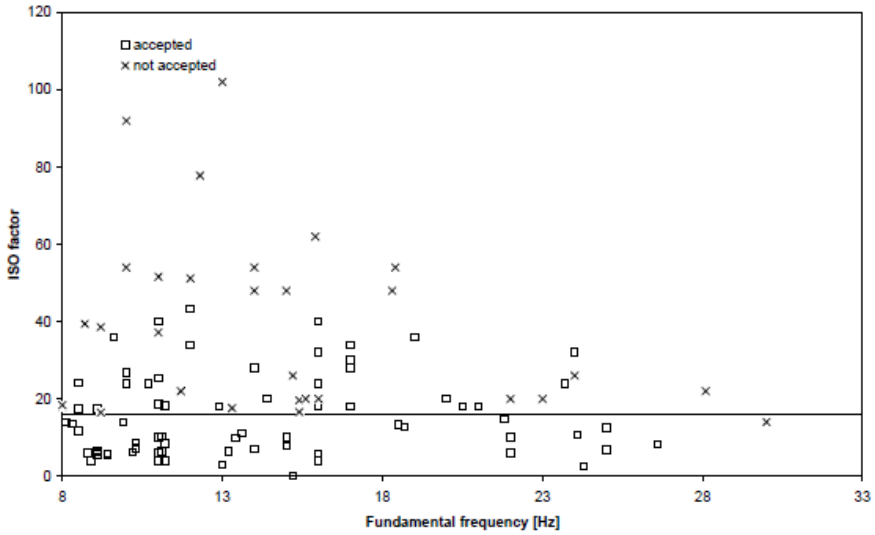

Figure 2-2. Weighted acceleration compared to acceptability

Vibration Dose Value (VDV) Approach

If intermittent vibrations want to be further analyzed, the SCI P354 includes the VDV. This approach allows the response to be greater than those specified for continuous vibrations but for short periods. VDV values are prescribed based on the probability of adverse comment and exposure period (16 h day and 8 h night).

To determine if a building is likely acceptable, it's necessary first to establish the maximum possible walking length, L_p, and frequency, f_p. With these parameters, the velocity of walking, v, and duration of the walking activity, T_a, can be determined through the following equations:

$$v = 1.67 f_p{}^2 - 4.83 f_p + 4.50 \qquad \left(m/s^2\right) \tag{2-28}$$

$$T_a = \frac{L_p}{v} \qquad (s) \tag{2-29}$$

Lastly, the number of times, n_a, that the walking pattern selected will take place on a period (based on the chosen VDV) is determined using the equation below:

$$n_a = \frac{1}{T_a}\left[\frac{VDV}{0.68 \times a_{w,rms}}\right]^4 \tag{2-30}$$

Intuitively, the floor will be judged as acceptable if the floor is expected to have fewer walking times than n_a in the exposure period.

FE Analysis

The SCI P354 lists several suggestions for performing Finite Element Analysis similar to those in DG11. To mention some: 1) Shell sections are recommended for representing slabs, 2) All connections should be modeled as rigid, 3) The floor mass should include the self-weight and permanent loads, 4) Continuous cladding is taken as a restraining vertical translation of the perimeter beams but allowing rotation.

2.4. Laboratory and In-situ Floor Testing

In the literature, there can be found many experimental investigations focused on characterizing the modal properties that affect the dynamic response of floors, especially the estimation of the natural frequencies, damping ratios, and accelerations. In general, the same techniques and instrumentation are commonly used regardless of the material or intended use of the specimens or whether it is in-situ or laboratory testing. In the following paragraphs, the most used types of testing will be addressed in order of simplicity.

2.4.1. Output – Only / Unreferenced Excitations

"Unreferenced excitations" is a term used when the force/input measurements are not recorded. This type of excitation is the easiest way to estimate the dynamic response of a floor system, given that it requires less expensive equipment (Barrett, 2006). Among these types of excitations are bouncing, ambient vibrations, heel-drop, walking, and non-instrumented impulse hammer.

The steady-state resonance response can be achieved by bouncing the structure at subharmonics of the natural frequency. One of the disadvantages of this method is that the

damping values estimated from the decay response are overestimated due to the human body that remains on top of the slab after the bouncing stops (Barrett, 2006).

Ambient vibrations, on the other hand, account for the behavior of the structure under service conditions, for instance, wind and live loads (Sanchez, 2008). This can be useful for approximating the floor's natural frequencies.

Another excitation is heel-drop, which consists of raising the heels 2 in. from the floor and releasing, producing an impact load equivalent to the individual's weight (Sanchez, 2008). Davis et al. (Davis et al., 2014) developed a simplified procedure, especially useful for the retrofit of structures with reported complaints. This method involves heel-drop excitations, a handheld spectrum analyzer to measure the floor accelerations, and a seismic accelerometer, combined with specific walking rates and paths. A heel-drop force can excite 1 Hz to 20 Hz, an appropriate range to cover human walking excitations. An impulse hammer generates an impulse force similar to that of a heel-drop. However, the hammer imparts a load three times smaller than the heel drop.

Although simple and more convenient in most cases, it should be remembered that the information provided by these unreferenced tests is limited. Barrett (Barrett, 2006) mentioned that natural frequencies and relative mode shapes are the only parameters that can be determined; thus, there is not enough information to estimate damping confidently and validate FE Models, as the input force is not recorded.

Once the natural frequency of the floor is determined, walking excitations can be used to determine the largest floor response. This is done by selecting a walking rate that corresponds to a subharmonic of the natural frequency to get a resonant buildup, but that is also between 1.6 Hz and 2.2 Hz, which is the range of human walking speed on a flat

surface (DG11, 2016). The walking paths can be selected at locations of interest, such as cantilevers, and parallel or perpendicular to the floor framing.

Specifically, Davis et al. (Davis et al., 2014) used this simplified method for the retrofit of a low-frequency patio floor made of a deep steel roof deck supported on open-web steel joists and normal-weight concrete pavers, along with other accessories such as roofing membrane and rigid body insulation.

Recent studies have reported the use of heel-drop impacts for other types of floor systems, such as prestressed slabs (Zhou et al., 2016) and conventional concrete slabs (Mohd Azaman et al., 2018).

Zhou et al. (2016) performed unreferenced heel-drop loads by men weighing between 125 lb. (57 kg) – 150 lb. (70 kg). Each measurement was repeated at least three times to average the responses and avoid randomness. The measured data, recorded as response accelerations in the time domain, needed to be converted to the frequency domain using techniques such as the fast Fourier transform, as shown in Figure 2-3. In this study, the damping values were determined using the logarithmic decay approach, isolating the first mode.

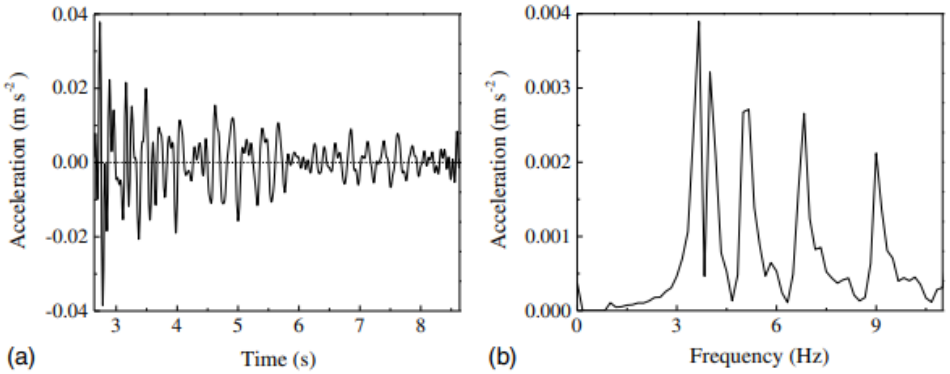

Figure 2-3. Example of heel-drop response in time domain and frequency domain [From Zhou et al. (2016)]

2.4.2. Shaker-based Experimental Modal Analysis (EMA)

EMA is the current most accurate method for characterizing the dynamic properties of a system. Given that the input excitations and output responses are measured in EMA, high-quality data is obtained to determine the damping, natural modes, and resonant frequencies. In turn, the results allow the calibration of FE models, comparison to serviceability limits, and the creation of FRF functions (Barrett, 2006).

One of the main setbacks of the shaker-based EMA is that it requires an electrodynamic shaker to excite the floor, which accounts for the most expensive equipment involved in the tests, and in most cases, makes it unviable. The testing times are also longer, given the logistics of moving the shaker, measuring, and processing data (DG11, 2016).

The testing procedure typically starts by sending a burst-chirp function as input to the shaker. The shaker is located at a grid-point location, usually at mid-bay or where it is assumed to have small participation in lower modes. (Alvis, 2001).

Impact hammer test is also a type of EMA. This type of test would overcome the difficulties related to shaker-based tests, given that it is faster, cheaper, and portable while also offering good results.

2.5. Amplitude Dependent Damping

As mentioned earlier, damping is one of the main parameters that describe the modal behavior of a structure and yet is difficult to estimate using the current techniques, such as the half-power method, curve fitting, and decay curves.

The difficulty in predicting damping can be explained by the nature of a type of nonmaterial damping known as viscous damping. Viscous damping occurs when an

opposing force is generated in response to the motion of an object. Given that the decay curves of actual structures are similar to the viscous model curves, a simplification is assumed where the structure's damping is taken as the viscous damping. This simplification is not necessarily correct since viscous damping is dependent on the excitation frequency; therefore, damping will be constant for small and large frequencies but will show a linear behavior for frequencies in between, where it will increase as the excitations amplitudes are also increased (e.g., Avci, 2016).

Avci (2016) discusses a procedure to achieve more accurate predictions. The author tested a footbridge structure to obtain its modal parameters, which were used to update the FE models. For this objective, a shaker was placed at different locations on the structure, applying chirp signals at 4 to 20 Hz. The procedure can be summarized in the following steps: 1) Obtain the natural system's natural frequency, 2) Test the structure at its natural frequency, 3) Apply the same sinusoidal excitation to the FE Model and the damping ratio obtained through the effective mass procedure, 4) Compare the measured accelerations to the FE Model response.

It's important to mention that the results with this technique were contrasted to the half-power method, curve fitting, and decay curves, observing that the latter yielded much higher damping ratios despite only having the first mode contributions, concluding that the most reliable method is one that accounts for amplitude-dependent damping properties.

2.6. Alternate Plate and Floor Systems

Concrete-filled steel deck acting compositely with steel beams is the most popular floor system in steel-framed buildings in the US. However, new systems are being

developed to overcome the extended erection times associated with installing formwork, if required, and concrete curing.

Sandwich Panels and Honeycomb Panels

For instance, several variations of sandwich panels are being studied for construction applications. Its configuration consists of metals as skin layers and various core types such as concrete, honeycomb, and polymeric materials, as shown in Figure 2-4. The skin layers, significantly stiffer than the core material, resist in-plane and lateral loads, while the core resists transverse shear loads (Cousins et al., 2009).

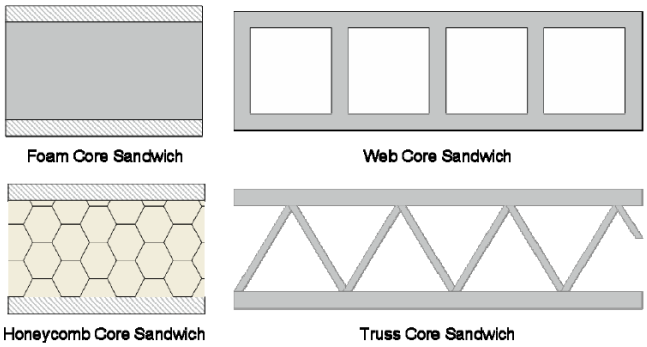

Figure 2-4. Sandwich Panel Configurations. From [Cousins et al. (2009)]

One of the main advantages of the sandwich panels is the ability to customize the configuration for specific applications. For instance, the insulation properties can be improved using a denser core material or increasing its thickness. In general, sandwich construction technology brings benefits over conventional structures, such as better thermal and acoustical insulation, good fatigue resistance, and mass manufacturing (Cousins et al., 2009).

In the 1980s, several studies were conducted for steel-concrete-steel sandwich panels. However, it was observed that the bond strength between the layers was rather weak and required adding some type of shear connectors. Researchers have recently studied using glass fiber reinforced polymers (GFRPs) as the skin layers combined with

polymeric cores. This configuration has been successfully used in timber structures due to its ease of installation and modular construction capabilities but hasn't been studied for high-rise buildings (Ryu et al., 2018).

Specifically, for the present research, steel plates and polymeric core sandwich panels are potentially suitable for the intended use. Ryu et al. developed an interesting configuration, shown in Figure 2-5, that enhances the performance under fire conditions while keeping the system relatively light. More importantly, using a polymeric core reduces the noise and vibrations (Ryu et al., 2018).

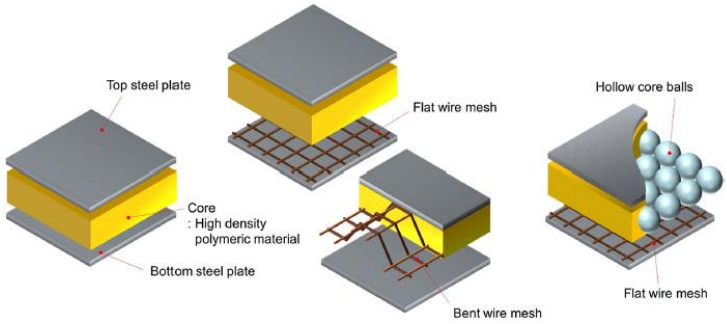

Figure 2-5. Sandwich panels with steel plates infilled with a polymeric material. From [Ryu et al. (2018)]

The honeycomb panels are another alternative to polymeric cores, as shown in Figure 2-6. The typical configuration consists of a geometric pattern instead of a solid polymer core.

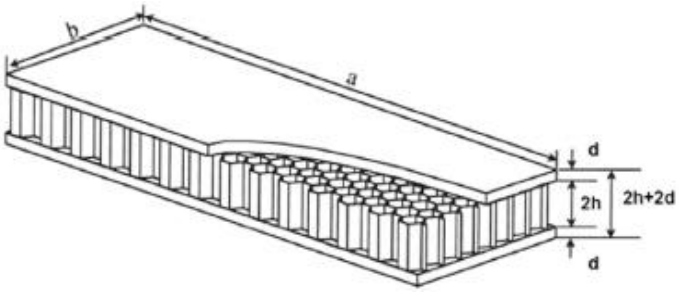

Figure 2-6. Honeycomb core Sandwich Panel. From [Arunkumar et al. (2016)]

Vibration and Damping

Several tests have been conducted on steel and polymer sandwich panels for vibration assessment. For instance, the vibration performance of the innovative system, shown in Figure 2-5, was studied by conducting unreferenced walking and heel drop tests (Lee et al., 2020). The natural frequencies were obtained from walking, and the damping from heel drop excitations. The natural frequencies obtained after framing and cladding completion were in the order of 28 Hz. On the other hand, the damping ratio calculated through the log-decrement approach after the completion of construction was 4.57%. This value looks promising, as it exceeds the recommended damping values per DG11; however, the simplified tests (unreferenced heel-drop) performed are not ideal nor provide enough information to characterize the response of the structure and should be instead used to estimate natural frequencies only, as described by Davis et al. (Davis et al., 2014).

Moreover, Han and Yu (2021) assessed the influence of the interface adhesion between the layers in the loss factor prediction. Impact hammer tests were conducted on rectangular specimens 7 mm long, 4 mm wide, and 1 mm thick. The results showed that while the interface strength between the layers did not have a significant impact on the loss factors, the adhesive layer did influence the vibration-damping performance, thus, modeling the sandwich panels as a 5-layer structure, as shown in Figure 2-7, yielded more accurate results when compared to experimental testing (Han & Yu, 2021).

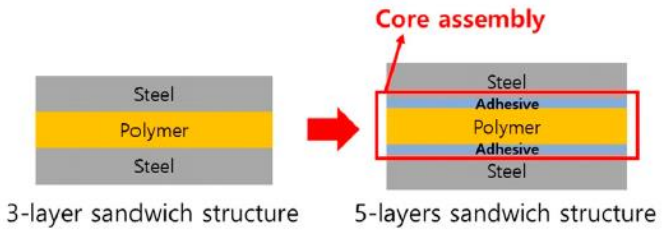

Figure 2-7. Steel-polymer sandwich panel structure for loss factor prediction. From [Han & Yu (2021)]

This research reported loss factors, η, ranging from 0.016 to 0.10 for electro-galvanized steel-polymer sandwich composites and the polymer volume fraction, varying the core material to different polymers. The loss factor was calculated through the half-power bandwidth method. To obtain the damping ratio, β, the loss factor is divided by two, obtaining damping values ranging from 0.8% to 5%. It's important to mention that one typical frequency response curve was included, showing natural frequencies from 0 to 3500 Hz.

2.7. Modular Systems

When looking in the literature for the term "panelized," it is typically used in the context of light-framing wood structures. Panelized construction is related to off-site construction, where the building is divided into two-dimensional panels for walls and floors. (Islam et al., 2022). Volumetric construction, conversely, is a form of three-dimensional modular construction typical for roofing. The main difference is that panelized construction requires the elements to be assembled on-site, while in volumetric construction, the 3D panels are shipped already assembled (Ahn et al., 2022). Panelized construction has many advantages over volumetric modular construction, such as site safety, cost and speed, and smaller equipment capacity, namely, smaller cranes and transportation demand (Ahn et al., 2022).

Although mainly used in the wood industry, both terms also apply to steel systems, as will be further discussed in the following sections.

2.7.1. Modular Systems Under Research

Several modular systems under the panelized configuration are being developed at the research level. For instance, Yang et al. (Yang et al., 2018) developed a modular system

(Figure 2-8) consisting of precast concrete slabs on top of space trusses that allow the installation of MEP before erection. The plan was designed to resist gravity and seismic loads of steel high-rise buildings. Each module has a maximum size of 20 ft x 8 ft x 8 in. thick, which fits a conventional truck. Regarding the connections, the modules can be assembled through bolted connections. This study developed a 3-story prototype model that showed a promising seismic performance.

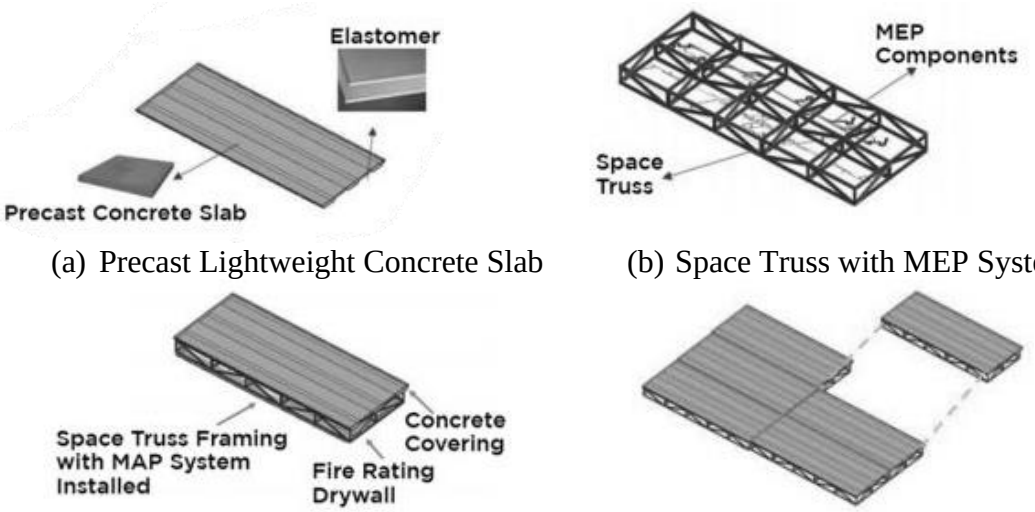

(a) Precast Lightweight Concrete Slab (b) Space Truss with MEP System

(c) Module unit (d) Floor system Assembling

Figure 2-8. Space Trusses on CLT – Modular System. From [Yang et al. (2018)]

Other examples of modular, panelized floor systems are summarized in Figure 2-9. All configurations aim to be lightweight, fast, simple to fabricate and erect, and stackable for transportation. Different materials are proposed to enhance other characteristics, such as resistance to corrosion and fire and load-carrying capacity.

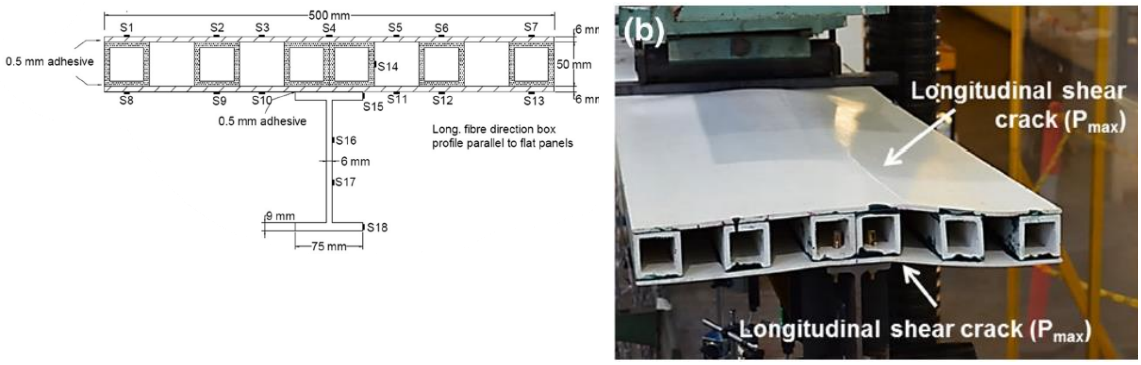

(a) Modular FRP- Steel composite beams. From [Satasivam & Bai (2016)]

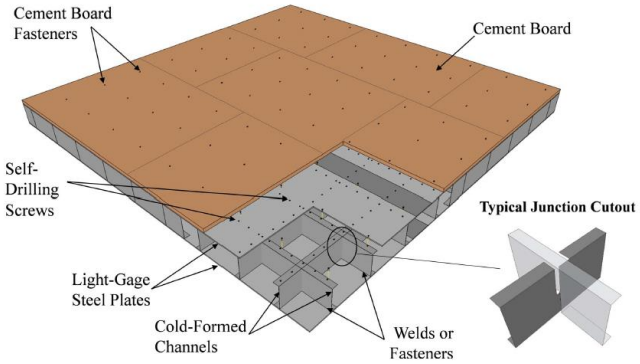

(b) Lightweight Two-Way Steel Floor System. From [MacLachlan et al. (2019)]

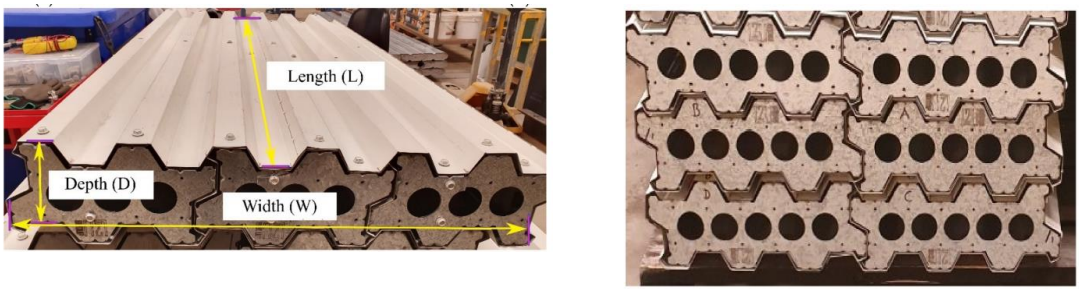

(c) Hollow Cellular Panels for Modular Flooring System. From [John et al. (2022)]

Figure 2-9. Other examples of Modular Systems

2.7.2. Modular Steel Buildings (MSB)

Modular Steel Buildings (MSB) often refer to room-sized volumetric units prefabricated in a factory and installed on-site as “building blocks” (Chen et al., 2017). MSB's typical configuration includes hollow sections that allow full or partial installation of floors, lighting, plumbing, heating, and architectural finishes in the shop. Its applications include low-rise buildings with occupancies like dormitories, offices, hospitals, schools,

and hotels (Khan & Yan, 2020). Among the challenges of this type of system is the detailing of the joint connections, as many columns and beams meet at the exact location; thus is the focus of many researchers, as shown in Figure 2-10.

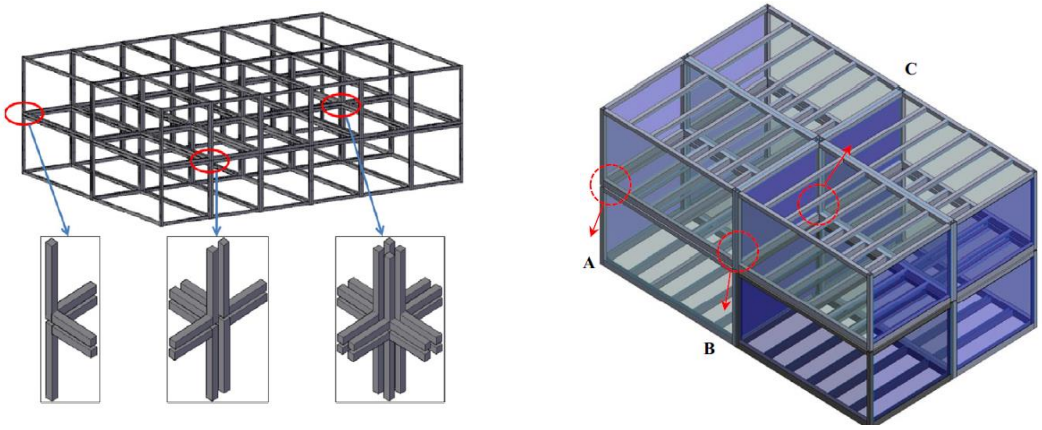

(a) Connections in MSB. From [Chen et al. (2017)]

(b) MSB assembled on site. From [Khan & Yan, (2020)]

Figure 2-10. Examples of modular steel buildings

2.7.3. Alternate Modular Systems to FastFloor

Other systems exploring different materials and configurations have been used in actual buildings and have successfully reduced erection times. Two cases are highlighted in the following paragraphs.

Hybrid CLT-Steel System

A Structure Magazine article (Odeh & Kuehnel, 2019) highlighted an innovative six-story residence hall in Rhode island, integrating exposed cross-laminated timber (CLT) panels supported by steel framing. Figure 2-11 shows the structure during the construction process and the hybrid system profile. As can be observed, the floor structure incorporated several layers: a 5-ply CLT floor pan, acoustic isolation mats, poured gypsum concrete topping, and a vinyl composition tile, which enhanced the floor structure's vibration and acoustic performance.

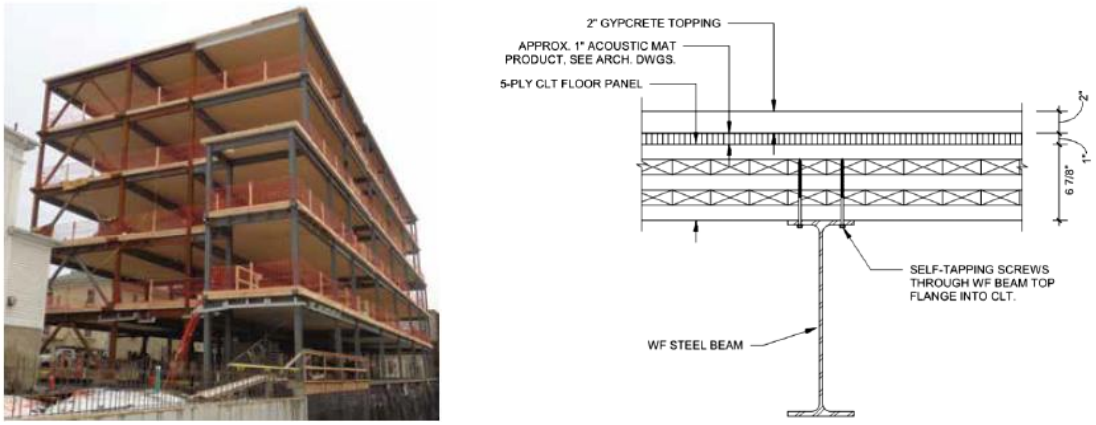

(a) Structure during construction *(b) CLT Floor profile*

Figure 2-11. Hybrid CLT – Steel System. From [Odeh & Kuehnel (2019)]

The CLT-Steel Hybrid system was chosen despite being around 10% more costly than other options, such as precast concrete with steel supports and heavy timber structure. The designers considered that the advantages associated with the system outweighed the extra costs. Specifically, CLT brings benefits related to sustainability, aesthetics, in-built fire proofing, speed, safety, camber, and logistics.

Further explaining the later advantages, the versatility of CLT panels allowed the manufacturer to fabricate panels of 8 ft x 50 ft, covering the whole width of the building, which allowed for faster construction. Regarding safety, the team observed that the modifications in-site were more straightforward as the CLT panels were cut using a chainsaw from the top without generating silica dust from concrete slabs. The CLT panels also had almost zero camber making the alignment without adjacent panels easier. Finally, the panels were stacked for transportation, reducing the required trucks.

Hollow-Core slabs and Deltabeam® Composite System

Deltabeam® consists of two horizontal flat plates joint through perforated webs, as shown in Figure 2-12. When combined with prefabricated hollow-core slabs, this system is an excellent alternative to post-tensioning construction (Vimmr, 2008). Among the

advantages of this system is the ability to achieve a flat roof, given that the hollow slabs and deltabeam® are flushed, which in turn facilitates the installation of HVAC systems below or inside the floor. Deltabeam® is also customizable regarding height, camber, and spans but has standard sizes for faster delivery. Fireproofing is integrated into the system. One of the drawbacks of this system is that it requires additional reinforcement between the hollow slabs and the deltabeam® followed by the pouring of concrete on-site to fill the deltabeam® and the joints between the slabs.

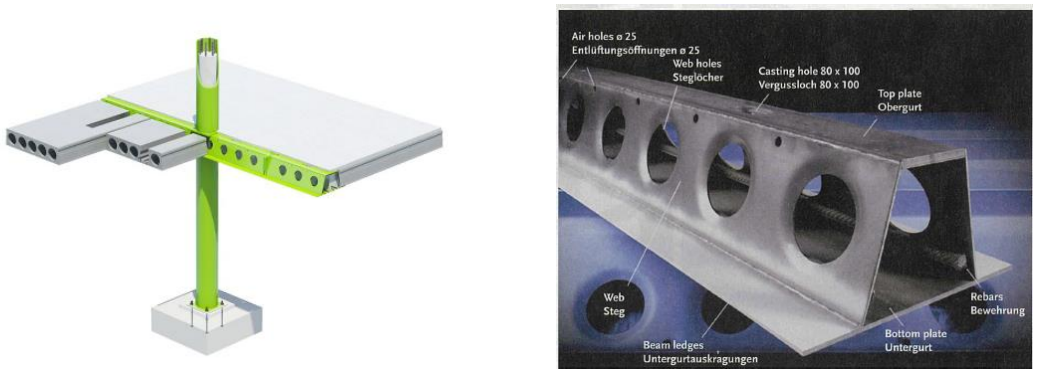

(a) Deltabeam® Frame *(b) Deltabeam® Section*

Figure 2-12. Deltabeam® Concept. From (Vimmr, 2008)]

Chapter 3. Introduction to FastFloor

3.1. The FastFloor Concept

FastFloor is the name given to the proposed non-proprietary modular floor system being studied, and this name will be used hereafter. The conceptual design of FastFloor consists of 10 ft x 40 ft individual modules formed by two beams attached to a bare plate on top. Each unit would be prefabricated in a shop. The dimensions allow the modules to fit and be stacked on a standard truck for transportation. During erection, the modules are placed on a pre-erected structure with columns and girders, as shown in Figure 3-1.

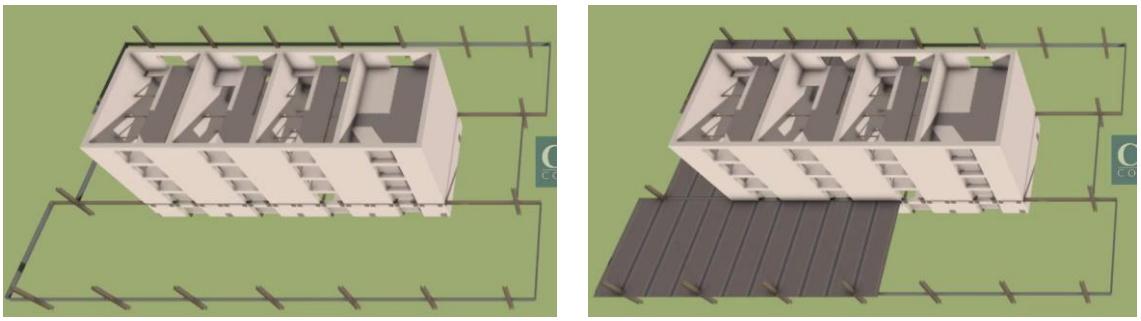

(a) Structure to be erected before FastFloor installation

(b) Placement of FastFloor modules

Figure 3-1. Construction sequence for FastFloor. From video by [Clark Construction, 2022]

Considering the identified challenges, several alternatives were evaluated in the project's early stages. For instance, by looking at the concept in Figure 3-1(a), it can be observed that before placing the modules, the columns don’t have bracing in the direction parallel to the modules, therefore plumbing the columns and ensuring their stability might require additional temporary elements to provide bracing. On the other hand, to ensure the diaphragm action under lateral loads, providing an adequate module-to-module connection, referred to as seam connection, is crucial. Other challenges involve the building performance under fire conditions and adaptability to special architectural requirements like cantilevers.

3.2. Specimen Alternatives

An archetype 40-story high-rise building layout, shown in Figure 3-2, was used as the starting point for determining the module's geometry. The layout has 40 ft x 30 ft bays with core walls between gridlines A-E and 2-3. A 10 ft cantilever is placed on the left of gridline G and at the right of gridline H. Each bay contains three 10 ft x 40 ft modules.

Figure 3-3 provides a summary of the options considered, along with advantages and challenges explained in Table 3-1, based on the geometric requirements of the archetype, fabrication, and erection.

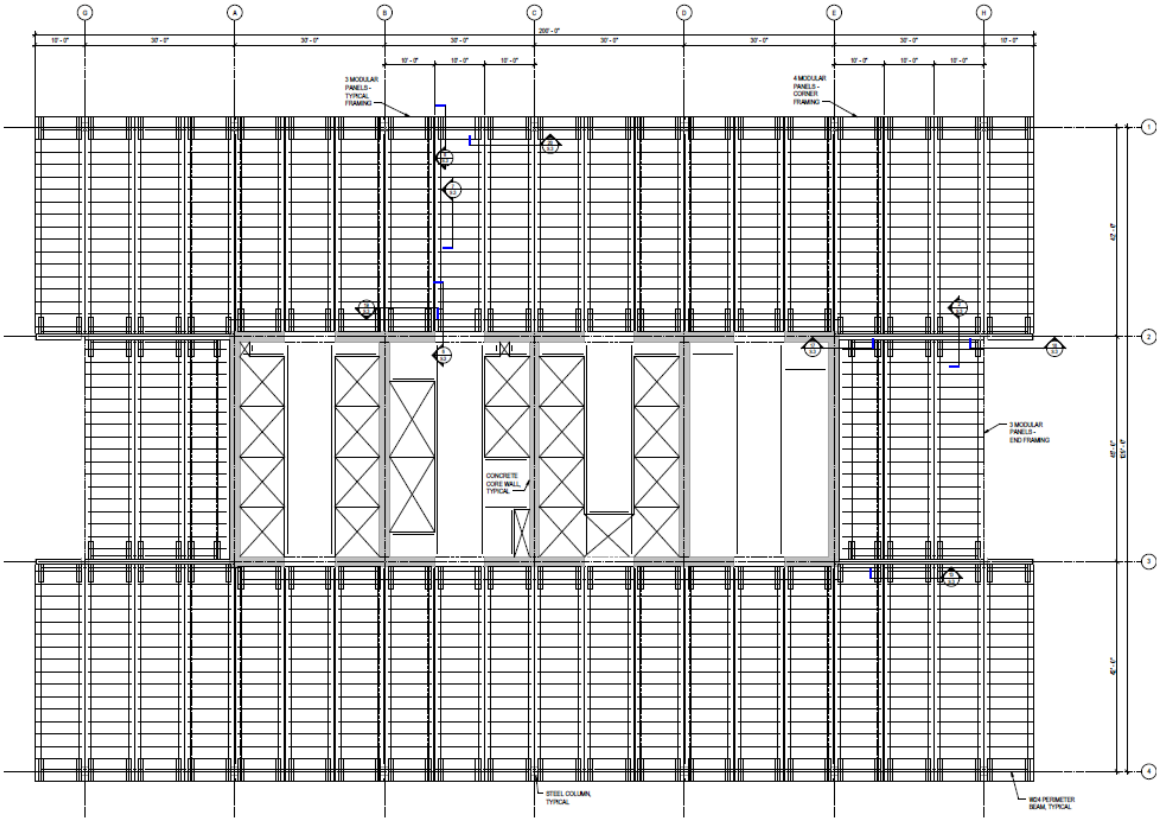

Figure 3-2. Archetype high-rise building – Plan View. From [Magnusson Klemencic Associates, 2016]

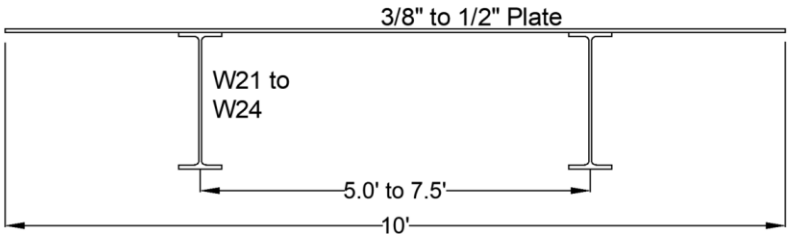

(a) Cantilevered Symmetric Module – Two beams and a plate

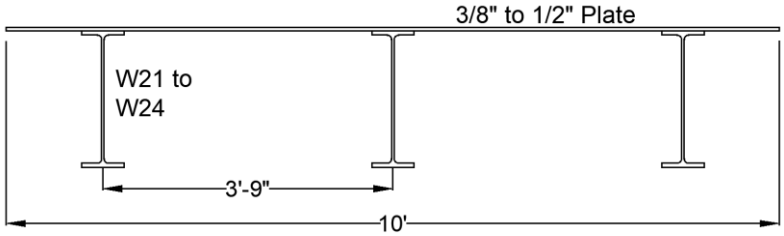

(b) Cantilevered Symmetric Module – Three beams and a plate

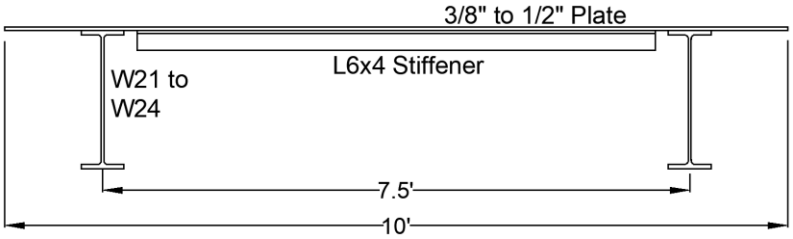

(c) Stiffened Symmetric Module

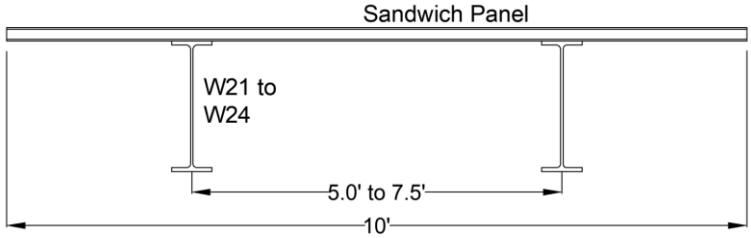

(d) Cantilevered Symmetric Sandwich Panel

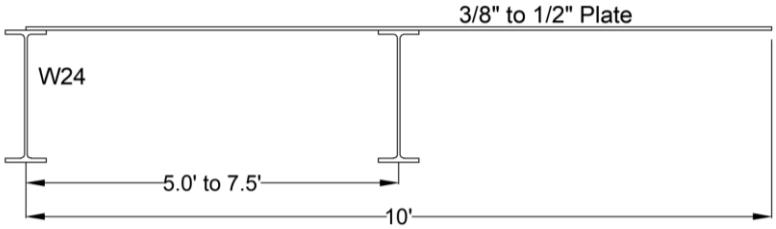

(e) Asymmetric Module

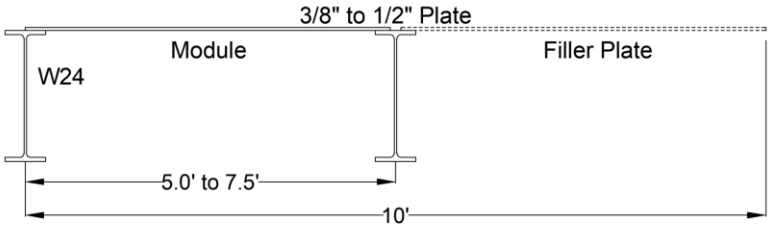

(f) Symmetric Module with Filler Plates

Figure 3-3. Specimen Alternatives – Geometric Configurations

Table 3-1. Alternatives of FastFloor Modules

Advantages	Challenges
(a) Cantilevered Symmetric Module – Two beams and a plate	
- Module weight is under the target value of 7.5 tons to keep the crane costs affordable. - 10 ft x 40 ft total dimensions - All shop welds done from same side. (One station) - All modules have the same configuration. - Easiest to accommodate building geometry.	- Seam connection between adjacent plates will require a procedure to get them in alignment. - The seam will require seal for fire stop/smoke. - Seam connections will be in "the air." - Acoustics might be an issue.
(b) Cantilevered Symmetric Module – Three beams and a plate	
- All shop welds done from same side. (One station) - All modules have the same configuration. - Better for floor vibrations	- Seam connection between adjacent plates will require a procedure to get them in alignment. - Module weight exceeds the target value of 7.5 tons to keep the crane costs affordable.
(c) Stiffened Symmetric Module	
- Plate in between beams has additional stiffness due to the angles. - All shop welds done from same side. (One station) - All modules have the same configuration. - Easiest to accommodate building geometry.	- Around ten additional pieces per module (angles) and more welding in the shop. - Seam connection between adjacent plates will require a procedure to get them in alignment. - The seam will require seal for fire stop/smoke. - Seam connections will be in "the air." - Acoustics might be an issue.
(d) Cantilevered Symmetric Sandwich Panel	
- 10 ft x 40 ft total dimensions.' - The polymer/Honeycomb core provides additional damping while keeping the slab thickness small. - Better acoustic performance	- Proprietary issues if using a commercial product. - Seam connection between adjacent plates requires unique detailing to pass through the core. - The seam will require seal for fire stop/smoke. - Seam connections will be in "the air."
(e) Asymmetric Module	
- Module weight is under the target value of 7.5 tons to keep the crane costs affordable. - 10 ft x40 ft module centerline - Seam connection is on the beams – easier alignment and no caulking for fire stop.	- Shipping/handling due to asymmetric configuration. - 5 ft cantilever plate is hard to handle. Temporary stiffeners might be required. - May need to flip the module for welding at the top and bottom while in the shop (Two stations)
(f) Symmetric Module with Filler Plates	
- Module weight is under the target value of 7.5 tons to keep the crane costs affordable. - Access to beam connections from the top before the filler plate is placed. - Seam connection is on the beams – easier alignment and no caulking for fire stop.	- Twice as many pieces – 5 ft wide coverage. - 5 ft x 40 ft plates are hard to handle in the field. - Plate loose edges are harder to detail. - Welding of A plate requires welding at the top and bottom, and connection configuration for B plates must be carefully designed.

3.3. Selected Module Configuration

Based on the advantages and challenges previously identified, the module configurations chosen for vibration testing correspond to the configuration in Figure 3-3(e) Asymmetric module and Figure 3-3(f) Symmetric Modules with Filler Plates. The behavior is assumed to be similar, so vibration testing will be done using configuration Figure 3-3(e).

The modules have simply supported conditions at both ends of the beam. Shear tabs will be used for the connection to core-walls (Figure 3-4 (a)) and at interior bays (Figure 3-4 (b)), and seated connections will be used at the perimeter of the structure where cantilevers are needed (Figure 3-4 (c)).

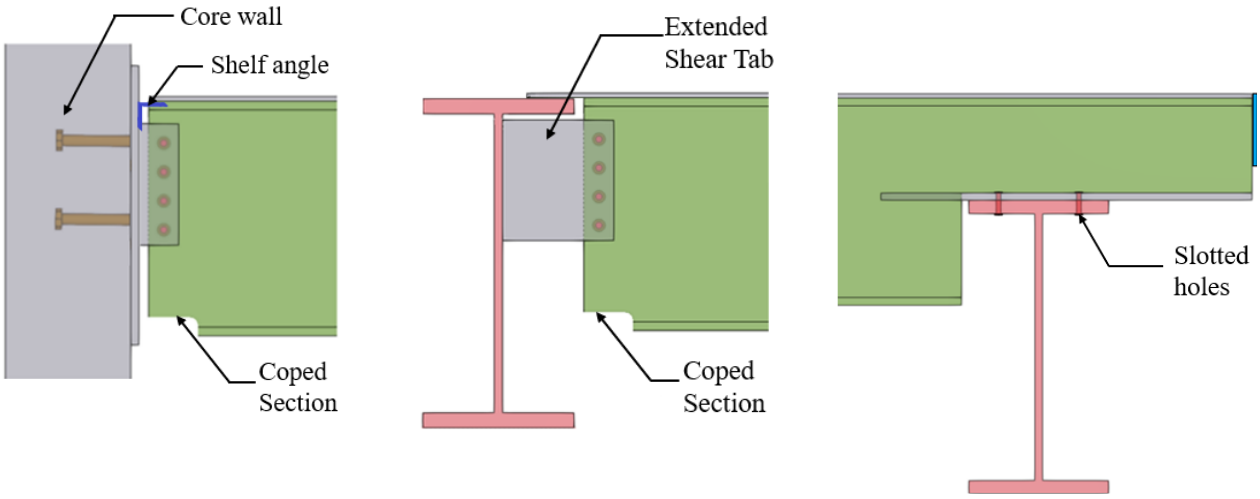

(a) Beam-to-Core Wall: Shear Tab

(b) Beam-to-Girder Connection: Extended Shear Tab

(c) Beam-to-Girder Connection: Seated connection

Figure 3-4. Beam connections

As shown in *Figure 3-5*, the asymmetric module configuration can be aligned with the columns, allowing the beams to provide bracing to the columns. Additionally, it can be placed in the cantilever portion of the building. On the other hand, one disadvantage is having different modules to fit the connection to columns.

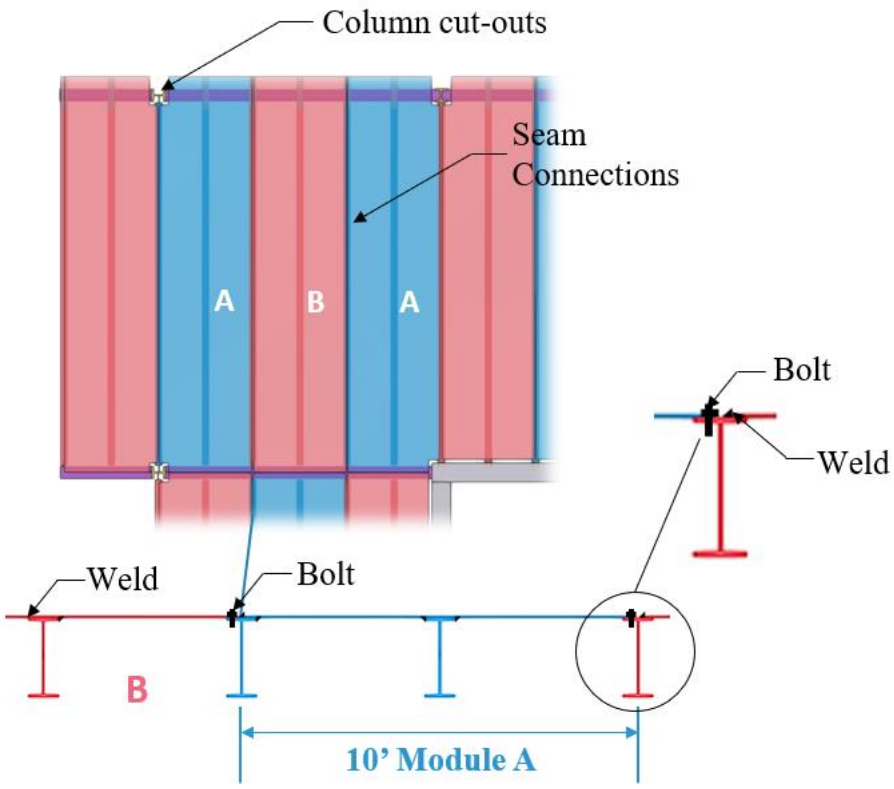

(a) Plan view of Archetype building and Cross section of selected Module Configuration

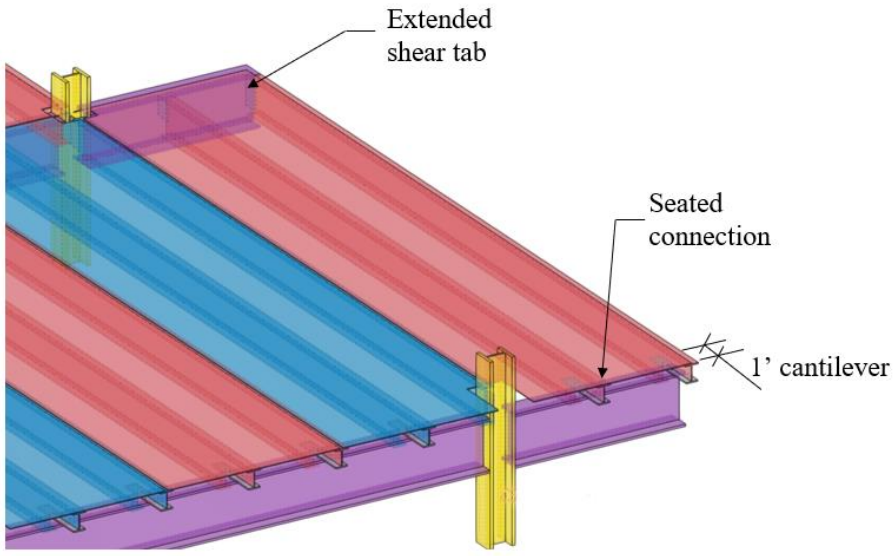

(b) 3D view of selected module fitted in archetype building

Figure 3-5. Selected module configuration located at a portion of archetype building

Chapter 4. Interviews

4.1. Motivation

Seven experts in fabrication and erection were chosen to provide feedback about the fabrication, transportation, and erection issues related to the FastFloor system. Based on an initial module configuration, the interviewees were asked to give input on fabrication, transportation, and erection sequence and to identify challenges and recommendations to improve the system's overall performance. Their feedback at the early stages of this project played an essential role in the final form of the modules.

4.2. Interviews Overview

In March 2022, the interviewees received a preliminary document, provided in Appendix A, which contained a questionnaire and drawings of a preliminary Module configuration, shown in Figure 4-1 and Figure 4-2. Questions were asked about the following categories of issues:

i. Fabrication, including working with the plate, fabrication procedures, camber, and penetrations.
ii. Transportation, including the type of truck and challenges fitting on a truck.
iii. Erection, including sequencing, lifting connections, and fit-up.

Subsequently, one-hour interviews were conducted individually to get feedback on the questions, other issues, and recommendations regarding modular floor systems. During the interviews, notes were taken.

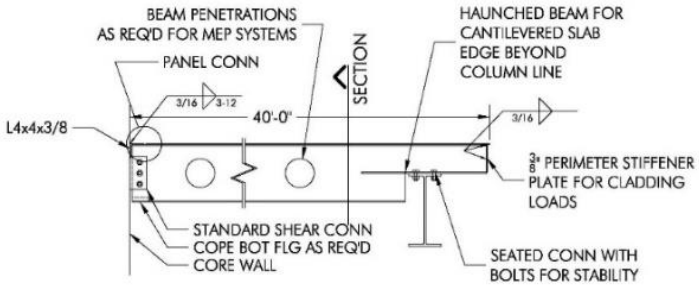

(a) Side view of typical Module

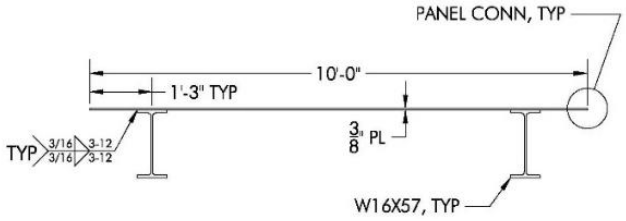

(b) Cross-section of a typical module

Figure 4-1. Preliminary Concept for Modular Floor System. . From [Magnusson Klemencic Associates, 2016]

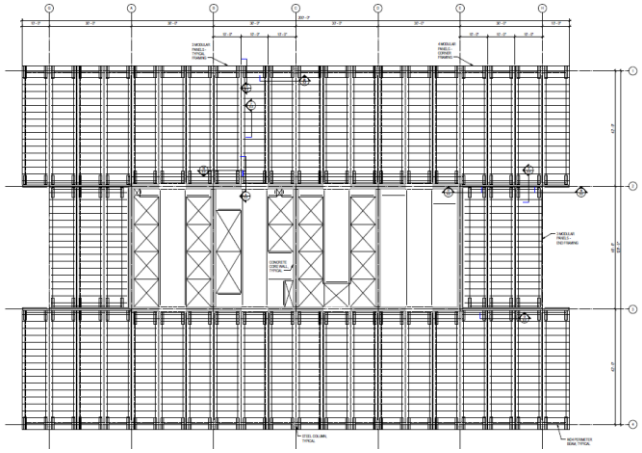

Figure 4-2. Plan View of Archetype High Rise Building. From [Magnusson Klemencic Associates, 2016]

4.3. Summary of Questionnaire Response

4.3.1. Overarching Thoughts

The interviewees agreed on fabrication off-site. The consensus was that the fabrication process is simple. Still, the biggest issue is related to the available space at the steel shop to store the module and the difference in timing between fabrication and erection. It is estimated that fabricators can make 2 to 4 modules daily (depending on the shop),

while 8 to 10 modules can be set on-site. This means there would need to be storage for modules ready to be sent to the site.

Regarding architectural requirements, two people said the modules must be adaptable for cantilevers ranging from 12.5 ft to 15 ft and radii on the outside of the building for architectural purposes. Special detailing may need to be provided for cladding attachment at the plate edge.

4.3.2. Fabrication

Regarding commercial availability, the interviewees stated that plates with dimensions up to 10 ft. x 20 ft. are available at service centers. Therefore, the proposed 10 ft. x 40 ft. plate size would likely need to be ordered from the mill. Two challenges related to this size were mentioned, such as flatness tolerances and the effect of welding on plate deformation.

The participants agreed on avoiding camber in the beams if possible. A hydraulic press can be used if required, but horses might be necessary to get the plate to fit the beam's shape for welding.

The recommended assembly sequencing involves fabricating the modules upside down and flipping them for transportation. For this purpose, several options were mentioned; for instance, magnets, lifting loops, plate clamps, and temporary lifting rings can be provided. For large quantities, a track welder could be set up; otherwise, welding automation is probably unnecessary.

4.3.3. Transportation

The use of a standard 8’-4” wide flatbed truck is recommended. The weight, therefore, must be limited to 40 to 45 kips. Bigger trucks are expensive and of limited

supply. Additionally, a 10 ft wide load requires special permits that can add 50% to the cost in some local jurisdictions such as New York City. It is expected that 10 ft wide loads are only a major issue in places like Manhattan. No escort is needed for loads under 12 ft wide.

Other limitations related to transportation of wide loads are that the following are not allowed: (1) driving at night and (2) driving on holidays and days before/after.

The modules should be erected directly from the truck; therefore, stacking the modules in the correct erection order must be considered. Three people suggested stacking three modules per truck. Two other people mentioned A-frames, similar to precast panels, so that the load fits withing the 8'-4" truck width (no wide load permit required). A crane with two lines would be needed if the modules are transported in this A-frame configuration.

Another important consideration is how to secure the modules on a truck. Tie-downs on a truck are 8.5 ft wide, which may be challenging for 10 ft wide modules. Holes can be placed on the plate next to the beams for the straps to pass through. Additionally, for the given module configuration with cantilevered plates, it was recommended to protect the edges of the plate from damage during tie-down. Blocking might be needed.

4.3.4. Erection/Construction Sequencing

The consensus was that lifting is an important consideration. For this purpose, a standard and certified system should be used. Three alternatives mentioned were: 1) a jig/strongback installed in the shop, removed after installation, 2) a removable bolted lug, and 3) Welded eyes bolts in four locations. The latter option might be a tripping hazard. A spreader beam may be needed on the crane, regardless. On another note, wind can hinder

the erection of the modules; especially for heavier modules; because of their weight, they will be harder to steady once they start moving.

Connections and fit-up also represent challenges during erection. Some options discussed are seated connections with slotted holes in both directions and shear tabs. Regarding connections at the core walls, it was mentioned that seat connections would be better since shear tabs don't have any allowance for tolerances parallel to the wall.

One recommendation for the side lap connections between adjacent modules is to use oversize holes in the plate to access connections from the top side. Given the flatness tolerance and deformations caused by welding during fabrication, power-actuated fasteners (PAF) might not be strong enough to align the modules. Other alternatives are: 1) welding a splice plate underneath the plate to one module and using blind bolts from the top to connect to the other module, 2) Intermittent butt welds and a splice plate underneath, 3) splice plate underneath the plate welded to one side and bolted to the other module. Unlike a typical steel deck after installation but before concrete is placed, a man lift could be used on the FastFloor modules right after erection to have access underneath the subsequent floor's modules. This was seen as an advantage for access during erection and could allow options for connections that need to be approached from the underside.

Later discussions suggested that tension-controlled bolts are not a good option for the bolted connection; and that if using a welded connection, the splice plate should be placed on top with fillet welds on the sides. Another concern is that welding is not possible if there is a coat of intumescent paint. Guardrails will need to be attached directly to the steel plate of the modules.

Chapter 5. Predictions related to floor vibration

5.1. Assumptions For How to Apply DG11 Analytical Procedure

Given that DG11 is calibrated for use with typical steel-framed structural systems with concrete-filled steel deck over steel beams, it is necessary to make assumptions about how to adapt DG11 to an all-steel modular floor system, to which currently there are no provisions and verify these assumptions using dynamic testing. Chapter 2 describes the basic procedures and some key parameters in DG11 as they pertain to a floor system with a concrete-filled steel deck on steel beams.

DG11 criteria, specifically Chapters 2 through 6, were used to perform the analytical vibration assessment as the starting point to determine the specimen's configuration for experimental testing. This involved several assumptions summarized in Table 5-1. Scenarios for the worst case, best case, and best guess were determined by selecting ranges for the variables based on optimistic predictions, DG11 guidelines, and the expected service conditions, as will be further explained.

Table 5-1. Summary of Assumptions Used in Vibration Calculations

Parameter	**Worst Case**	**Best Case**	**Best Guess**
Plate span length, U_{LP}	Beam CL-CL	Clear span	Clear span
Damping from RAF, β	0.5%	3.5%	1.5%
Total damping ratio, β	3.0%	6.0%	4.0%
Live load, L	0.0 psf	8.0 psf	8.0 psf
Superimposed Load, D_{super}	5.0 psf	15 psf	9.0 psf
Total Superimposed Load, D_{super}	9.0 psf	19 psf	13 psf
Effective plate width for plate and beam panels	25% of trib. Width	100% of trib. Width	100% of trib. width
Location of the bay under analysis	Interior (no free edges)	Exterior (with free edges)	Exterior (with free edges)
Load on girder (plf)	Interior	Exterior	Exterior
Plate boundary condition	Simply supported	Fixed-fixed	Simply supported

Panel Modes

DG11 does not include the plate panel contributions, given that the concrete-filled steel deck slab has significantly greater stiffness than the beam and girder panels. This was validated by solving Example 4.3 in DG11 with a slab panel. It was found that the natural frequency of the slab panel is approximately 2.7 times greater than the girder and beam panel modes. Consequently, the difference in the system's natural frequency with and without the slab panel contribution is around 3%. The detailed calculations are included in Appendix B.

For FastFloor, this simplification is not possible, given that the contribution of the slab panel, hereafter referred to as the Plate Panel, significantly affects the system's natural frequency. This accounts for the main modification made to DG11, where the plate panel contribution to the vibration behavior of the system is considered.

Plate Panel

To include the contributions of the plate panel, two assumptions were made. First, the plate boundary was assumed to be simply supported to keep the validity of Equation (2-10). Therefore, Equation (2-1) determines the plate mode deflection.

Second, to determine the plate moment of inertia, the supported weight, and the deflection, the unsupported plate length, L_{up}, was taken as the clear distance between beam flanges instead of the center-to-center beam spacing.

Composite Properties

When determining the transformed moment of inertia of the beam panel, it was assumed to act compositely with the plate. Conversely, given the configuration of

FastFloor, where the girders are not in contact with the plate, the girders were taken as non-composite. Thus, the inertia corresponds to that of the steel beam itself.

For the plate panel, the transformed moment of inertia was taken as the plate's inertia itself. For the stiffened configuration, the transformed moment of inertia included the stiffeners (angles).

Effective Plate Width

There are limit states associated with the configuration of an unstiffened plate, which would not be a concern for a concrete deck slab. The buckling of the plate may reduce the contribution of the steel plate to the moment of inertia of the beam panel or plate panel. The reduction is quantified here as a modification to the plate's effective width in terms of percent, ranging from 25% to 100% of the effective width. This assumption is to be verified through experimental testing.

Damping Ratio

The damping ratio of the floor system was another important assumption, given that the values given by DG11 are not intended for a system like FastFloor. A range of damping going from 3% to 6% was used for the analytical calculations. This variation tries to capture the additional damping when the raised access floor is placed on top of the FastFloor modules.

The damping ratios, corresponding to the structural system, ceiling and ductwork, and electronic office fit-out, were taken per the recommended values in DG11. However, it is essential to mention that the structural system might have a different damping since the overall configuration differs from that of DG11 cases. In addition, the contributions of

the Raised Access Floor (RAF) to the damping ratio were also considered. The total damping ratio is calculated as follows:

β = 0.005 to 0.035 (RAF) + 0.01 (structural system) *(5-1)*
+ 0.01 (ceiling and ductwork) + 0.005 (electronic office fit-out)
= 0.03 to 0.06

Loads

The loads used in the analytical and computational analyses were varied to evaluate different scenarios and the impact of each variable in the system's natural frequency. The loads were taken as follows:

Live Load	0 – 8 psf
Superimposed Dead Load	5 – 15 psf per TATE types of RAF + 4 psf per DG11 = 9 psf – 19 psf

Location of Bay Under Analysis

The effective beam panel width varies on the location under analysis. The analytical calculations were done for a typical beam without free edges, where C_j=2.0, and for beams parallel to a free edge, where C_j=1.0.

Effective Panel Weight, W

The plate panel contribution to the effective panel weight was added as an additional term to the equation below:

$$W = \frac{\Delta_j}{\Delta_p + \Delta_j + \Delta_g} W_p + \frac{\Delta_j}{\Delta_p + \Delta_j + \Delta_g} W_j + \frac{\Delta_g}{\Delta_p + \Delta_j + \Delta_g} W_g \qquad (5\text{-}2)$$

Where

Δ_p = Midspan deflection of the plate

W_j = Effective panel weight for the plate

Fundamental Frequency

The plate panel contribution to the system's natural frequency was added by including its deflection in the equation below. This implies that the assumed support condition of the plate is simply supported.

$$f_n = 0.18\sqrt{\frac{g}{\Delta_p + \Delta_j + \Delta_g}} \qquad (5\text{-}3)$$

Acceptability Criteria

The recommended peak acceleration limit per DG11 of 0.5%g is also used for FastFloor when determining the specimens for testing. However, it's crucial to highlight that experimental testing aims to obtain the natural frequencies and damping ratios.

5.2. DG11 Calculations

The asymmetric module from Section 3.2 was selected. Then, two variations were identified, one heavier version, SM-94-1/2, and one lighter version, SM-68-3/8, with different cross-sections and plate thicknesses, as shown in Table 5-2. These two configurations were chosen optimistically so that the heavier module has a chance of satisfying floor vibration criteria while the lighter module is more pushing the limits.

Table 5-3 summarizes the analytical predictions for each specimen. Detailed calculations are included in Appendix C.

The specimen identification is based on the type of test (SM for Single Module, further explained in Chapter 6), the weight of the W24 section (68 plf or 94 plf), and the thickness of the plate (3/8 in. or 1/2 in.). The specimens are therefore identified as shown in Table 5-2, and the cross sections are presented in Figure 5-1.

Table 5-2. Geometric configuration of specimens

Specimen	SM-68-3/8	SM-94-1/2
Beams	W24x68	W24x94
Girders	W33x263	W33x263
Stiffeners	NA	NA
Plate thickness (in.)	3/8	1/2
Beam spacing (ft)	5	7.5
Weight (psf)	35.5	45.8
Weight of 10'x 40' panel (ton)	5.78	7.84

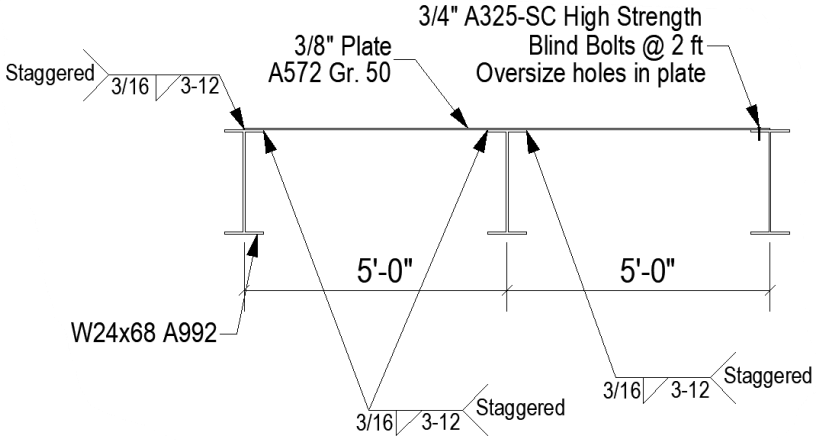

(a) Specimen SM-68-3/8

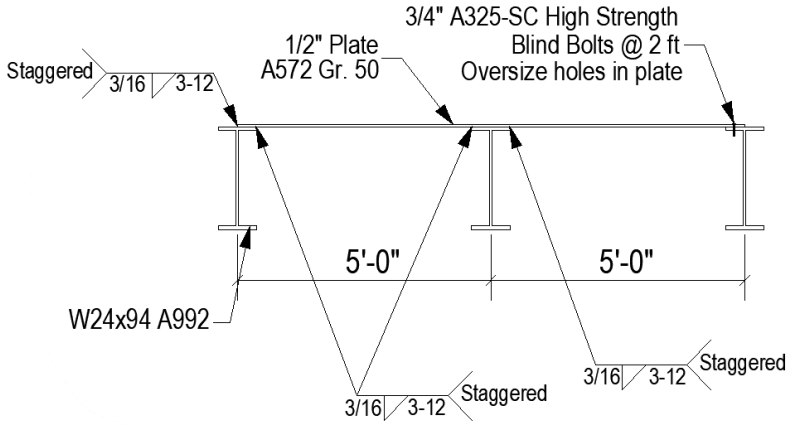

(b) Specimen SM-94-1/2

Figure 5-1. Cross-section view of 10 ft x 40 ft modules

Table 5-3. Analytical predictions for specimens

		SM-68-3/8	SM-94-1/2
Worst case	f_{nPBG} (Hz)	5.76	6.09
	f_{nBG} (Hz)	7.97	7.51
Best case	f_{nPBG} (Hz)	6.90	7.57
	f_{nBG} (Hz)	7.51	7.93
Best Guess	f_{nPBG} (Hz)	5.77	7.06
	f_{nBG} (Hz)	7.92	8.67
Worst case	a_{pPBG}/g (%)	3.06	1.37
	a_{pBG}/g (%)	0.91	0.62
Best case	a_{pPBG}/g (%)	0.87	0.50
	a_{pBG}/g (%)	0.67	0.42
Best Guess	a_{pPBG}/g (%)	2.39	1.16
	a_{pBG}/g (%)	0.96	0.61

Where

Subscript PBG = Plate, Beam, and Girder panel contributions

Subscript BG = Beam and Girder panel contributions

f_{nPBG} = System natural frequency with plate panel contribution

f_{nBG}= System natural frequency without plate panel contribution

a_{pPBG}/g = Ratio of peak acceleration to gravity acceleration with plate panel contribution

a_{pBG}/g = Ratio of peak acceleration to gravity acceleration without plate panel contribution

From the results obtained, it can be observed that the natural frequency, f_{nPBG}, including the plate panel contribution is lower than f_{nBG}, when neglecting the plate panel, which indicates that the plate flexibility reduces the bay frequency. The predicted accelerations, a_{pPBG}/g, including the plate panel contribution, are higher than a_{pBG}/g. The difference between the two approaches confirms that the plate panel contribution to the vibration behavior is not negligible as compared to DG11.

Additionally, Specimen SM-94-1/2 satisfies the floor vibration criteria for the Best-Case scenario, given that the accelerations are below the DG11 limit of 0.5%g. However,

both specimens fail the criterion using best-guess assumptions, so experimental testing is necessary to determine the appropriate assumptions.

5.3. SCI P354 Approach for Light Steel Frame Floors

Even though FastFloor does not meet the criteria to be considered light steel frame floors (Discussed in Section 2.3), given that the moments of inertia far exceed the limit value, calculations were done for both specimens (without RAF) following the criteria for light steel framed floors, given that the slab is a bare plate, similar to the slab types considered by the SCI. The detailed procedure is included in Appendix D.

Regarding the composite properties, the supporting members have a moment of inertia greater than the limit per SCI by a factor of over 30 for the smallest member size (W24x68). In addition, in SCI P354, it is assumed that the floor slab is a light material. Thus, the resulting transformed steel area is very small. For FastFloor, the moment of inertia is much larger because the plate is steel instead of one of the lightweight materials.

The variables n_x and n_y, correspond to the number of consecutive bays acting in the direction perpendicular and parallel to the floor joists, respectively. Both values were taken conservatively as 1.0, considering only the contributions of one module. These values affect the effective floor width and effective floor length, and thus the modal mass, *M*, involved in the Response Factor estimation, *R*. In Section 2.3, more information is provided on the mentioned variables.

Given that the analyzed specimens are substantially stiffer than the systems that would satisfy the criteria for lightweight floors, the acceleration response, a_{wrms}, yields low values, resulting in a Response Factor, *R*, smaller than the acceptable limit of 16. For Specimen SM-68-3/8 , R=7.29 and for SM-94-1/2, R=5.78. Although both specimens lie

in the accepted zone, this not necessarily means that the floor is acceptable for continuous vibrations because the modules don't satisfy the criteria to use this procedure.

5.4. SAP2000 Modelling According to DG11 – Chapter 7

5.4.1. Calibration of SAP2000

Before proceeding with the FE models of the single-module specimens, the modeling assumptions were validated by reproducing the model described in Example 7.1 of DG11, Chapter 7: Office floor with cantilever area. The given parameters are summarized in Table 5-4:

Table 5-4. Parameters of DG11 – Example 7.1

Masses	
Uniform mass:	
Concrete slab + Deck	41.0 psf
Typical mechanical, electrical, plumbing, and ceiling	4 psf
Electronic office build-out live load	8 psf
Total uniform load	53.0 psf
Mass applied to shell elements	**1.65 psf-s^2/ft**
Cladding:	
Weight	280 plf
Line mass along gridline F	**8.70 plf-s^2/ft**
Member masses:	Computed by the program
Viscous Damping Ratio	
Structural system	β=0.01
Ceiling and ductwork	β=0.01
Electronic office fit-out	β=0.005
Total damping	**0.025**
Slab Stiffness	2700 ksi
Poisson ratio	0.2

Two models were developed with different approaches. As shown in Figure 5-2, one model had the slab and member aligned at the centroid, while the second model had the members offset by 2 in. to account for the deck height. For both models, the thickness assigned to the slab corresponds to the depth of concrete above the ribs, and the stiffness

in the direction parallel to the ribs was adjusted by modifying the bending coefficient. The considerations for each approach are further explained below.

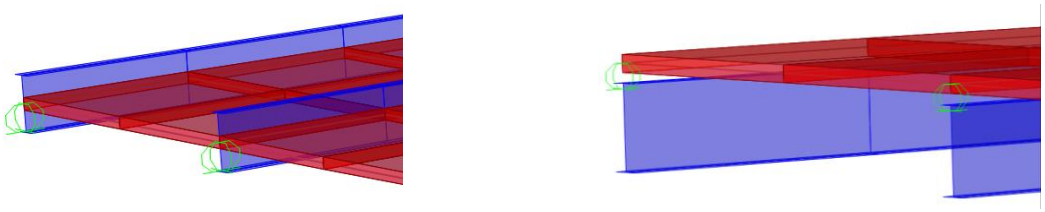

(a) Approach 1: Members and slab aligned at the centroid

(b) Approach 2: Introduction of gap equal to deck height between top flange and modeled slab

Figure 5-2. Models for validating DG11 – Example 7.1

Approach 1: Members and Slab Aligned at Centroid

DG11 uses this approach, where it is required to subtract the slab moment of inertia from the member transformed moment of inertia since it is already included in the shell stiffness. Table 5-5 compares the calculated geometric properties and the reported values in DG11.

Table 5-5. Comparison of calculated properties vs. reported values in DG11

Parameter	DG11	Calculated	Percentage of difference
Slab moment of inertia perpendicular to ribs (in.^{4}/ft)	34.3	34.3	0%
Slab moment of inertia parallel to ribs (in.^{4}/ft)	102	98.87	3.0%
Typical beam W16x26 transformed moment of inertia (in.^{4})	1,100	1,126	2.4%
Spandrel beam W16x26 transformed moment of inertia (in.^{4})	1,010	975.1	3.5%
Interior girder W24x55 transformed moment of inertia (in.^{4})	3,970	4,061	2.3%
Cantilevered girder W24x55 transformed moment of inertia (in.^{4})	3,670	3,727	1.6%

Furthermore, several property modifiers were calculated for Approach 1, as shown in Table 5-6. Detailed calculations are attached in Appendix E.

Table 5-6. Property modifiers assigned in SAP2000 Model

Parameter	Property Modifier Magnitude	SAP2000 Modification Factor
Slab Bending in parallel direction	2.88	Bending m22 Modifier
Typical beam W16x26 strong axis moment of inertia	3.66	Moment of Inertia about 3-axis
Beam W16x26 along gridline C strong axis moment of inertia	10	Moment of Inertia about 3-axis
Spandrel beam W16x26 strong axis moment of inertia	7.99*	Moment of Inertia about 3-axis
Interior girder W24x55 strong axis moment of inertia	2.94	Moment of Inertia about 3-axis
Cantilever girder W24x55 strong axis moment of inertia	2.71	Moment of Inertia about 3-axis
All framing members	0.00	Shear Area in 3-direction

*Increased by 2.5 to account for cladding restraint

The following modeling assumptions are made to obtain identical results to those in DG11.

The sections used for the framing members don't correspond to the specific W-shapes. Instead, a section is created where the cross-section area is defined according to the steel section used. In contrast, the moment of inertia around the x-axis corresponds to the transformed moment of inertia of the composite section. All other geometric properties, including the shear areas in both directions, are taken as zero.

When shear deformations were neglected, the results were much closer, as observed in the comparisons discussed in Figure 5-3, Figure 5-5, Figure 5-6, and Table 5-7. For instance, the frequency for the first mode was 3.29 Hz when including shear deformations, compared to 3.49 Hz when neglecting them, resulting in a 5.7% decrease. This is consistent

with (Barrett, 2006) observations, where neglecting shear deformations results in stiffer members and, therefore, greater frequencies.

Approach 2: Introduction of gap equal to deck height between top flange and modeled slab

SAP2000 allows changing the Insertion Point of the framing elements, which enables the possibility to offset the members with reference to the slab centroid. Since the modeled slab corresponds to the portion above the ribs, the members were offset to introduce a gap between the top flange and the modeled slab equal to the deck height, in this case, 2 inches. A Property Modifier is then assigned to account for the perpendicular direction, where the concrete between the ribs contributes additional stiffness.

Introducing this gap to the model allows SAP2000 to directly calculate the composite properties avoiding the need to use property modifiers, except for specific cases such as 1) Orthotropic slab stiffness, 2) Additional stiffness to account for cladding, 3) Additional stiffness to account for building continuity / adjacent slabs that are not included in the model. Therefore, only the modifiers related to the slab stiffness in the direction parallel to the ribs were kept to account for cladding restraints.

As observed in Figure 5-3, while Approach 1 had the closest mode shapes and natural frequencies to DG11, Approach 2 also showed similar results, as shown in Figure 5-6 and Table 5-7. For instance, the percentage of difference between DG11 and Approach 2 had a maximum value of 4.6% for the frequencies and 11.2% for the peak accelerations, for the 12th mode being slightly more conservative. For the first mode, the observed differences were 2.6% and 4.4% for the frequencies and accelerations, respectively. These results are reasonably close, and it’s generally easier to implement because it does not require calculating and implementing property modifiers.

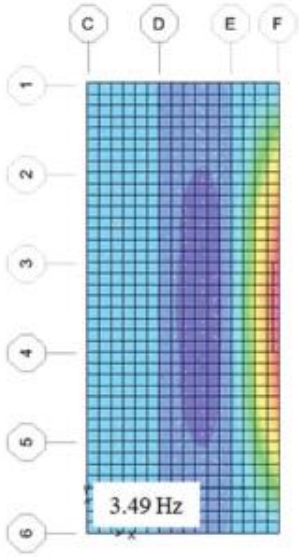

(a) DG11 Mode 1, f_n=3.49 Hz

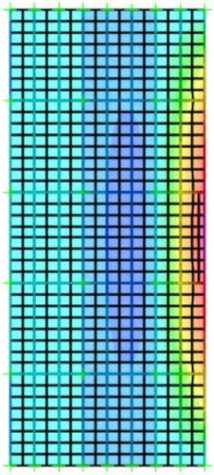

(b) Approach 1: Mode 1, f_n=3.42 Hz

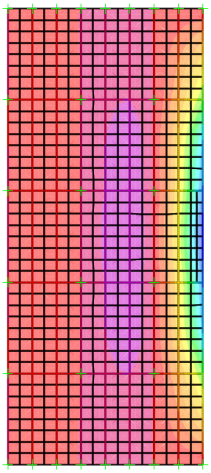

(c) Approach 2: Mode 1, f_n=3.58 Hz

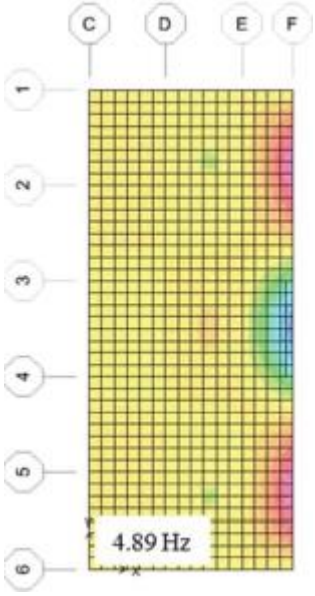

(d) DG11 Mode 3, f_n=4.89 Hz

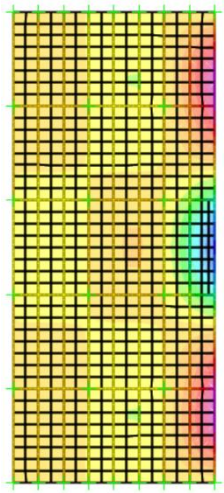

(e) Approach 1: Mode 3, f_n=4.78 Hz

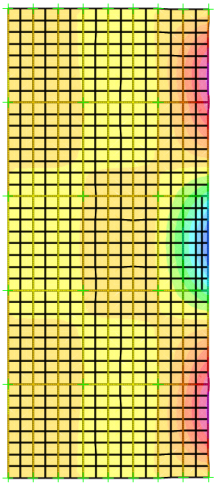

(f) Approach 2: Mode 3, f_n=4.52 Hz

Figure 5-3. Comparison between DG11 and computed frequencies and mode Shapes

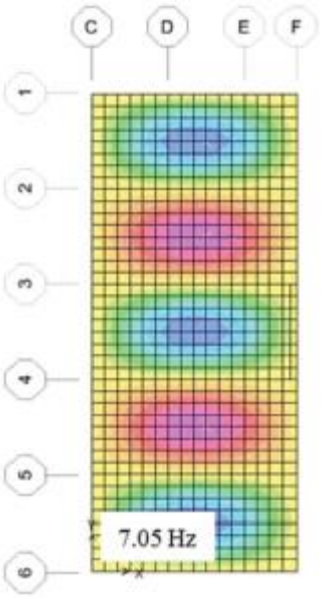

(g) DG11 Mode 5, f_n=7.05 Hz

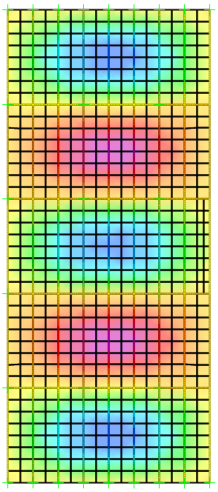

(h) Approach 1: Mode 5, f_n=7.05 Hz

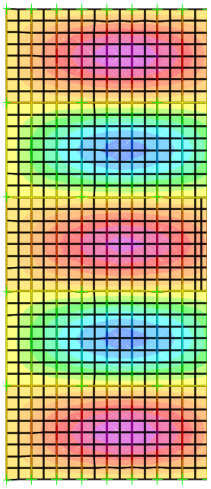

(i) Approach 2: Mode 5, f_n=7.01 Hz

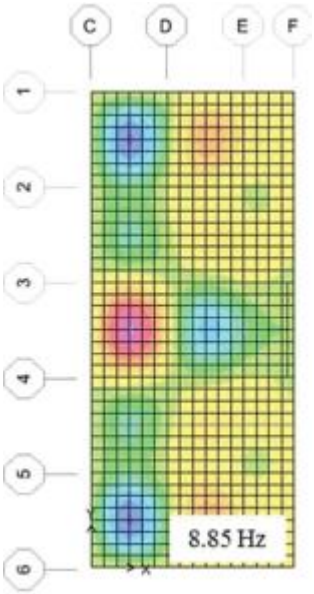

(j) DG11 Mode 10, f_n=8.85 Hz

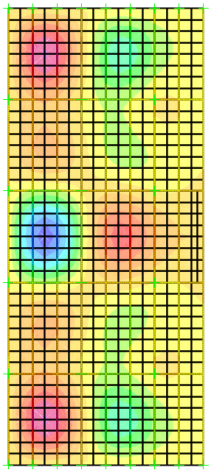

(k) Approach 1: Mode 10, f_n=8.82 Hz

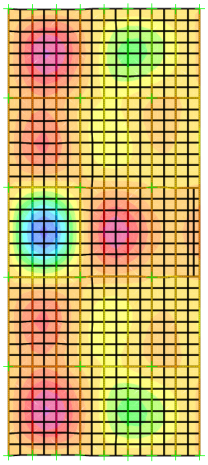

(l) Approach 2: Mode 10, f_n=8.62 Hz

Figure 5-3. Comparison between DG11 and computed frequencies and mode Shapes

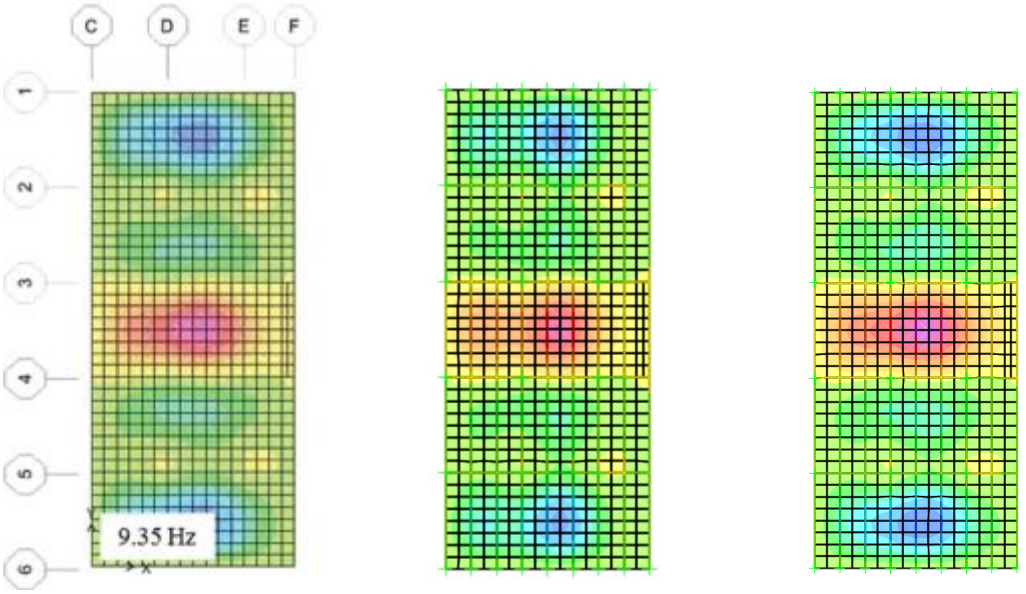

(m) DG11 Mode 12, f_n=9.35 Hz (n) Approach 1: Mode 13, f_n=9.34 Hz (o) Approach 2: Mode 13, f_n=8.92 Hz

Figure 5-3. Comparison between DG11 and computed frequencies and mode Shapes

Frequency Response Function (FRF) Prediction

For this structure, two potential walking paths were determined. Thus, frequency response functions were estimated for load and acceleration at the backspan and cantilever tip, as shown in Figure 5-4. The SAP2000 modeling approach is verified here against the values reported in DG11.

In Figure 5-5, Figure 5-6, and Table 5-7, the FRF plots and their associated peak frequencies and accelerations are compared. Approach 2 also led to acceptable values, with a maximum error of 11%. It's important to mention that the deck cross-section was assumed since no information was given in DG11; thus, the property modifier might differ from that used in the original model.

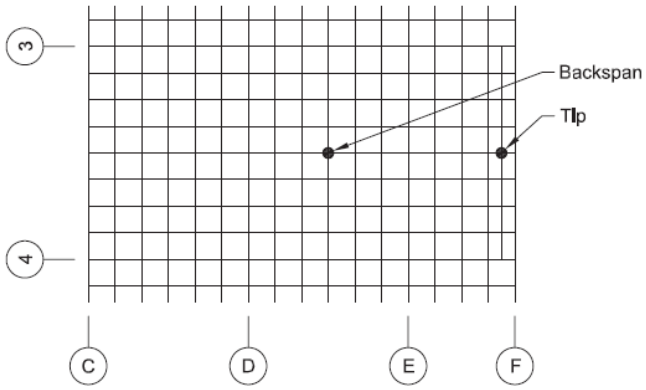

Figure 5-4. Backspan and tip analysis locations. From [DG11 (2016)]

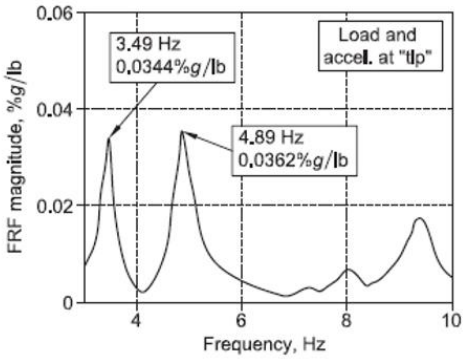

(a) DG11- Load and acceleration at tip. *From [DG11 (2016)]*

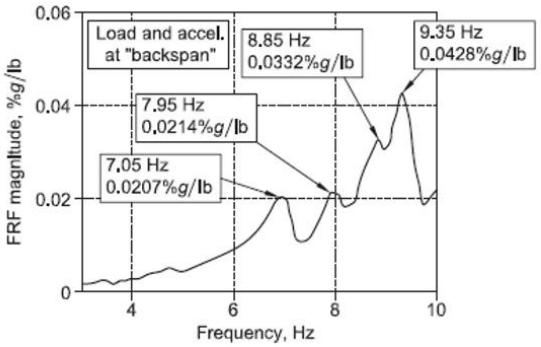

(a) DG11- Load and acceleration at backspan. *From [DG11 (2016)]*

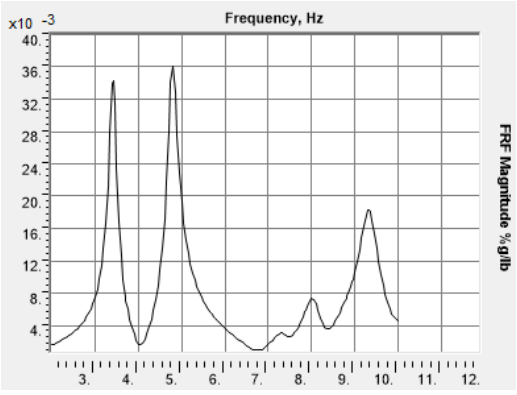

(b) Approach 1 – Load and acceleration at the tip

Figure 5-5. Tip Location FRF magnitudes, Example 7.1

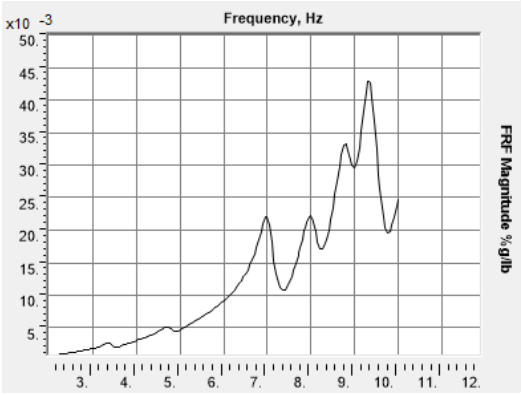

(b) Approach 1 – Load and acceleration at backspan

Figure 5-6. Backspan location FRF magnitudes, Example 7.1

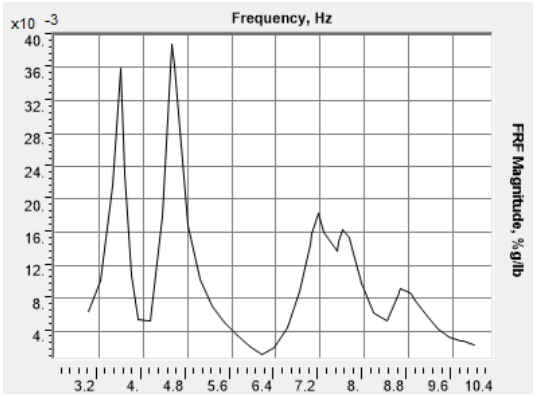

(c) Approach 2 – Load and acceleration at the tip

Figure 5-5. Tip Location FRF magnitudes, Example 7.1

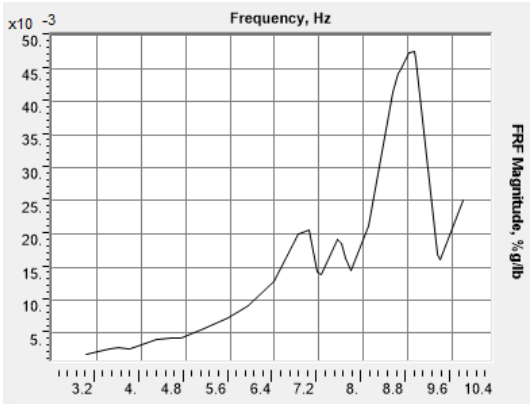

(c) Approach 2 – Load and acceleration at backspan

Figure 5-6. Backspan location FRF magnitudes, Example 7.1

Table 5-7. Comparison between models and DG11

		Tip Location FRF magnitudes		**Backspan location FRF magnitudes**			
DG11	Acceleration [%g/lb.]	0.0344	0.0362	0.0207	0.0214	0.0332	0.0428
	Frequency [Hz]	3.49	4.89	7.05	7.95	8.85	9.35
Approach 1	Acceleration [%g/lb.]	0.0343	0.0361	0.022	0.022	0.033	0.0429
	Frequency [Hz]	3.46	4.80	6.95	7.96	8.78	9.32
Difference Between DG11 and Approach 1	Acceleration [%]	0.29	0.28	6.28	2.8	0.6	0.23
	Frequency [%]	0.86	1.84	1.42	0.13	0.79	0.32
Approach 2	Acceleration [%g/lb.]	0.0359	0.0388	0.021	0.0192	-	0.0476
	Frequency [Hz]	3.58	4.52	7.00	7.53	-	8.92
Difference Between DG11 and Approach 2	Acceleration [%]	4.4	7.2	1.4	10.3	-	11.2
	Frequency [%]	2.6	7.6	0.7	5.3	-	4.6

It is concluded that the SAP modeling approach used in this work, specifically Approach 1 for modeling beams and slabs, is consistent with DG11. It is also concluded that Approach 2, which directly models the offset between the beams and slab, produces

results within approximately 10% of the approach used in DG11 and, thus, is deemed acceptable for use in this study.

5.4.2. Single Module Models

The four configurations of the single module specimens used for experimental tests, listed in Table 5-2 and Figure 5-1, with and without RAF, were replicated in SAP2000, including the actual loads in the experimental setup; therefore, for the scope of this research, the purpose of these models is to compare mode shapes and natural frequencies between the experiments and models. These models will not be used to judge acceptability for floor vibrations because they do not include live load and consideration of fit-out.

The modeling procedure was the same as Approach 2 in the previous section, which includes the offset in the model instead of using property modifiers, as shown in Figure 5-7. It's important to mention that the restraint condition at the supports included a pinned support, with an additional rotational restraint along the y-axis, that simulates the bolted connection between the bottom of the beam and the girder in the experiment. The parameters assigned to the models are shown in Table 5-8.

Table 5-8. Parameters assigned to single-module models

Masses	**SM-68-3/8**	**SM-94-1/2**
Uniform mass:		
Steel plate	15 psf	20 psf
RAF (ConCore1000 floor panels, Posilock pedestal heads)	9 psf	9 psf
Total uniform load without RAF	15 psf	20 psf
Mass applied to shell elements without RAF	**0.47 psf-s^2/ft**	**0.62 psf-s^2/ft**
Total uniform load with RAF	24 psf	29 psf
Mass applied to shell elements with RAF	**0.75 psf-s^2/ft**	**0.9 psf-s^2/ft**
Member masses:	Computed by the program	
Slab Stiffness	29,000 ksi	

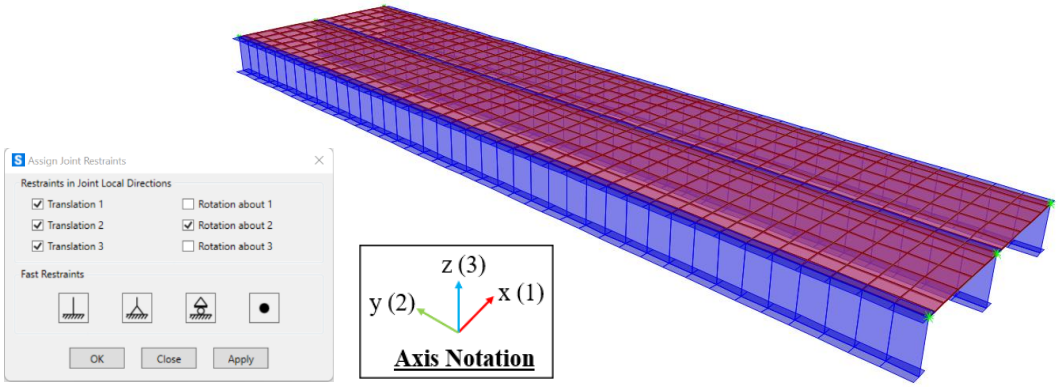

Figure 5-7. Typical Model Configuration for single modules in SAP2000

Table 5-9 summarizes the first mode per specimen and frequencies. Figure 5-8 through Figure 5-11 show the first six mode shapes and frequencies for each specimen, normalized by its peak deformation. These results will be compared with experimental results in Chapter 7.

Table 5-9. Summary of First-Mode Natural Frequencies for Single Module Specimens

Specimen Code	**SM-68-3/8**	**SM-94-1/2**	**SM-68-3/8 RAF**	**SM-94-1/2 RAF**
Plan dimensions	30 ft x 40 ft	30 ft x 40 ft	30 ft x 40 ft	30 ft x 40 ft
Beam sections	W24x68	W24x94	W24x68	W24x94
Beam spacing (ft) (CL distance)	5.0	5.0	5.0	5.0
Plate thickness (in.)	3/8	1/2	3/8	1/2
SDL (psf)	0.0	0.0	9	9
LL (psf)	0.0	0.0	0.0	0.0
f_{n1FE} (Hz) (Bending Mode 1)	12.66	14.12	10.6	12.54

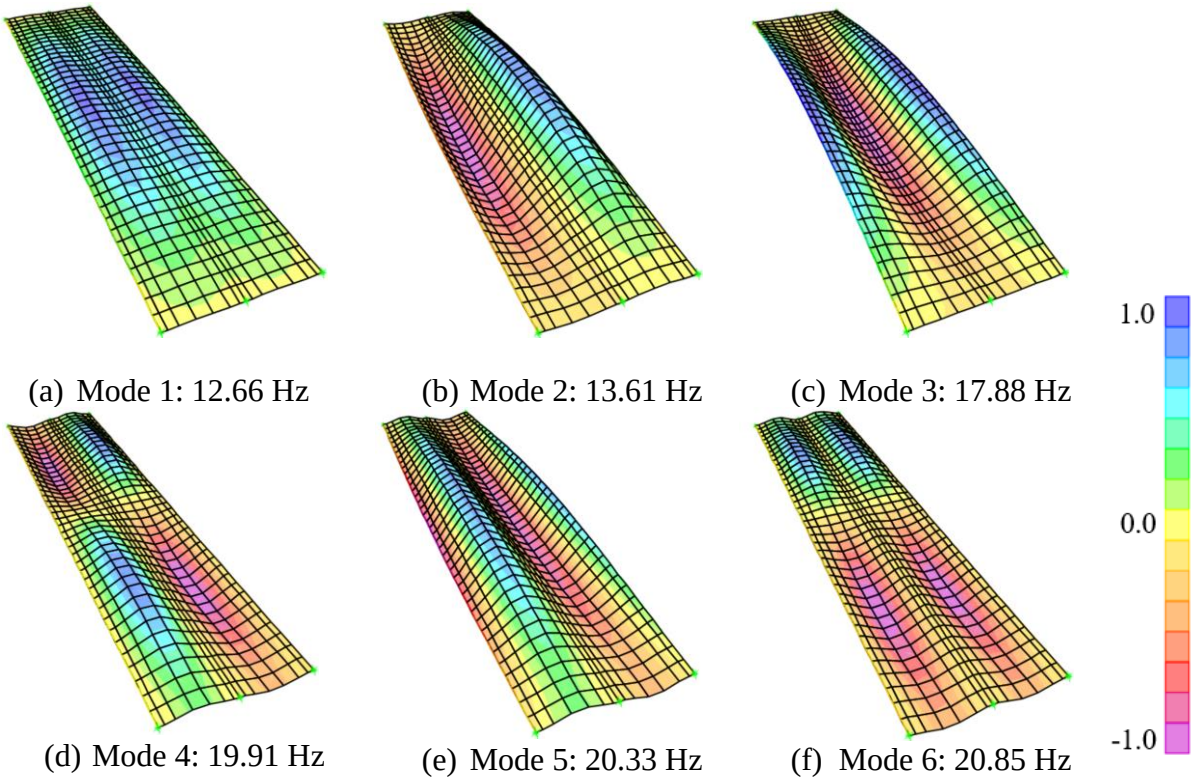

(a) Mode 1: 12.66 Hz (b) Mode 2: 13.61 Hz (c) Mode 3: 17.88 Hz

(d) Mode 4: 19.91 Hz (e) Mode 5: 20.33 Hz (f) Mode 6: 20.85 Hz

Figure 5-8. Computed Frequencies and Mode Shapes for SM-68-3/8

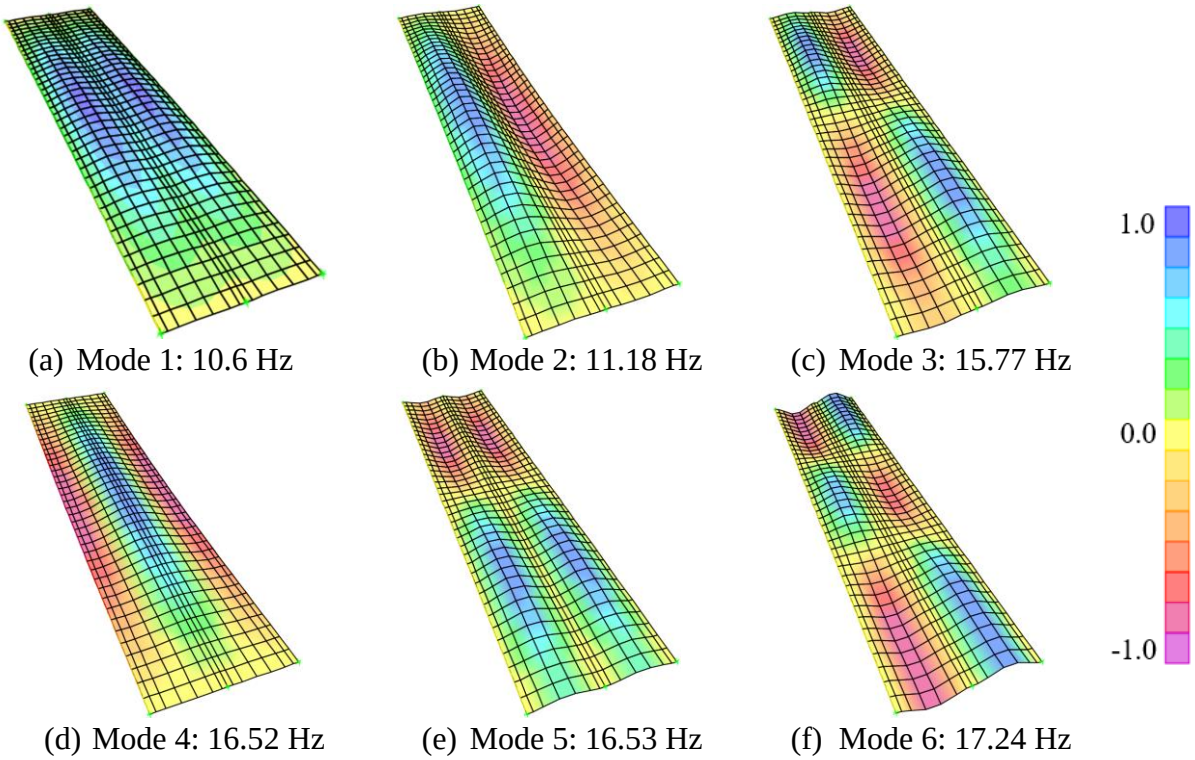

(a) Mode 1: 10.6 Hz (b) Mode 2: 11.18 Hz (c) Mode 3: 15.77 Hz

(d) Mode 4: 16.52 Hz (e) Mode 5: 16.53 Hz (f) Mode 6: 17.24 Hz

Figure 5-9. Computed Frequencies and Mode Shapes for SM-68-3/8 RAF

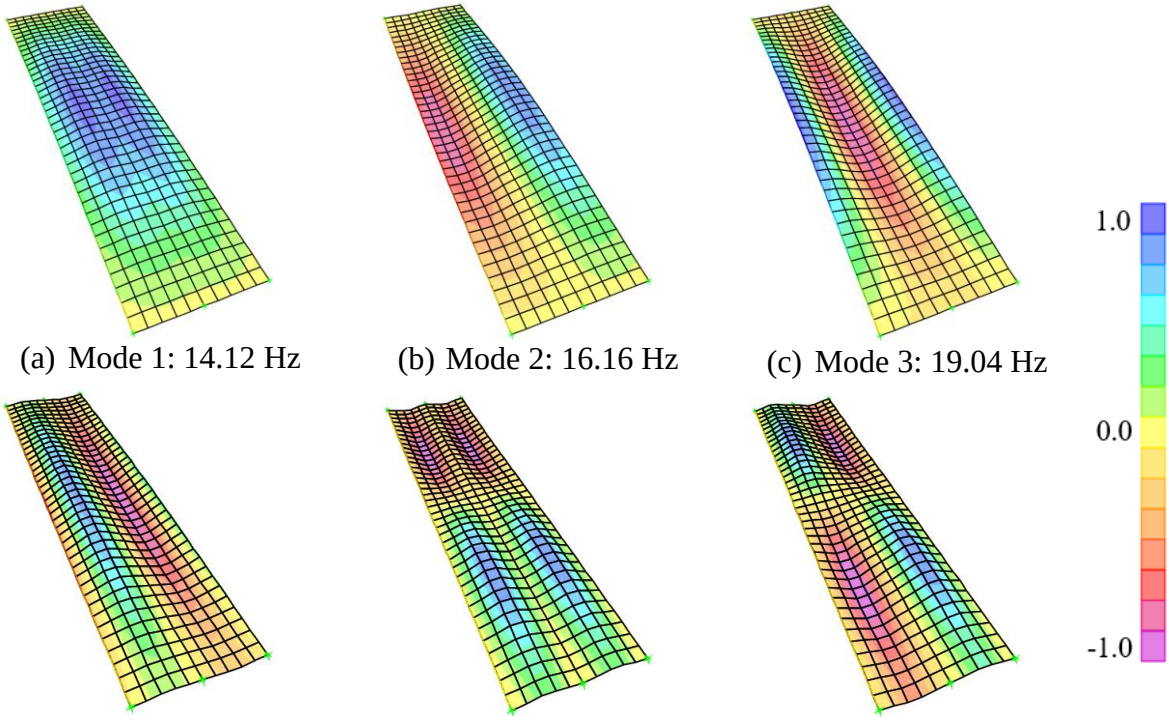

(a) Mode 1: 14.12 Hz (b) Mode 2: 16.16 Hz (c) Mode 3: 19.04 Hz

(d) Mode 4: 27.14 Hz (e) Mode 5: 27.65 Hz (f) Mode 6: 27.72 Hz

Figure 5-10. Computed Frequencies and Mode Shapes for SM-94-1/2

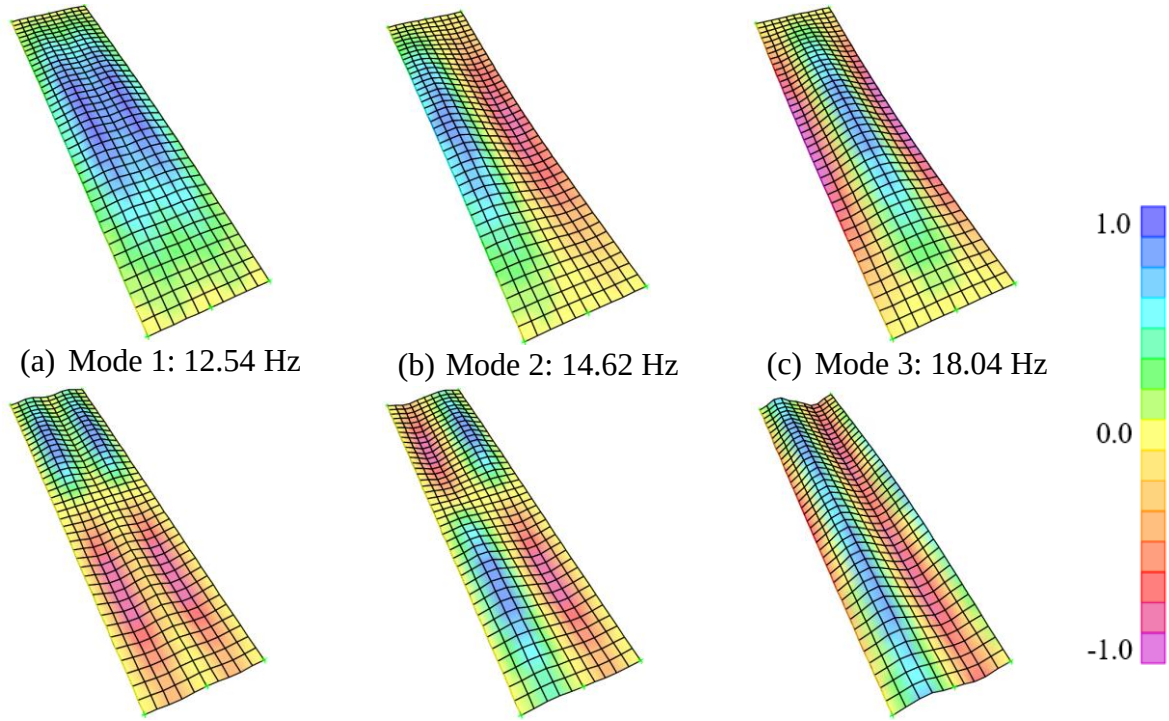

(a) Mode 1: 12.54 Hz (b) Mode 2: 14.62 Hz (c) Mode 3: 18.04 Hz

(d) Mode 4: 23.02 Hz (e) Mode 5: 23.02 Hz (f) Mode 6: 23.93 Hz

Figure 5-11. Computed Frequencies and Mode Shapes for SM-94-1/2 RAF

5.4.3. Full Bay Models

Four models were created in SAP2000, keeping the geometries of the tested specimens but including a total of three modules corresponding to a bay per the archetype building discussed in Section 3.2. These models aim to replicate the actual conditions in a real building and judge its acceptability under DG11 provisions. Expected loads and damping for vibration assessment were assigned, including those from additional fit-out. The parameters assigned to the models are shown in Table 5-10 and Table 5-11:

Table 5-10. Parameters assigned to single-module models

Masses	**FB-68-3/8**	**FB-94-1/2**
Uniform mass:		
Steel plate	15 psf	20 psf
Typical mechanical, electrical, plumbing, and ceiling	4 psf	4 psf
RAF (ConCore1000 floor panels, Posilock pedestal heads)	9 psf	9 psf
Electronic office build-out live load	8 psf	8 psf
Total uniform load without RAF	27 psf	32 psf
Mass applied to shell elements without RAF	**0.84 psf-s^2/ft**	**0.99 psf-s^2/ft**
Total uniform load with RAF	36 psf	41 psf
Mass applied to shell elements with RAF	**1.12 psf-s^2/ft**	**1.27 psf-s^2/ft**
Member masses:	Computed by the program	
Slab Stiffness	29,000 ksi	

Table 5-11. Viscous Damping Ratio from Best Guess Assumptions

Without RAF	
Structural system	β=0.01
Ceiling and ductwork	β=0.01
Electronic office fit-out	β=0.005
Total damping without RAF	**0.025**

With RAF	
Structural system	β=0.01
Ceiling and ductwork	β=0.01
Electronic office fit-out	β=0.005
RAF	β=0.015
Total damping with RAF	**0.040**

The detailed procedure for judging acceptability will be shown for FB-68-3/8, and then, a summary of all the predictions for full-bay models will be provided.

The modeling procedure follows the same used for Single-Module models, with slight changes. 1) The girders were included, 2) The support conditions were changed to a combination of pins and rollers, with no rotational restraints, and 3) A more refined mesh was added at the middle of the unsupported plate to take measurements at critical points. The typical configuration is shown in Figure 5-12.

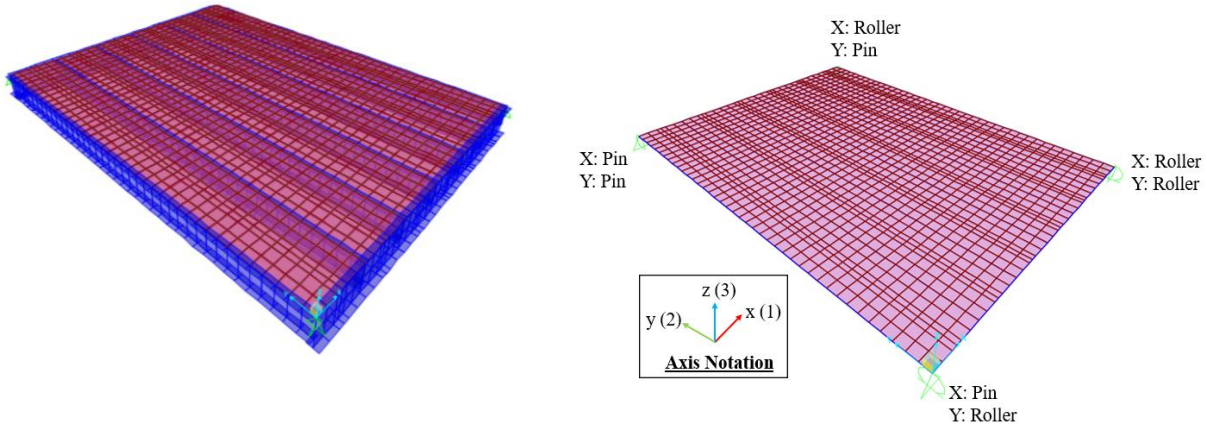

(a) Typical Extruded View for full-bay (b) Support conditions for Full-Bay Models

Figure 5-12. Typical Model Configuration for Full-Bay in SAP2000

Low-Frequency Floor Procedure

The full model FB-68-3/8 was analyzed to get natural frequencies and mode shapes. Only the first mode had a frequency under 9 Hz, which is the cutoff in DG11 for low-frequency floors because of resonant build-up with one of the first four subharmonics of the walking force. Thus, the predicted mode maximum acceleration is determined using the low-frequency floor procedure previously discussed in Section 2.3.

First, the dynamic coefficient and the resonant build-up factor are calculated using Equations (2-13) and (2-14). Consequently, different FRF- magnitude are analyzed for the critical locations shown in Figure 5-13(b), where load cases were created for each location

to apply a 1.0 lb. force. The locations were selected based on where the maximum values of the mode shapes occur, as there is no information regarding walking paths based on architectural layouts. It can be observed that the model has a symmetric behavior, which would be expected based on the geometry, with maximum FRF Magnitude at MidPlate 3 and MidPlate 4. The FRFs are shown in Figure 5-14.

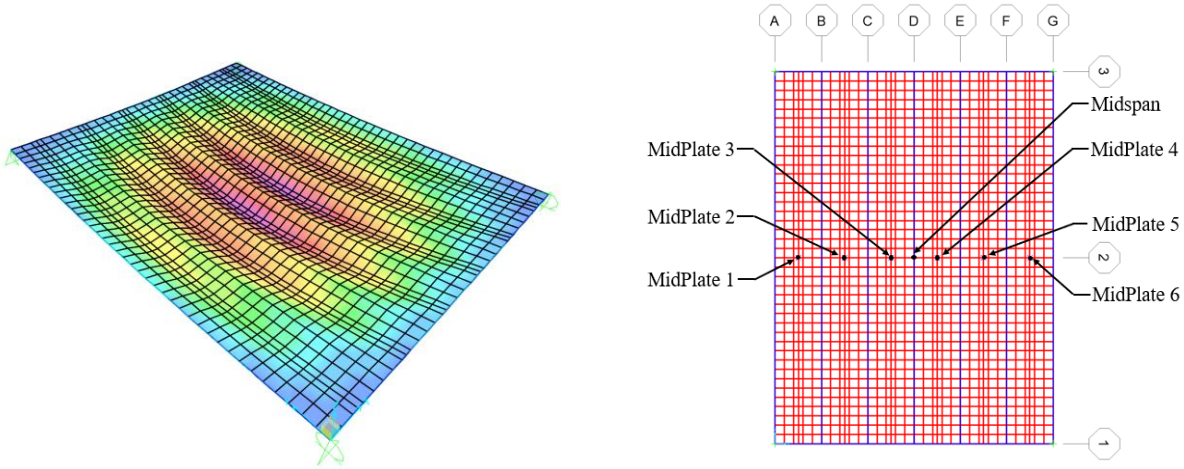

(a) First Mode Shape. f_{n1}=8.71 Hz (b) Analysis Locations

Figure 5-13. Analysis Locations for Low-Frequency Mode Shape

$$\begin{aligned}\alpha &= 0.09e^{-0.075 f_n} \\ &= 0.09e^{-0.075(8.71\ \text{Hz})} \\ &= 0.0468\end{aligned} \qquad \textit{(2-13)}$$

$$\begin{aligned}\rho &= 12.5\beta + 0.625 \text{ if } 0.01 \le \beta < 0.03 \\ &= 12.5(0.025) + 0.625 \\ &= 0.938\end{aligned} \qquad \textit{(2-14(a))}$$

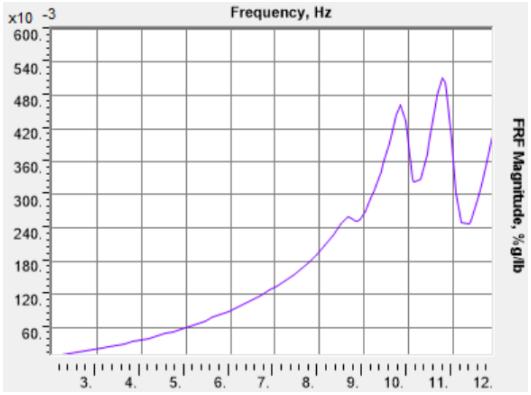

FRF_{Max}=0.259 %g/lb at 8.66 Hz

(a) FRF magnitudes at MidPlate1

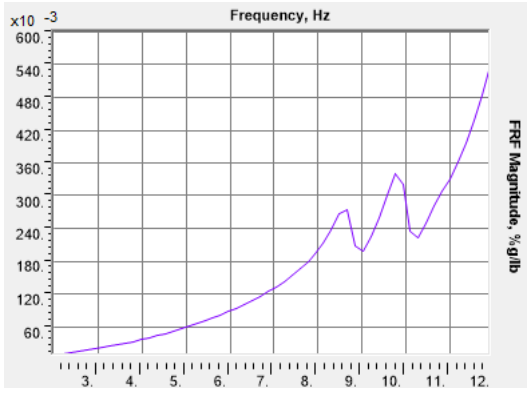

FRF_{Max}=0.274 %g/lb at 8.66 Hz

(b) FRF magnitudes at MidPlate2

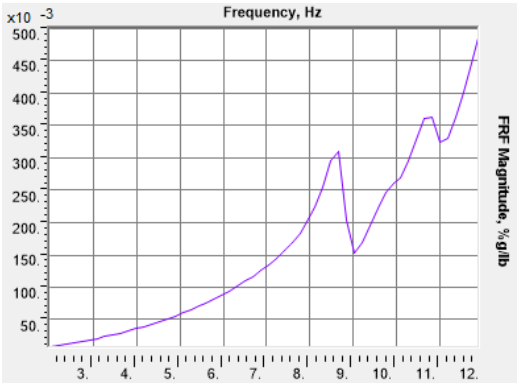

FRF_{Max}=0.31 %g/lb at 8.66 Hz

(c) FRF magnitudes at MidPlate3

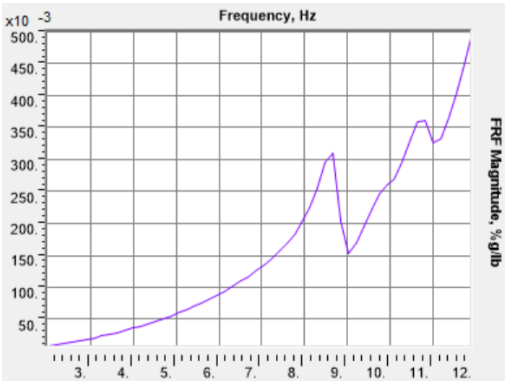

FRF_{Max}=0.31 %g/lb at 8.66 Hz

(d) FRF magnitudes at MidPlate4

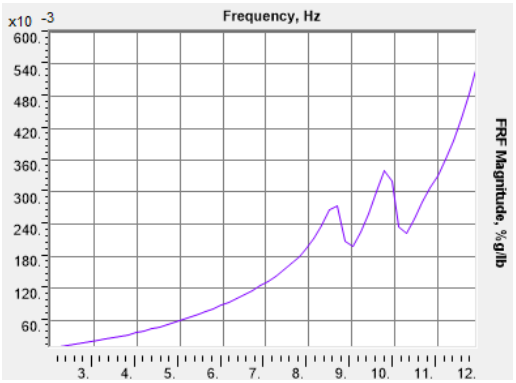

(e) FRF_{Max}=0.274 %g/lb at 8.66 Hz
FRF magnitudes at MidPlate5

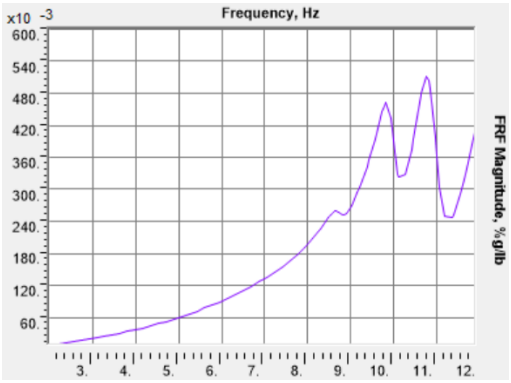

(f) FRF_{Max}=0.259 %g/lb at 8.66 Hz
FRF magnitudes at MidPlate6

Figure 5-14. FRF Magnitudes at critical locations

$$a_p = FRF_{Max}\alpha Q\rho \qquad (2\text{-}12)$$
$$= (0.31\%\ g/\text{lb})\ (0.0468)\ (168\ \text{lb})\ (0.938)$$
$$= 2.29\ \%\ g > 0.5\%\ g$$

Complaints are expected since the predicted peak acceleration for configuration FB-68-3/8 exceeds DG11 (Equation (2-12)). Generally, the bay's midspan is a location of interest. For the configuration of FastFloor, this spot coincides with a beam. Therefore, it is worth analyzing that location to note the difference between the predicted peak accelerations. Following the same procedure as for the other critical locations and based on the FRF shown in Figure 5-15, the peak acceleration at midspan for the first mode is $a_p = 0.702\%\, g$, which, despite exceeding the 0.5% g limit, is significantly closer. It can be concluded that the acceleration "issues" for FastFloor are rather localized. These results are based on the "best guess" assumptions presented in Section 5.1 and represent a preliminary result. In the future, after tests are conducted with RAF, the models will need to be updated accordingly, and acceptability will be re-evaluated.

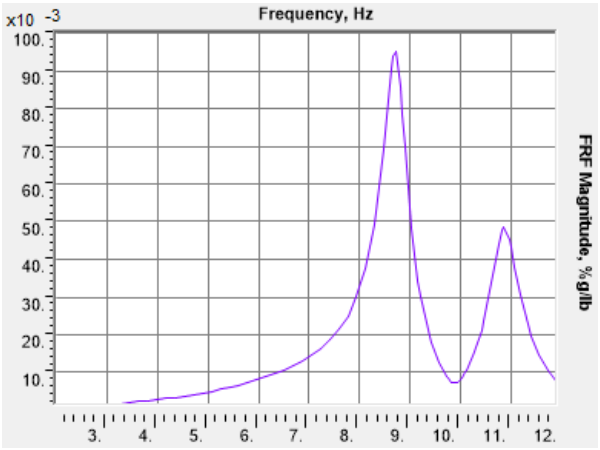

FRF_{Max}= 0.0952 %g/lb at 8.71 Hz

Figure 5-15. FRF Magnitudes at Midspan

High-Frequency Floor Procedure

Based on the procedure discussed in Section 2.3, the first 40 modes were analyzed to cover frequencies up to 20 Hz for Configuration FB-68-3/8. For Joint Midspan 3, previously studied for Low-Frequency floors, the dominant mode was identified as the 13th

corresponding to the higher FRF Magnitude, as seen in Figure 5-16. The natural frequency of the dominant mode is 16.62 Hz, which can be matched by the 8th harmonic (Table 2-1).

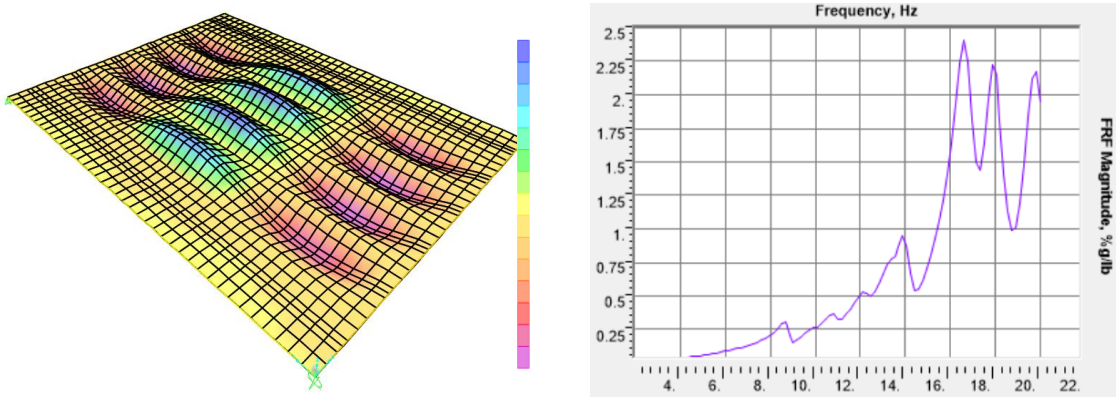

Mode 13, $f_{n,13}$= 16.62 Hz FRF_{Max}= 2.43 at $f_{n,13}$= 16.62 Hz

Figure 5-16. Dominant Mode Shape and FRF Magnitude for Joint Midplate 3

The dominant mode controls the step frequency:

$$f_{step} = \frac{f_{\text{n,dominant}}}{h} = \frac{16.62 \text{ Hz}}{8} = 2.078 \text{ Hz} \qquad (2\text{-}15)$$

The response of each mode is then calculated for all modes up to 20 Hz. For example, for the dominant mode, the effective impulse is calculated from Equation (2-16), and the peak acceleration from Equation (2-17).

$$a_{ESPA} = \sqrt{\frac{2}{N}\sum_{k=1}^{N} a_k^{\,2}} \qquad (2\text{-}16)$$

$$a_{p,22} = 2\pi f_{n,22}\phi_{i,22}\phi_{j22}I_{eff,22} \qquad (2\text{-}17)$$

$$= 2\pi(16.62 \text{ Hz})\left(10.4\sqrt{\text{in./kip-s}^2}\right)^2\left(\frac{0.696 \text{ lb-s}}{1000 \text{ lb/kip}}\right)\left(\frac{100\%g}{386 \text{ in./s}^2}\right)$$

$$= 2.03 \%g$$

The mass-normalized shape values are taken from SAP2000 by selecting the table for joint displacements, that despite being shown in units of length, according to the CSI Analysis Reference Manual (Computers and Structures, Inc., (2017), the mode shapes are normalized and scaled, with respect to the mass matrix.

The acceleration waveform, per Equation (2-19), is evaluated over the footstep period, t=0 to $t=T_{step}$ (Equation (2-18)) in 0.005 s increments. The calculations for the 13th mode are as follows:

$$T_{step} = \frac{1}{f_{step}} = \frac{1}{2.078 \text{ Hz}} = 0.481 \text{ s} \tag{2-18}$$

$$a_{22}(t) = a_{p,22} e^{-2\pi f_{n,22} \beta t} \sin\left(2\pi f_{n,22} t\right) = \left(2.03\%g\right)\left(e^{-2\pi(16.62 \text{ Hz})(0.025)t}\right)\sin\left(2\pi\left(16.62 \text{ Hz}\right)t\right) \tag{2-19}$$

The total response between footsteps is estimated using Equation (2-20) by superimposing the acceleration waveforms for all modes.

$$a(t) = \sum_{k=1}^{\text{Nmodes}} a_k(t) = \sum_{k=1}^{40} a_k(t) \tag{2-20}$$

Lastly, as the peak acceleration from Equation (2-20) is not comparable to the limit based on the sinusoidal accelerations, an equivalent sinusoidal peak acceleration is calculated from Equation (2-21).

$$a_{ESPA} = \sqrt{\frac{2}{N}\sum_{k=1}^{N} {a_k}^2} = 7.8\%\text{g} \tag{2-21}$$

Following the same procedure explained above, peak accelerations were obtained for all full-bay configurations, and results are summarized in Table 5-12 and Table 5-13. For the case of low-frequency floors, only Specimen FB-68-3/8 with and without RAF and FB-94-1/2 with RAF had frequencies below 9 Hz. That is why only these configurations are included in Table 5-12.

Table 5-12. Summary of peak accelerations for Low-Frequency Floors

				At Joint MidPlate 3		At Joint Midspan	
Configuration	**$f_{n,1}$, Hz**	**Dynamic coefficient, α**	**Resonant build-up factor, ρ**	***FRF_{max}, %g/lb***	***a_p (%g)***	***FRF_{max}, %g/lb***	***a_p (%g)***
FB-68-3/8	8.71	0.047	0.938	0.31	2.29	0.095	0.70
FB-68-3/8 RAF	7.79	0.050	1.0	0.21	1.75	0.047	0.40
FB-94-1/2 RAF	8.70	0.047	1.0	0.12	0.93	0.0483	0.38

Table 5-13. Summary of equivalent peak accelerations for High-Frequency Floors

Configuration	**Dominant Mode**	**Number of Modes < 20 Hz**	**$a_{,ESPA}$ (%g)**
FB-68-3/8	13	40	7.80
FB-68-3/8 RAF	15	58	7.16
FB-94-1/2	6	7	0.95
FB-94-1/2 RAF	6	12	0.80

Although all predictions show an exceedance of DG11 0.5%g limit, based on the assumed "best guess" parameters, these results should be considered preliminary. Based on experiments, the parameters that need to be updated include damping ratios and boundary conditions pertaining to the support conditions and connection between the beams and plate, exploring options like rotational springs. Regarding masses, the mass of one person can be included to simulate the conditions during impact hammer tests.

In addition, the models only correspond to one bay since the plate is flexible compared to a concrete-filled steel deck, and therefore, less floor area is expected to get

mobilized by floor vibrations. However, as mentioned earlier (Section 2.3), DG11 recommends a three-by-three grid of bays to analyze an interior bay, leading to more mass contributing and a decrease in the acceleration response.

Table 5-14 summarizes the first mode per specimen and frequencies.

Table 5-14. Summary of First-Mode Natural Frequencies for Full-Bay Specimens

Specimen Code	**FB-68-3/8**	**FB-94-1/2**	**FB-68-3/8 RAF**	**FB-94-1/2 RAF**
Plan dimensions	30 ft x 40 ft	30 ft x 40 ft	30 ft x 40 ft	30 ft x 40 ft
Beam sections	W24x68	W24x94	W24x68	W24x94
Beam spacing (ft) (CL distance)	5.0	5.0	5.0	5.0
Plate thickness (in.)	3/8	1/2	3/8	1/2
SDL (psf)	0.0	0.0	9	9
LL (psf)	8	8	8	8
f_{n1FE} (Hz) (Bending Mode 1)	8.71	9.5	7.79	8.70

5.5. Alternate Module Configuration Based on Predictions

The predictions shown in the previous section conclude that the FastFloor modules considered so far will not satisfy floor vibration criteria. Thus, an alternative was developed by taking the geometry of the heavier module SM-94-1/2 and adding five lines of stiffeners every 5 ft around midspan, as shown in Figure 5-17 and Figure 5-18. The stiffeners chosen are angles L6x4x5/16 with the long leg oriented vertically.

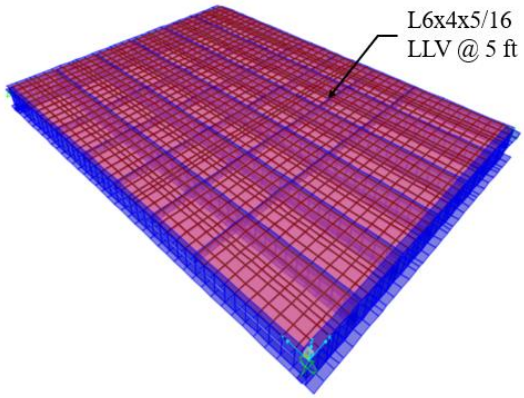

Figure 5-17. Stiffened Configuration for Full-Bay in SAP2000

Based on the same assumed parameters in Table 5-10, the natural frequencies and mode shapes were determined for this new stiffened configuration. The first mode was observed to be higher than 9 Hz (Figure 5-18), so the high-frequency floor procedure was followed to judge acceptability for vibrations. The critical analysis locations were relocated to midspan between the stiffeners where the highest deformations were observed in the updated mode shapes, as shown in Figure 5-18.

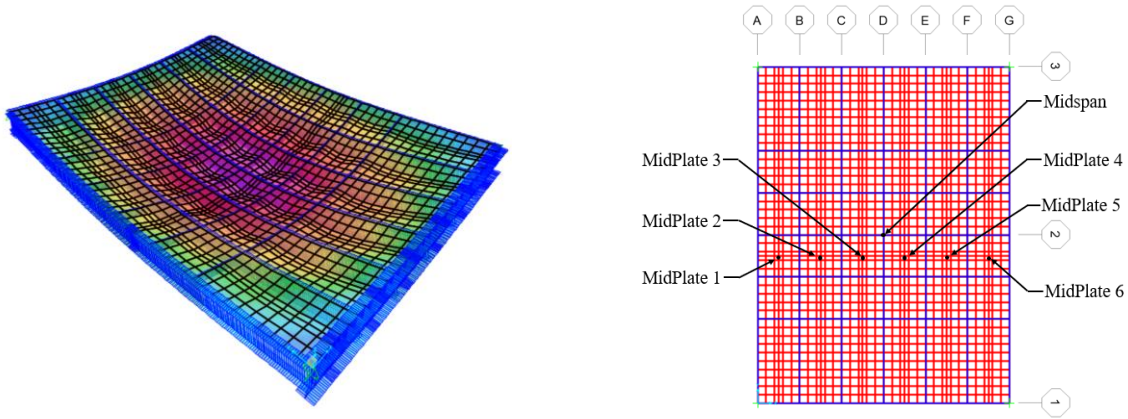

(a) First Mode Shape. f_{n1}=9.66 Hz (b) Analysis Locations

Figure 5-18. Analysis Locations for High-Frequency Mode Shape

The FRF magnitudes were checked for each location, observing the highest acceleration value for Mode 5 at location MidPlate 2, as shown in Figure 5-19.

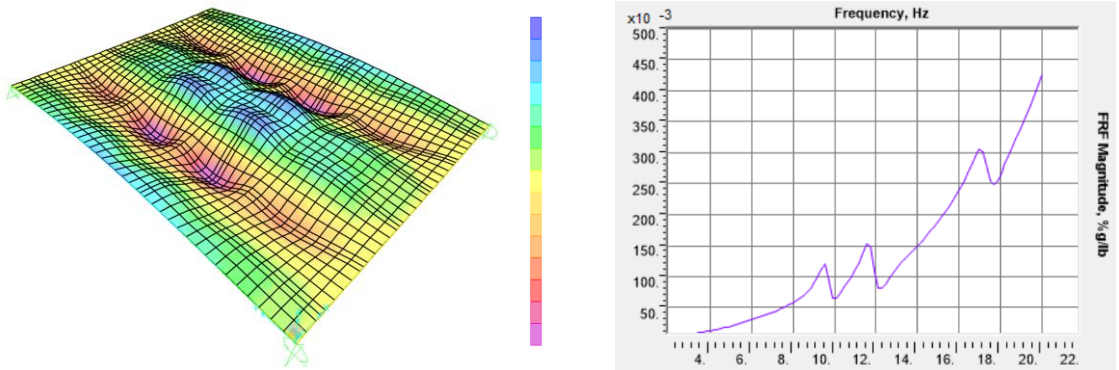

Mode 4, $f_{n,4}$= 17.23 Hz FRF_{Max}= 0.305 at $f_{n,5}$= 17.23 Hz

Figure 5-19. Dominant Mode Shape and FRF Magnitude for Joint Midplate 2

The equivalent sinusoidal peak acceleration, calculated from Equation (2-21), is 0.401%g, less than DG11 tolerance limit of 0.5%g, so this configuration is predicted to work for vibrations.

There need to be new predictions once the models and DG11 calculations are updated to match the experiments. Thus, based on this proposed stiffened configuration, similar options can be further explored by varying parameters such as size, spacing, and location of stiffeners.

5.6. Comparison between full-bay models and analytical predictions for "Best Guess."

The analytical predictions summarized in Table 5-3 are comparable with the FE models performed. Specifically, the "Best Guess" parameters coincide with the ones used for FE modeling the specimens with RAF. Therefore, a comparison between the frequencies and accelerations is discussed in the following paragraphs. Table 5-15 summarizes the frequencies and accelerations.

Table 5-15. Analytical vs. computational predictions for specimens

Parameter		**FB-68-3/8 RAF**	**FB-94-1/2 RAF**
Including plate panel contribution	f_{nPBG} (Hz)	5.77	7.06
Neglecting plate panel contribution	f_{nBG} (Hz)	7.92	8.67
DG11 FE model	f_{nFE} (Hz)	7.79	8.70
Including plate panel contribution	a_{pPBG}/g (%)	2.39	1.16
Neglecting plate panel contribution	a_{pBG}/g (%)	0.96	0.61
DG11 FE model	a_{pFE}/g (%)	1.75	0.93

It can be observed that the frequencies are much closer between the FE models and analytical frequencies when neglecting the plate panel contribution. Regarding the peak accelerations, for both specimens, the FE accelerations lie between the analytical

acceleration, leaning slightly closer to the accelerations when including the plate panel. These results are inconclusive, given that they are based on assumed parameters and follow the DG11 provision for a system to which it is not calibrated. Therefore, comparison with experimental tests plays an important role at this stage.

5.7. Effect of Plate Tension Due to Gravity Loads

The full-bay models were also analyzed to determine the amount of tension in the plate and how it changes the frequencies. This analysis was divided into two parts: first, maintaining the same boundary conditions and parameters shown in Section 5.4.3, several nonlinear load cases were created to apply tension loads as a percentage of the plate's yield strength, F_y=50 ksi, ranging from 0 to 100%. The tension loads were applied as area loads to the shell elements at the edges of the exterior beams, as shown in Figure 5-20.

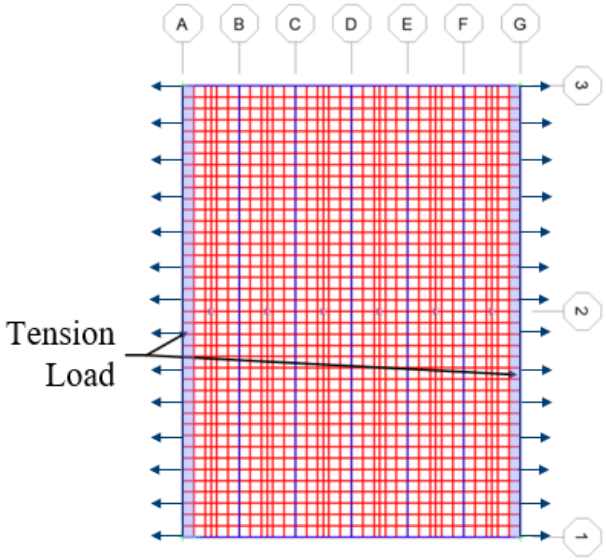

Figure 5-20. Location of assigned tension loads

The creation of individual nonlinear cases that considered P-Delta effects and its corresponding modal cases based on the stiffness at the end of each nonlinear case allowed the model to capture the plate tension effect on the first mode frequencies. The same

behavior was observed for the four full-bay models, where a faster increment in the frequencies is observed until 10% of F_y, as observed in Figure 5-21 and Figure 5-22

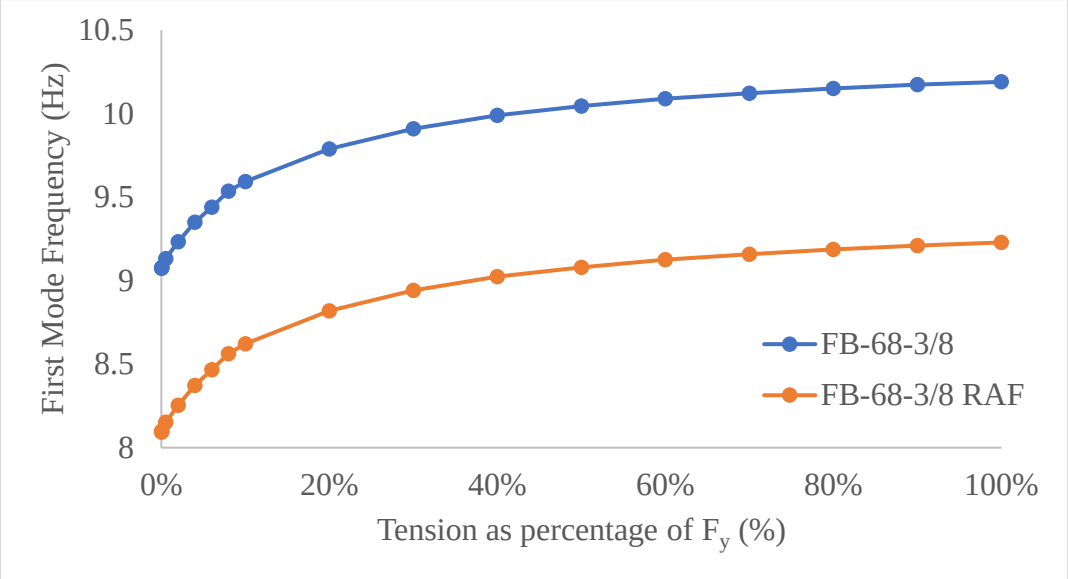

Figure 5-21. Frequency vs. Tension as a percentage of F_y for FB-68-3/8 with and without RAF

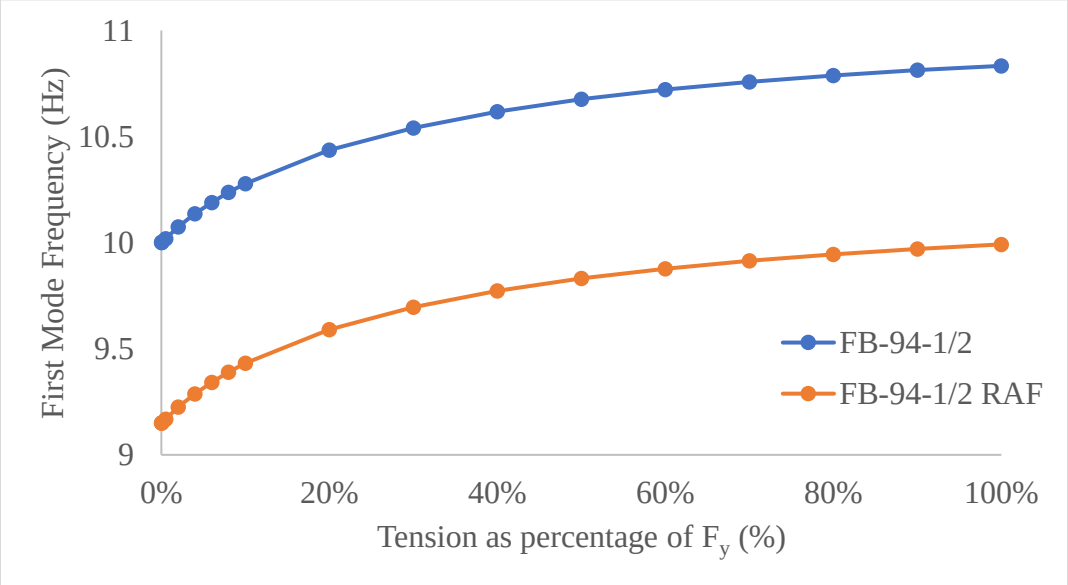

Figure 5-22. Frequency vs. Tension as a percentage of F_y for FB-94-1/2 with and without RAF

The second part of the analysis consisted of determining the expected tension in the plate caused by the actual gravity loads expected for vibration analysis. Translational restraints in the direction perpendicular to the beams were added along the edges of the

plate to obtain the tension from the reactions. Dead and Live loads were changed to nonlinear cases to consider the P-Delta effects.

A resultant reaction was obtained by averaging all the joint reactions and dividing over the width of the shell element times the plate thickness. The predicted tension loads varied between 0.17% and 0.26% of f_y. Thus, it is concluded that the plate's tension load will not significantly affect increasing the natural frequency.

Chapter 6. Vibration Testing Setup

6.1. Test Specimens

The vibration testing specimens were conceived as either single module specimens or full bay specimens, as shown in Figure 6-1. Based on the six specimen configurations shown in Section 4.2, Specimens SM-68-3/8-5 and SM-94-1/2-5, corresponding to the lightest and heaviest sections, were selected for single module tests, with and without raised access floor, to verify and retrofit the assumptions made in the analytical and computational predictions. It was decided that the full bay tests shown in Figure 6-1(b) will be included in a future phase of this research. The rest of this section refers to single-module specimens only.

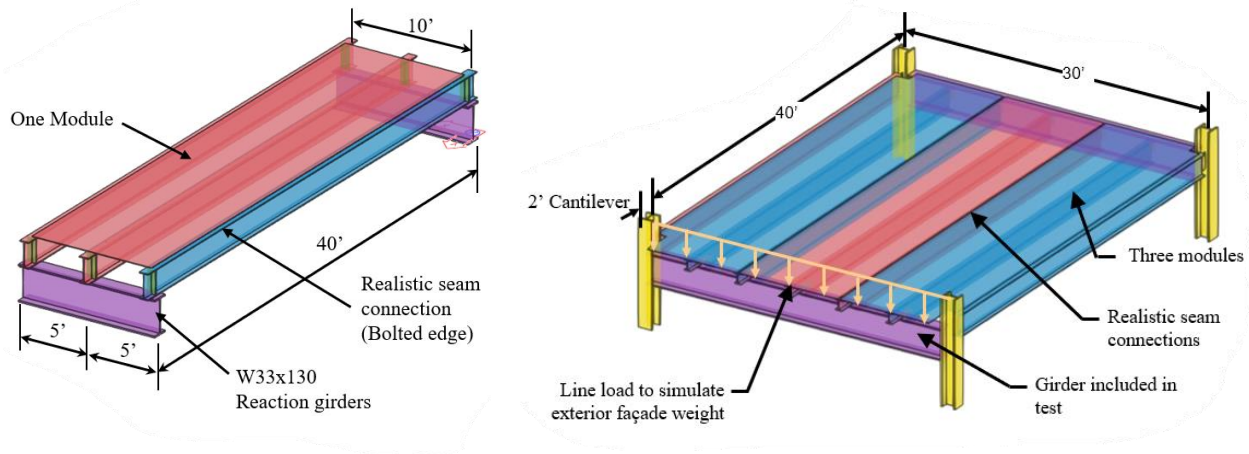

(a) Single module Specimens (b) Full bay Tests

Figure 6-1. Proposed Vibration Testing

The specimens consist of W24 beams with a 10 ft x 40 ft plate. The beams were ASTM A992 Grade 50, and the plates were ASTM A572 Grade 50. In addition to using these specimens to evaluate floor vibrations, it was also desired to use them to investigate the fabrication, erection, and transportation of the modules. For this purpose, the fabrication (Described in Section 4.2) process and transportation from the steel shop to the laboratory were monitored. In addition, the specimens were specified following the

asymmetric configuration described in Section 3.3. As shown in Figure 6-2, one edge beam was sent bolted to represent the beam that is part of an adjacent module using Shuriken® nut holders and bolts. Oversize holes were specified in the plate to increase the tolerance during the assembly.

Regarding the beam-to-plate welds, Figure 6-2(b) and Figure 6-2(c) show the 3/16 in. 3 in. long spaced 12 in. staggered fillet weld detail and locations. Finally, each beam was bolted to the top flange of W33x130 reaction girders using 3/4 in. A325 bolts. Appendix F includes the fabrication drawings.

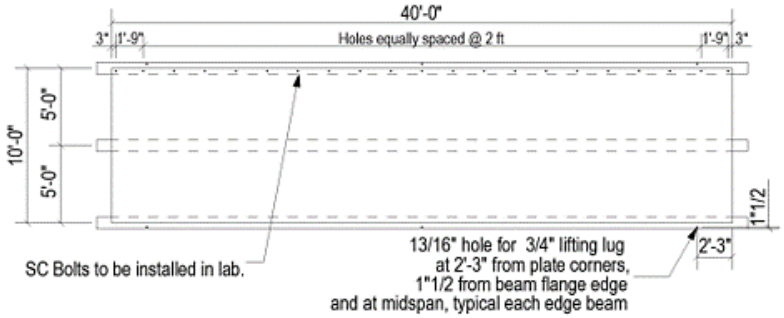

(a) Plan view

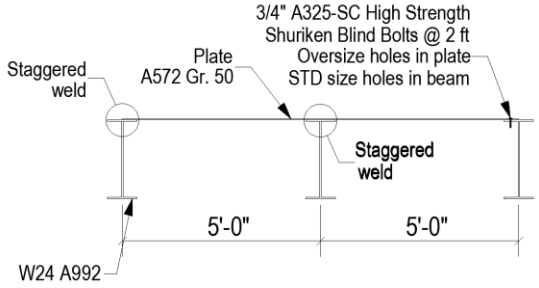

(b) Cross section view

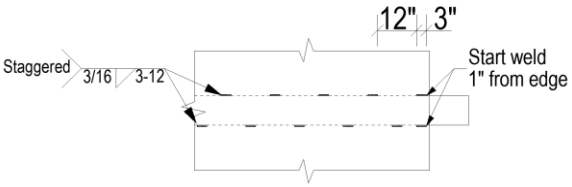

(c) Staggered Weld detail

Figure 6-2. Details of the Specimen

6.2. Fabrication of Single-Module Specimens

On May 22nd and 23rd, the specimens SM-68-3/8 and SM-94-1/2 were fabricated at the Cooper Steel Facilities in Shelbyville, TN.

Fabrication Process

Initially, three hollow sections were placed on top of the existing structure for assembly. Then, the steel plate was picked using four lifting lugs, during which some permanent deformation was observed, as shown in Figure 6-3. Subsequently, the beams were picked up using clamps (Figure 6-4) and then placed on top of the plate to have the modules fabricated upside down.

Figure 6-3. Bare plate deformation

Figure 6-4. Clamps used for moving the beam.

First, the center beam was positioned. The welders confirmed the measurements and clamped the beam to the hollow sections (Figure 6-5). The plate and the beam were tack-welded at the ends to secure their location.

Figure 6-5. Placing of center beam

A similar process was followed for the edge beam, but spacers, shown in Figure 6-6, were necessary to fully support the beam flange.

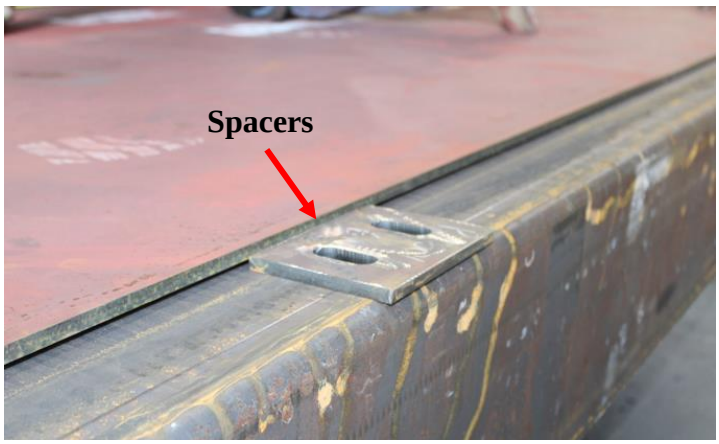

Figure 6-6. Spacers use for unsupported portion of edge beam flange

Once both beams were tack welded at the ends, a gap could be observed between the plate at the beams due to the out-of-flatness of the plate and natural camber of the beams, as observed in Figure 6-7. In addition, the beams had out-of-plane deformation. Both issues were improved by using a hydraulic jack (Figure 6-8).

Figure 6-7. Gap between plate and beams before and after the use of the hydraulic pump

Figure 6-8. Use of hydraulic press to reduce the gap between the plate and beams

The welders proceeded with tack welding along the lengths of the beams, including overhead welding for the edge beam. Subsequently, the fitter continued drawing the location of the staggered welds, as shown in Figure 6-9. All welding was conducted without flipping the module, so overhead welds were used for the edge beam.

Figure 6-9. Staggered Welds

Flipping Process

The most challenging part of the fabrication was flipping the specimen after it was fabricated upside down, as shown in Figure 6-10.

Figure 6-10. The final state of the modules

For flipping the modules, only two lug bolts are used. For this reason, bigger bolts were necessary to resist the module self-weight, and additional holes were drilled on the edge beam flanges. In addition, the asymmetrical modules were hard to handle, so the third beam was bolted, and temporary braces were welded between the beams. The flipping process is shown in Figure 6-11.

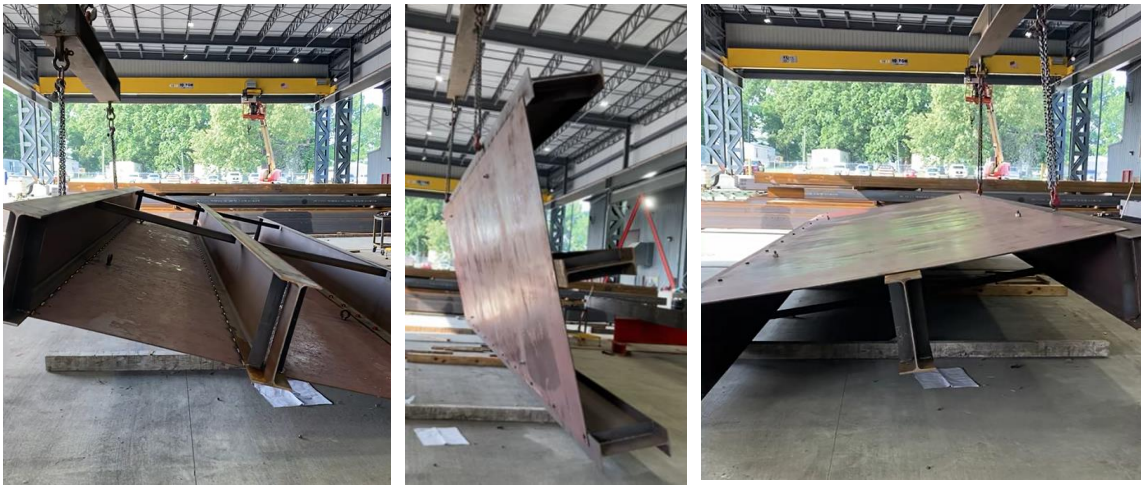

Figure 6-11. Flipping Process

Lastly, using the four lifting lugs, the specimens were stacked on the flatbed, as shown in Figure 6-12, Figure 6-13, and Figure 6-14. In the latter, it is observed that the modules are wider than the truck.

Figure 6-12. Lifting of whole module for placing on truck

Figure 6-13. Modules stacked on the flatbed

Figure 6-14. End view of specimens on flatbed

6.3. Equipment for Referenced Impulse Hammer Tests

The impact hammer used is PCB Piezotronics 086D50, shown in Figure 6-15, with a self-weight of 12.1 lb. It is equipped with a force sensor with a measurement range ± 5000 lb., which allows recording the input loads by connecting the hammer to an analyzer.

Figure 6-15. Impact Hammer Model 086D50

6.4. Instrumentation

Ten PCB 393B12 seismic accelerometers (Figure 6-16) will be used to measure the acceleration response. The accelerometers have a Sensitivity of 10 V/g and a frequency range of 0.15 Hz to 1000 Hz. Each one weighs 7.4 oz and is 2.18 in height.

A DT9857 Dynamic Signal Analyzer, Figure 6-17, by the company Data Translation®, is equipped with 16 IEPE inputs and two stimulus waveform output channels. Through the software QuickDAQ, the analyzer can generate output excitations, perform single-channel FFT operations, record, and export data for further analysis, among other functionalities.

Figure 6-16. Seismic Accelerometers PCB 393B12

Figure 6-17. Dynamic Signal Analyzer DT9857

6.5. Testing procedure

Impact hammer was the method used for Experimental Modal Analysis (EMA). The test was used to determine the natural frequencies and mode shapes, for the Specimens SM-68-3/8 and SM-94-1/2, without RAF.

The same procedure was followed for both specimens. The hammer struck the specimens at a specific location, defined as the reference DOF. The accelerometers would be relocated, as shown in Figure 6-19, maintaining the same location excitation for the impact hammer throughout the set of measurements. This is called a fixed-input, roving

response setup. The hatched circles represent locations where measurements were not included in the final analysis, given that the DT Analyzer Channel wasn't working properly.

After each hit, the free vibration response of the structure is measured. The window chosen corresponded to 10 seconds, meaning the time between excitations.

In all tests, both the excitations and the responses were recorded. Figure 6-18 shows a schematic of the test setup.

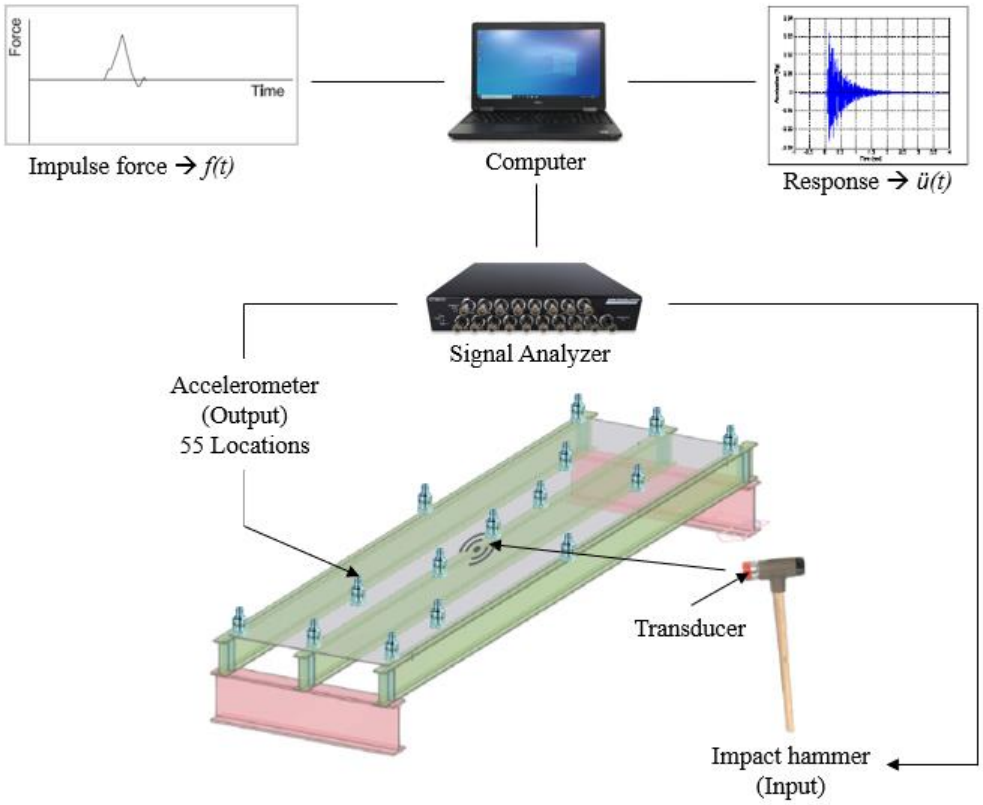

Figure 6-18. Schematic of Impulse Hammer tests

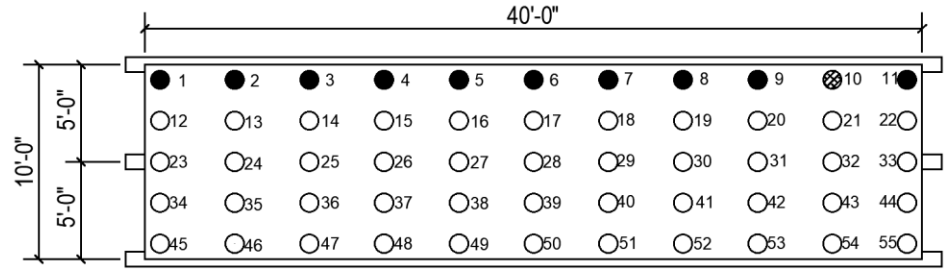

(a) Location 1 of accelerometers

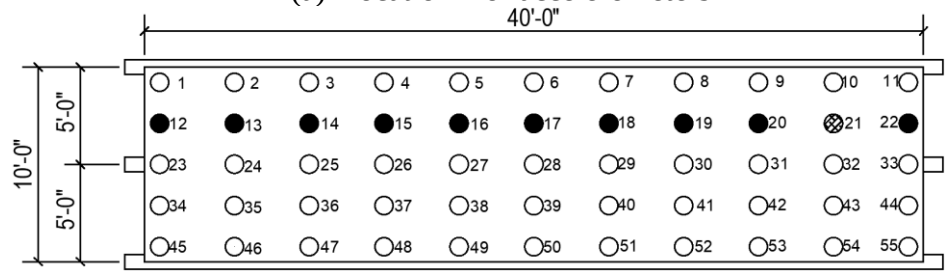

(b) Location 2 of accelerometers

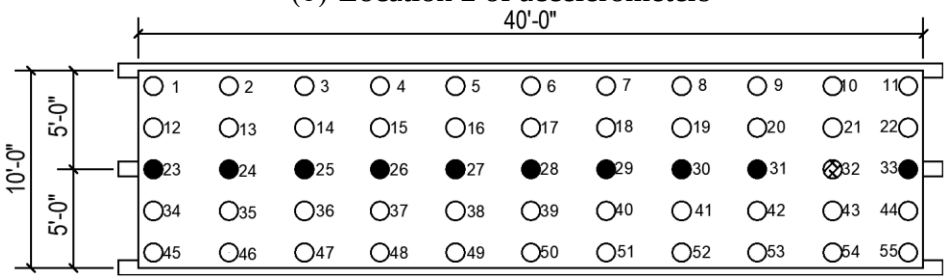

(c) Location 3 of accelerometers

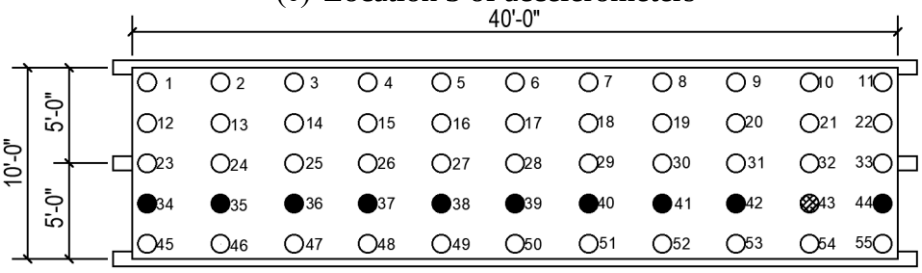

(d) Location 4 of accelerometers

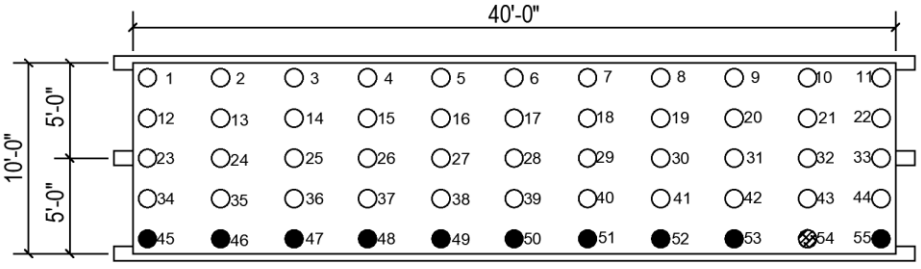

(e) Location 5 of accelerometers

Figure 6-19. Location of accelerometers

It’s important to clarify that the acceleration values obtained will not represent enough information to determine if the specimen is satisfying the vibration requirements, given that the modules to be tested are not a significant representation of an entire story of a real building as they will not include all the built out corresponding to MEP, ceilings, finishes and live loads. As previously mentioned, the parameters that will be used to compare to FE models are the natural frequencies, damping with and without RAF, and mode shapes. Updated FE models can be used, in the future, to evaluate acceptability.

Chapter 7. Experimental Results

The tests were conducted at the West Virginia University Structural Engineering Laboratory, following the procedure explained in Chapter 6. Figure 7-1 shows the accelerometers arranged at midspan, covering locations 23 through 33, per Figure 6-19. The person was on top of the plate to apply the strikes during the measurements.

Figure 7-1. Accelerometers at midspan

The sampling rate was 2000 Hz, time resolution was 0.005 seconds, and the number of samples was set to 1000. The window, time between strikes, was 10 seconds. Three averages were taken per set of measurements.

After each test, the quality of the measurements was judged based on the plot of every FRF and the associated Coherence. For instance, in Figure 7-2, the FRF shows clear peaks that indicate resonant frequencies. The coherence showed good behavior in frequencies greater than 10 Hz, as a value of one indicates free-noise measurements. All measurements that showed bad coherences were discarded, and the tests were repeated.

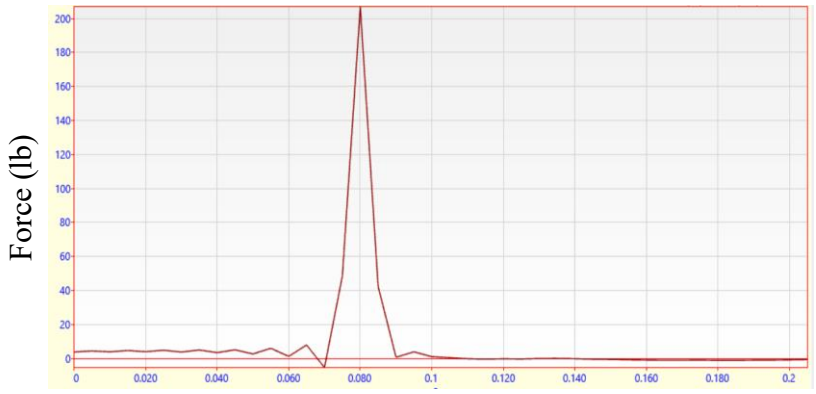

(a) Impact load in time domain

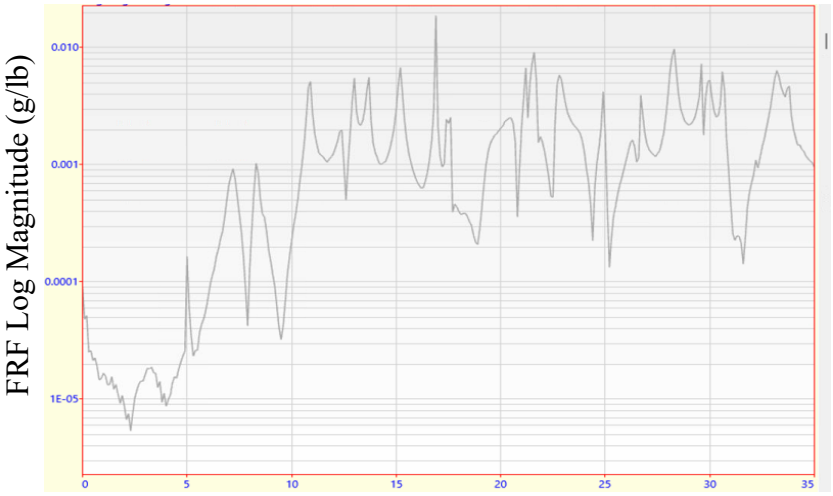

(b) FRF of one accelerometer location

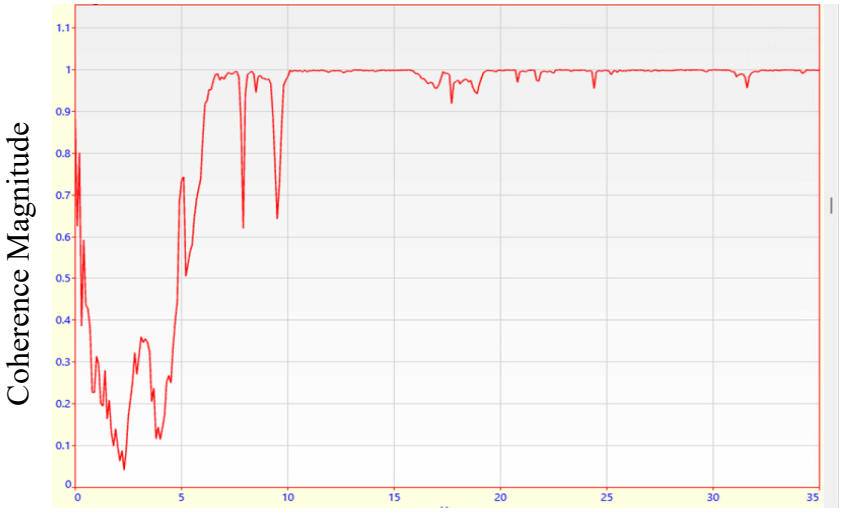

(c) Coherence associated with FRF

Figure 7-2. Example of recorded data during tests

Once all 55 locations were measured, the associated accelerance FRF were overlaid to observe the peaks. The imaginary part of the FRF contains the coordinates of the mode shapes at the location of each accelerometer. Figure 7-3 shows the FRFs, for all 55 locations, in Magnitude and Imaginary form. It can be observed from Figure 7-3(b) that the hammer test excited several modes, represented by the peaks at the natural frequencies of the system.

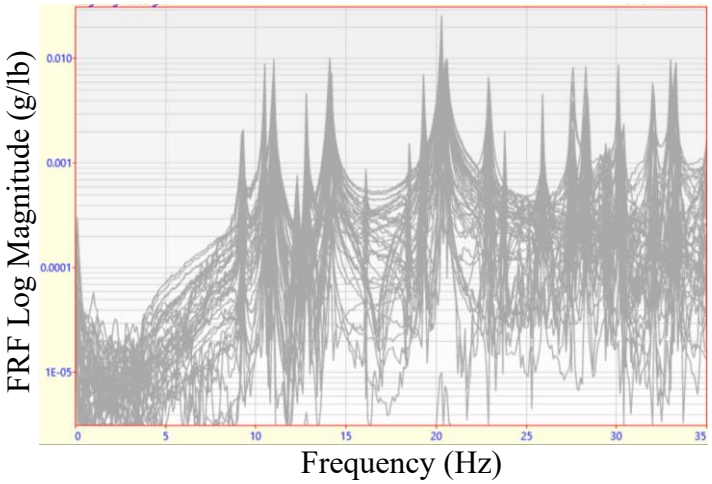

(a) FRF Magnitude for all locations of Specimen SM-68-3/8

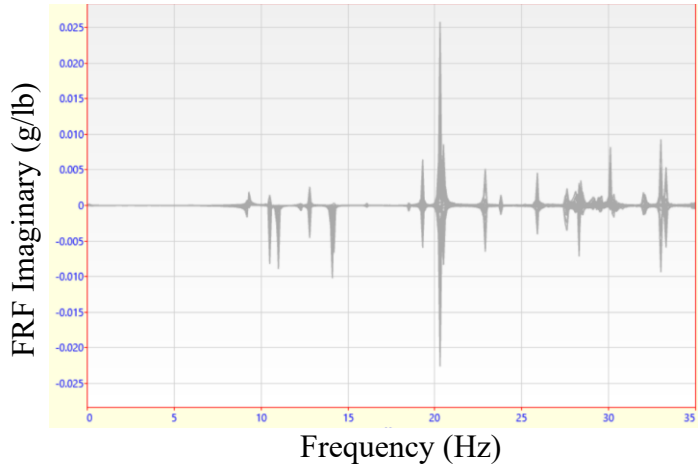

(b) FRF Imaginary portion for all locations of Specimen SM-68-3/8

Figure 7-3. FRF Magnitude and Imaginary part for Mode Shape Determination

The first five mode shapes and their associated frequencies were extracted for both specimens using MEscope (Vibrant Technology, Inc., 2022). To visualize the mode shapes,

a structure was created with 55 nodes, to which the FRFs were assigned. For the locations without measurements, interpolation was used.

For both specimens, regardless of the excitation location, the frequencies for each mode were the same; this is because, in FRF, the response is normalized with respect to the magnitude of the impulse, allowing the response comparison due to different excitations (Sanchez, 2008).

Comparison Between Experimental and FE Mode Shapes

The experimental mode shapes and frequencies are compared to the single-module models. In general, likely mode shapes were observed in switched order and frequencies, as observed in Figure 7-4 and Figure 7-5.

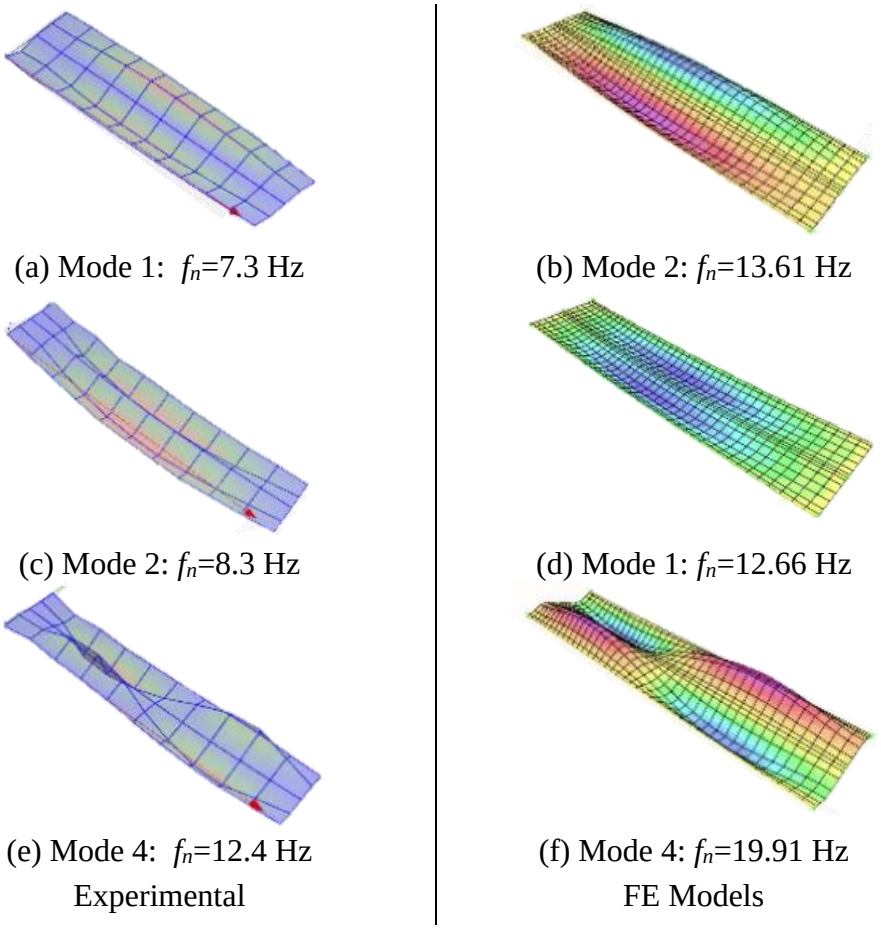

(a) Mode 1: f_n=7.3 Hz (b) Mode 2: f_n=13.61 Hz

(c) Mode 2: f_n=8.3 Hz (d) Mode 1: f_n=12.66 Hz

(e) Mode 4: f_n=12.4 Hz (f) Mode 4: f_n=19.91 Hz

Experimental FE Models

Figure 7-4. Comparison of selected likely mode shapes of Specimen SM-68-3/8

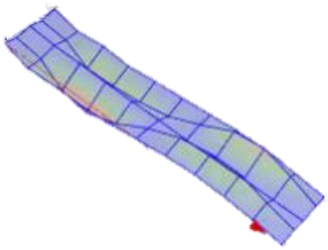

Mode 5: f_n=15.1 Hz

Experimental

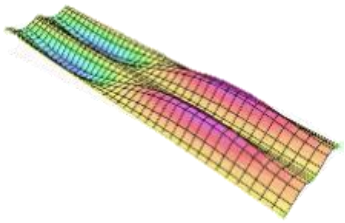

Mode 6: f_n=20.85 Hz

FE Models

Figure 7-4. Comparison of selected likely mode shapes of Specimen SM-68-3/8

In the case of Specimen SM-94-1/2, the mode shapes reflected more asymmetry in the plate response, possibly due to the different boundary conditions along the edge beams (Bolted on one edge and welded on the other).

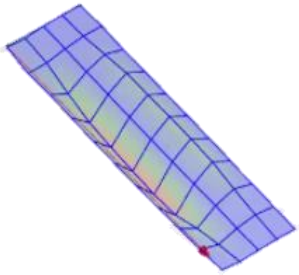

Mode 1: f_n=9.2 Hz

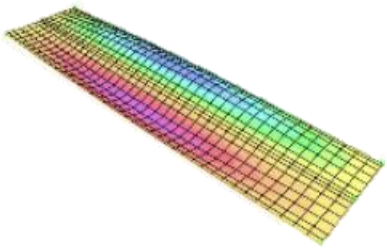

Mode 2: f_n=16.15 Hz

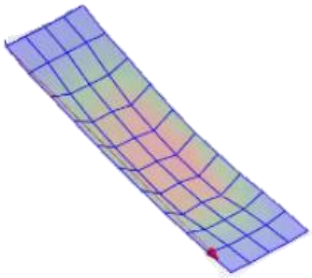

Mode 3: f_n=11 Hz

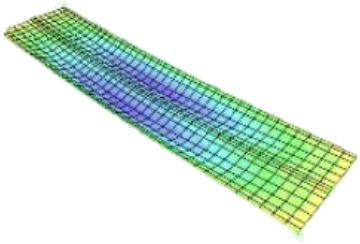

Mode 1: f_n=14.12 Hz

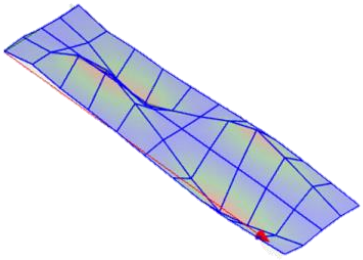

Mode 7: f_n=16.1 Hz

Experimental

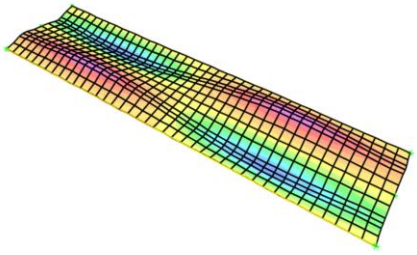

Mode 6: f_n=27.25 Hz

FE Models

Figure 7.5. Comparison of selected likely mode shapes of Specimen SM-94-1/2

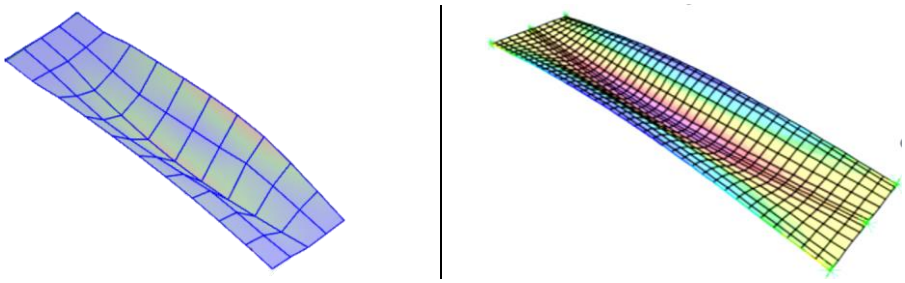

Mode 10: f_n=20.3 Hz | Mode 3: f_n=19.03 Hz

Experimental | FE Models

Figure 7-5. Comparison of selected likely mode shapes of Specimen SM-94-1/2

To complement the visual comparison discussed above, the Modal Assurance Criterion (MAC) values were estimated for the modes shown in Figure 7-4 and Figure 7-5.

The Modal Assurance Criterion (MAC) is a measure used to assess quantitatively the similarity between two mode shapes. A value of 1 indicates perfect similarity, while a value of 0 indicates no similarity at all. Typically, the MAC is used to compare mode shapes from experimental modal analysis and FE models, aiding in model validation and refinement processes (Pastor et al., 2012).

The calculation of the MAC values consists of the dot product of the two mode shapes at discrete points and then normalizing the result based on the magnitudes of the individual mode shapes (Barrett, 2006). The equation used is as follows :

$$\mathrm{MAC}(i,j) = \frac{|\phi_j^T \phi_i|^2}{\left(\phi_j^T \phi_j\right)\left(\phi_i^T \phi_i\right)} \qquad (7\text{-}1)$$

Where

ϕ_i and ϕ_j = Mode shape vectors being compared.

A MATLAB code was developed to perform the calculations in Equation (7-1). To obtain the FE data, the mass-normalized shape values were exported from SAP2000,

matching the number of DOF and location in the experimental setup, neglecting the values corresponding to the nodes where no measurements were taken (Refer to Figure 6-19).

On the other hand, the experimental shape values correspond to the real part. The imaginary part of the mode shape gives information about the phase, and it is not considered in the MAC calculation. Curve fitting was done through the Complex Mode Indicator Function (CMIF) in MEscope to obtain the mode shapes of interest. This function identifies the frequency and mode shapes associated with a peak in the FRFs, by calculating Singular Value Decomposition (SVD) on each set of FRFs (Barrett, 2006).

The results are presented in Figure 7-6 and Table 7-1 for Specimen SM-68-3/8 and Figure 7-7 and Table 7-2 for Specimen SM-94-1/2 as 3D plots and the associated matrix.

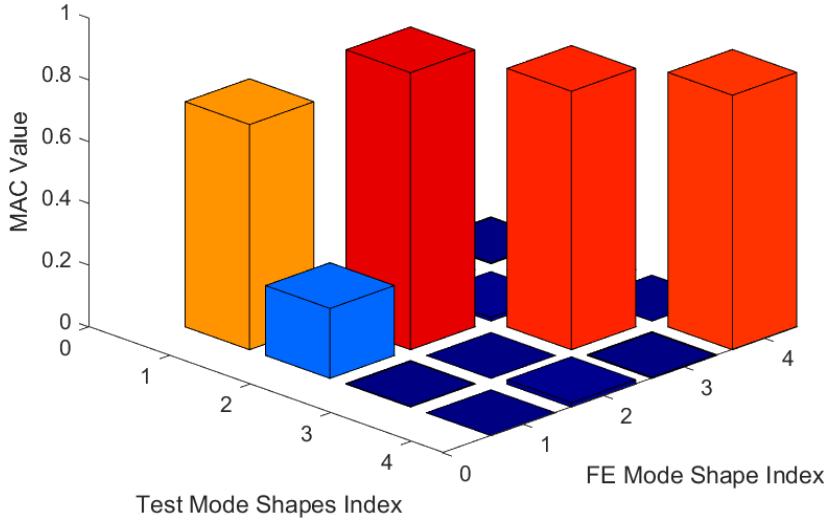

Figure 7-6. CrossMAC 3D plot for Specimen SM-68-3/8

Table 7-1. CrossMAC Matrix for Specimen SM-68-3/8

	Test Shapes	S1	S2	S3	S4
FE Shapes	**Frequency (Hz)**	7.3	8.3	12.4	15.1
S1	13.6	0.729	0.226	0.002	0.000
S2	12.6	0.000	0.897	0.000	0.014
S3	19.9	0.042	0.012	0.837	0.003
S4	20.8	0.004	0.000	0.000	0.824

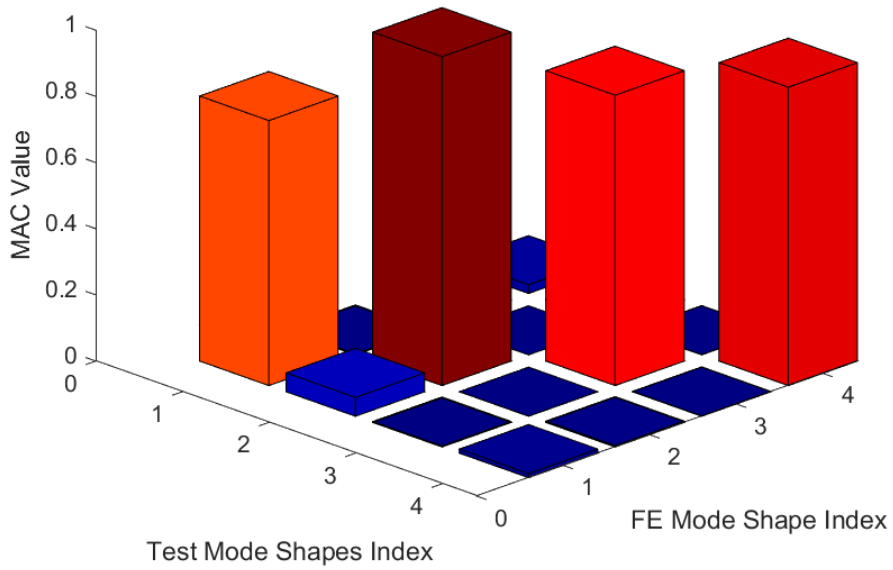

Figure 7-7. CrossMAC 3D plot for Specimen SM-94-1/2

Table 7-2. CrossMAC Matrix for Specimen SM-94-1/2

	Test Shapes	S1	S2	S3	S4
FE Shapes	**Frequency (Hz)**	16.1	14.1	27.6	19
S1	9.2	0.801	0.057	0.003	0.012
S2	11	0.003	0.994	0.000	0.004
S3	16.1	0.006	0.000	0.878	0.001
S4	20.3	0.027	0.001	0.001	0.902

The CrossMAC values confirm the correlation between the selected mode shapes from the experimental and computational models, which could be visually evidenced. For the case of Specimen SM-68-3/8, the diagonal terms lay between 0.8 and 0.9, indicating a moderate correlation between the mode shapes, with possible differences or deviations. In addition, the off-diagonal terms had small values, which is a desirable outcome, suggesting that each mode shape captured a distinct and specific vibration mode of the system. Regarding Specimen SM-94-1/2, a similar behavior was observed for the selected mode shapes.

It's important to mention that other experimental modes were not observed in the FE models, and some had asymmetric deformations with respect to the beam centerline. Therefore, only a few likely mode shapes were chosen for comparison.

Additionally, given that the MAC only considers modal shapes, comparison is possible in this case, despite significant frequency differences. A separate frequency comparison has to be done to determine the correlation between modes and, thus, will have to be reevaluated after the FE models are refined.

Parameters To Be Revised to Improve Computational Predictions

As discussed below, significant differences exist between the tests and FE models. For both specimens, the measured frequencies were smaller than the computational predictions. This means the specimens can have more mass or less stiffness than the assumed parameters. The mass isn't likely the issue as it corresponds to self-weight. Conversely, the stiffness is related to the boundary conditions, probably explaining the observed differences. A list of recommendations of what can be changed in the models to better match the experiment is provided below:

- Support conditions and connection between the beams and plate:

For single-module models, the assumed support conditions consisted of pins and a rotational restrain in the direction of the beams. Also, the framing members were modeled with fixed ends. Based on the results, it's likely that a rotational spring/partial fixity better describes the actual boundary condition at the supports.

- Insertion point of framing members

The insertion point is related to the position of an object with reference to the line drawn to represent that object in the model. Although the stiffness of the sections remains the

same regardless of the specified insertion point, the boundary conditions change (Computers and Structures, Inc.,n.d.), contributing to the differences observed in the specimen's stiffness. For instance, the specified insertion point prevents the top flange fibers from shortening and introduces a longitudinal tension force. This is especially critical for the single-module specimens since all supports are fully pinned, unlike full-bay models, where the insertion point should not affect since the supports are a combination of rollers and pins.

- Shear areas of framing members

In all models, the shear areas of the framing members were neglected to follow DG11 procedures. This assumption was observed to result in higher frequencies, as discussed in Section 2.2 and Section 5.4.

- Effective width of steel for plate

As explained in Section 5.1, the buckling of the plate may reduce the contribution of the steel plate to the moment of inertia of the beam panel or plate panel. The actual effective width of the plate is to be verified through experimental testing.

- Additional mass corresponding to the person performing the strikes with the impact hammer, although this is not expected to have a significant influence on the results.

Chapter 8. Conclusions and Recommendations for Future Research

8.1. Conclusions

In this thesis, FastFloor, a new modular all-steel system, was developed for commercial applications. The system is conceptualized as individual modules with a simple configuration to preserve fast fabrication times. Each module consists of wide flange beams and a bare plate on top. The key benefits include increasing the speed of construction by eliminating concrete pouring and curing times, flexibility of use, and quality of construction. FastFloor will also allow lighter structures, reducing waste, delays, and carbon footprint.

One of the main challenges at the early stages has been finding a configuration that satisfies floor vibrations while also addressing issues related to fabrication, transportation, and erection. Seven experts in fabrication and erection were asked to identify challenges and recommendations based on an initial module configuration by conducting individual interviews. Their feedback played an essential role in the final form of the modules, as it provided insight into crucial aspects such as plate handling, location of seam connections, fabrication sequence, and ways to stack and transport the modules on standard flatbeds, among others.

DG11 criteria were used to perform the analytical and computational vibration assessment as the starting point to determine the specimens' configuration. In addition to the assumptions made on how to adapt DG11 to an all-steel system, to which currently there are no provisions, three scenarios (worst case, best case, and best guess) were established by selecting ranges for the variables based on optimistic predictions, DG11 guidelines, and the expected service conditions, respectively.

Regarding the analytical predictions, it was observed that, depending on the scenario, the specimens satisfied or not DG11 limit of 0.5%g for accelerations; for instance, the peak accelerations ranged from 0.42%g to 1.37%g for SM-94-1/2, and 0.67% to 3.06%g for SM-68-3/8, for the best case and worst case, respectively.

On the other hand, the computational assessment per DG11 was done by developing eight FE Models. Four single-module models representing the conditions in the experimental setup, with and without RAF, to compare mode shapes and natural frequencies; and four full-bay models, with and without RAF, to replicate the actual conditions in a real building and judge the acceptability of the system under DG11 predictions.

Although all the FE predictions showed an exceedance of DG11 0.5%g limit, based on the "best guess" parameters, these results should be considered preliminary. It was concluded that experimental testing was necessary to determine the appropriate assumptions.

Impact hammer was the method used for Experimental Modal Analysis (EMA). The test was used to determine the natural frequencies and mode shapes, for the Specimens SM-68-3/8 and SM-94-1/2, without RAF. A total of 55 locations were measured through a fixed-input, roving response setup.

The results showed that the first mode corresponded to local deformations on the plate, as opposed to the predictions where a bending mode was expected to be the fundamental mode. In general, likely mode shapes were found in a different order and with different associated frequencies. Regarding the natural frequencies, the experimental results showed that the specimens have lower frequencies than those of the FE Models,

meaning that the specimens are less stiff than the assumptions. These results are one step forward in evaluating floor vibration acceptability and refining the Fastfloor module to satisfy floor vibration criteria.

8.2. Recommendations for Future Research

The experimental results from impact hammer tests can be refined by making some changes in the setup: 1) The measurement locations and the time record length can be increased so that the response dies out. These changes would improve the data quality and consistency of the modal tests; 2) More averages should be done per test to reduce the measurement noise. In the presented thesis, three averages were done per test. This number could be increased to 5 to 10 times for future measurements.

Additional types of excitations can be explored to verify the modal parameters, such as shaker with burst chirp signal and constant amplitude sinusoidal signal and reference heel-drop on force plate.

A second phase of this research includes the evaluation of the specimens with RAF, as shown in Figure 8-1. A similar test setup to that proposed in Chapter 6 is recommended, with a variation. The accelerometers should be located simultaneously on top of the plate and the RAF, covering all 55 locations, to capture both behaviors.

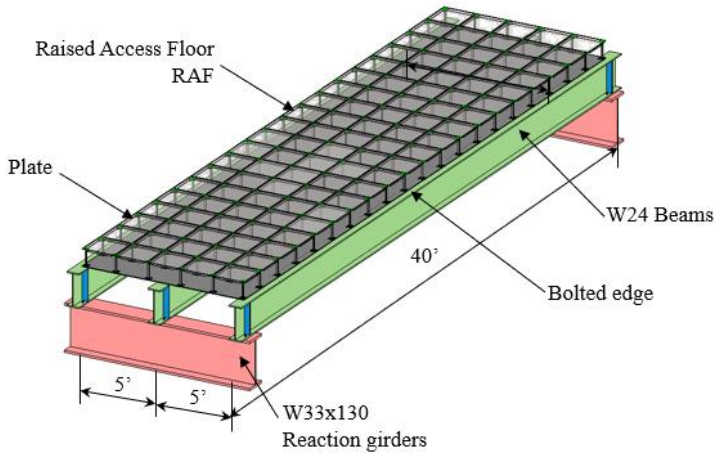

Figure 8-1. Specimens with RAF installed

After performing the totality of the experimental tests, the analytical and computational predictions can be updated to better match the test results. Thus, there will be enough information to determine whether the modular floor system will satisfy the floor vibration criteria. Additionally, updated alternatives based on the initial configuration (e.g., stiffened modules) can be further explored.

Regarding the models, there are a few options that can improve the computational results as compared to the experimental tests. The parameters to be updated include:

1) Changing the support conditions and connection between the beams and plate, exploring options like rotational springs and partial fixities, 2) Evaluating the effect of the insertion point of framing members, 3) Adding additional mass such as that of the person performing the strikes with the impact hammer.

References

Ahn, S. J., Han, S., Altaf, M. S., & Al-Hussein, M. (2022). Integrating off-site and on-site panelized construction schedules using fleet dispatching. *Automation in Construction*, *137*, 104201. https://doi.org/10.1016/j.autcon.2022.104201

Alvis, S. R. (2001). *An Experimental and Analytical Investigation of Floor Vibrations* [PhD. Dissertation]. Virginia Polytechnic Institute and State University.

Arunkumar, M. P., Jagadeesh, M., Pitchaimani, J., Gangadharan, K. V., & Babu, M. C. L. (2016). Sound radiation and transmission loss characteristics of a honeycomb sandwich panel with composite facings: Effect of inherent material damping. *Journal of Sound and Vibration*, *383*, 221–232. https://doi.org/10.1016/j.jsv.2016.07.028

Avci, O. (2016). Amplitude-Dependent Damping in Vibration Serviceability: Case of a Laboratory Footbridge. *Journal of Architectural Engineering*, *22*(3), 04016005. https://doi.org/10.1061/(ASCE)AE.1943-5568.0000211

Barrett, A. R. (2006). *Dynamic Testing of In-Situ Composite Floors and evaluation of Vibration Serviceability Using the Finite Element Method* [PhD. Dissertation]. Virginia Polytechnic Institute and State University.

Catbas, F. N. (Ed.). (2014). *Dynamics of Civil Structures, Volume 4: Proceedings of the 32nd IMAC, A Conference and Exposition on Structural Dynamics, 2014*. Springer International Publishing. https://doi.org/10.1007/978-3-319-04546-7

Chen, Z., Liu, J., Yu, Y., Zhou, C., & Yan, R. (2017). Experimental study of an innovative modular steel building connection. *Journal of Constructional Steel Research*, *139*, 69–82. https://doi.org/10.1016/j.jcsr.2017.09.008

Clark Construction (2022). FastFloor Modules vs. Typical Construction . Personal Communication

Computers and Structures, Inc. (n.d.). Hysteretic damping form. Retrieved May 29, 2023, from https://www.csiamerica.com/products/sap2000/analysis-reference/manuals/sap2000-v22-0-0-analysis-reference-manual/chapter-4-nonlinear-static-pushover-analysis/hysteretic-damping-form

Computers and Structures, Inc. (n.d.). Damping FAQ - Technical Knowledge Base. Retrieved May 29, 2023, from https://www.csiamerica.com/support/technical-faq/damping-faq

Computers and Structures, Inc. (n.d.). Insertion point - Technical Knowledge Base. Retrieved June 16, 2024, from https://wiki.csiamerica.com/display/kb/Insertion+point

Computers and Structures, Inc. (2017). CSI Analysis Reference Manual (ISO# GEN062708M1 Rev.18). Computers & Structures, Inc.

Cousins, T. E., Murray, T. M., & Harris, D. K. (2009). *Use of a Sandwich Plate System in a Virginia Bridge*.

Davis, B., Liu, D., & Murray, T. M. (2014). Simplified Experimental Evaluation of Floors Subject to Walking-Induced Vibration. *Journal of Performance of Constructed Facilities*, *28*(5), 04014023. https://doi.org/10.1061/(ASCE)CF.1943-5509.0000471

Han, S., & Yu, W.-R. (2021). Effect of interfacial properties on the damping performance of steel–polymer sandwich cantilever beam composites. *Journal of Vibration and Control*, 107754632110482. https://doi.org/10.1177/10775463211048269

Islam, M. S., Chui, Y. H., & Altaf, M. S. (2022). Design and Experimental Analysis of Connections for a Panelized Wood Frame Roof System. *Buildings*, *12*(6), 847. https://doi.org/10.3390/buildings12060847

John, K., Rahman, S., Kafle, B., Weiss, M., Hansen, K., Elchalakani, M., Udawatta, N., Hosseini, M. R., & Al-Ameri, R. (2022). Structural Performance Assessment of Innovative Hollow Cellular Panels for Modular Flooring System. *Buildings*, *12*(1), 57. https://doi.org/10.3390/buildings12010057

Khan, K., & Yan, J.-B. (2020). Finite Element Analysis on Seismic Behaviour of Novel Joint in Prefabricated Modular Steel Building. *International Journal of Steel Structures*, *20*(3), 752–765. https://doi.org/10.1007/s13296-020-00320-w

Lee, J. H., Park, M. J., & Yoon, S. W. (2020). Floor Vibration Experiment and Serviceability Test of iFLASH System. *Materials*, *13*(24), 5760. https://doi.org/10.3390/ma13245760

MacLachlan, D., Robertson, B., Boadi-Danquah, E., & Fadden, M. (2019). Parametric Analysis of Vibrations in a Lightweight Two-Way Steel Floor System. *Journal of Structural Engineering*, *145*(11), 04019134. https://doi.org/10.1061/(ASCE)ST.1943-541X.0002417

MKA (2016). Modular Office Plan . Personal Communication

Mohd Azaman, N. A., Abd Ghafar, N. H., Azhar, A. F., Fauzi, A. A., Ismail, H. A., Syed Idrus, S. S., Mokhjar, S. S., & Abd Hamid, F. F. (2018). Investigation of Concrete

Floor Vibration Using Heel-Drop Test. *Journal of Physics: Conference Series, 995*, 012027. https://doi.org/10.1088/1742-6596/995/1/012027

Murray, T. M., Allen, D. E., Ungar, E. E., & Davis, B. D. (2016). Vibrations of Steel-Framed Structural Systems Due to Human Activity Design Guide Series 11, Second Edition. *American Institute of Steel Construction*.

Odeh, D. J., & Kuehnel, P. (2019, August). *The Hybrid CLT-Steel Residence Hall*. 22–24.

Pastor, M., Binda, M., & Harčarik, T. (2012). Modal Assurance Criterion. *Procedia Engineering*, *48*, 543–548. https://doi.org/10.1016/j.proeng.2012.09.551

Ryu, J., Kim, Y. Y., Park, M. W., Yoon, S.-W., Lee, C.-H., & Ju, Y. K. (2018). Experimental and numerical investigations of steel-polymer hybrid floor panels subjected to three-point bending. *Engineering Structures*, *175*, 467–482. https://doi.org/10.1016/j.engstruct.2018.08.030

Sanchez, T. A. (2008). *Experimental and Analytical Study of Vibrations in Long Span Deck Floor Systems* [MSc. Thesis]. Virginia Polytechnic Institute and State University.

Satasivam, S., & Bai, Y. (2016). Mechanical performance of modular FRP-steel composite beams for building construction. *Materials and Structures*, *49*(10), 4113–4129. https://doi.org/10.1617/s11527-015-0776-2

Smith, A. L., Hicks, S. J., & Devine, P. J. (2009). *Design of floors for vibration: A new approach* (Revised ed). Steel Construction Institute.

Vibrant Technologies. (2022, December 29). *Operating Manuals | Vibrant Technology, Inc.* Vibrant Technology, Inc. https://www.vibetech.com/support/operating-manuals/

Vimmr, V. (2008). *The Deltabeam composite system: A big opportunity for hollow-core slabs*. *74*(11), 44–52.

Yang, T. Y., Zhuo, S. R., & Li, Y. J. (2018). Seismic Behavior and Design of Innovative Modular Steel Floor System. *Key Engineering Materials*, *763*, 287–294. https://doi.org/10.4028/www.scientific.net/KEM.763.287

Zhou, X., Cao, L., Chen, Y. F., Liu, J., & Li, J. (2016). Acceleration Response of Prestressed Cable RC Truss Floor System Subjected to Heel-Drop Loading. *Journal of Performance of Constructed Facilities*, *30*(5), 04016014. https://doi.org/10.1061/(ASCE)CF.1943-5509.0000864

Appendix

A. Interviews Questionnaire and Detailed Responses

Acknowledgements

The interview participants help was much appreciated with the interviews. Fabricators: David Wright, Rong Meng, Duff Zimmerman, and Erection specialists: Chad Fox, Will Jacobs, Dave McCrary, and Cori Amadon.

FastFloor Project
Investigating Fabrication and Erection Issues
3/8/2022

Objectives:
The objective of this survey is to evaluate issues of fabrication, transportation, erection, and construction sequence for modular floor systems such as the system shown in Figure 1. This objective will be accomplished by interviewing members of the Industry Advisory Panel and others and taking detailed notes. The results will be consolidated into a brief report (intended for internal use, not public distribution), that identifies:

a) Likely processes / sequences to be used in fabrication and erection of modular floor systems.
b) Challenges associated with fabrication and erection of the preliminary modular floor system concept shown in Figure 1 and Figure 2.
c) Necessary changes to the modular floor system to accommodate fabrication, transportation, and erection.

Instructions:

1. Please review the drawings on Page 2.
2. Look through the questions on Pages 3 and 4. It is not necessary to prepare any formal response.
3. We will have a zoom interview with you to get your feedback on the questions and any other issues you see with these modular floor systems.

Preliminary FastFloor Module Used for Assessment – send to interviewee

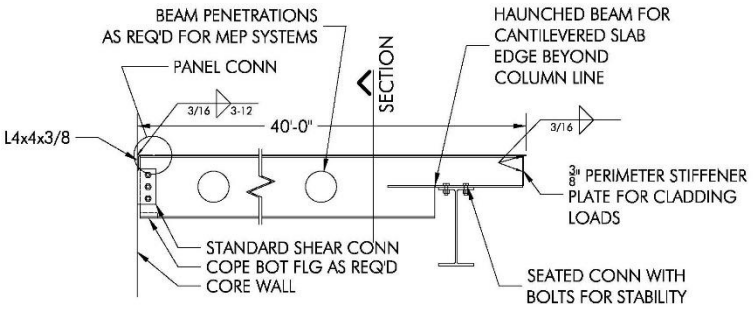

a) Side view of typical module

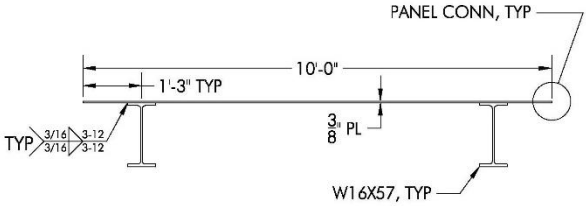

b) Cross-section of typical module

Figure 1 – Preliminary Concept for FastFloor Modular Floor System

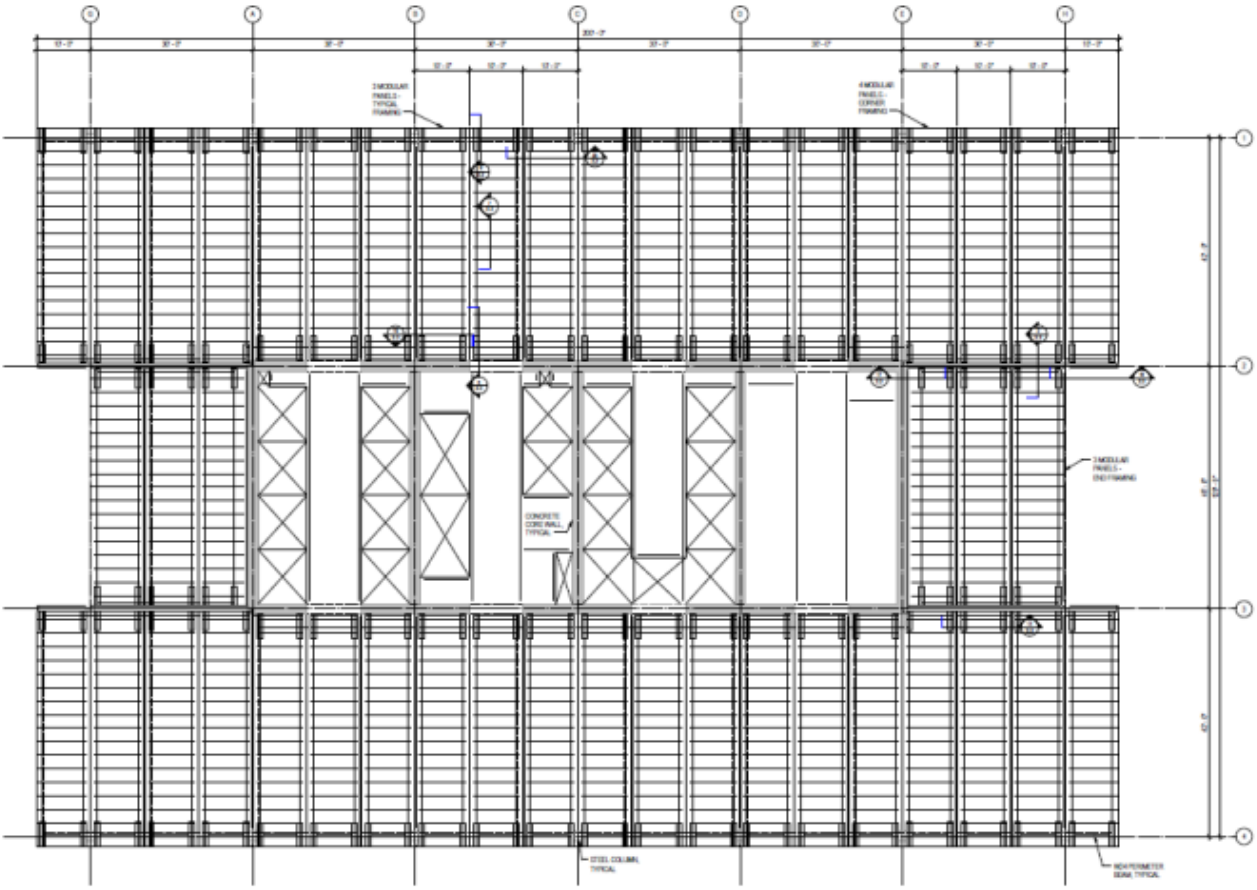

Figure 2 – Example Floor Plan

Questions:

The following questions will create a framework for the interviews, but discussion can veer from these questions as desired. Referencing Figure 1 and Figure 2.

1. Fabrication
    a. Working with the Plate
        i. What are the dimensions of 3/8" plate that is available? Is 10'x40' available, or need a splice?
        ii. If the 3/8" plate needs to be spliced, how would you do it? Weld procedure?
        iii. Any challenges handling 3/8" plate that is this large (floppy, not flat, etc.)?
    b. Fabrication
        i. Would this module be fabricated upside down?
        ii. Would you use automatic welding or hand welding for the plate to beam welds?
        iii. If beams welded to plate when upside down, is there trouble flipping it over afterward?
    c. Camber and Penetrations
        i. What would be the process for cambering, e.g., camber the beams, then weld plate to cambered beams? When to apply camber.
        ii. Penetrations through 3/8" plate for vertical MEP? Recommendations for how to reinforce around opening?
        iii. Penetrations through beam webs for MEP – any issues?
    d. Overarching View of Fabrication
        i. Are there challenges handling the module in the shop? Picking a 40'x10' module and there is no bracing of the beams – is this an issue?
        ii. Any other issues you see for fabricating this module?
        iii. Are there any unusual costs / time associated with fabricating this module?
        iv. Could the majority of fabricators do this type of work, or is this specialized work that only big fabricators can do?
        v. Would fabrication on site make sense?
2. Transportation
    a. Transporting on a truck
        i. How many of these modules can you fit on a truck?
        ii. Would you use a standard flatbed? Are there other options such as putting wheels on the modules?
        iii. Any potential for nesting on a truck?
        iv. Challenges associated with stability on a truck?
    b. Overarching Questions
        i. Are there any unusual costs associated with transportation?
        ii. Any other issues you see for transporting these modules?
3. Erection / Construction Sequencing
    a. Lifting
        i. Challenges for lifting? Pick points?

ii. Would you need any special attachments / equipment on the crane to be able to pick up the module?
iii. Limits on what can be lifted with crane? Is this a regional limitation?

b. Connections and Fit-Up
    i. Challenges for fit-up on site for modules that use seated connections on both ends?
    ii. Suggested panel-to-panel connections?
    iii. Any issues if panel-to-panel connections are PAF through a thin plate (assuming sufficient strength)?
    iv. Challenges associated with bolted panel-to-panel connections (can't reach underside)?

c. Overarching Questions
    i. What would be construction sequence in the field? Core wall, columns, girders, modules, panel-to-panel connections?
    ii. Any issues working on this type of surface / erecting railing around perimeter, etc.?
    iii. Are there any unusual costs or time requirements associated with erection?
    iv. Any other issues you see associated with erection?

B. DG11 – Example 4.1, including slab panel

1. INPUT: GEOMETRIC PROPERTIES

Beam section: W18x35

$d_j := 17.7\ in$

$A_j := 10.3\ in^2$

$I_{xj} := 510\ in^4$

$SW_j := 35\ \frac{lbf}{ft}$

$S_b := 10\ ft$

$L_j := 35\ ft$

Girder section: W21x50

$d_g := 20.8\ in$

$A_g := 14.7\ in^2$

$I_{xg} := 984\ in^4$

$SW_g := 50\ \frac{lbf}{ft}$

$L_g := 30\ ft$

Deck Slab

$L_p := 40\ ft$

$f_c := 4\ ksi$

$E_c := 110^{1.5} \cdot \sqrt{f_c\ ksi} = 2307\ ksi$

$d_d := 2\ in$

$d_c := 3.25\ in$

Module dimensions

$L_{module} := 105\ ft$

$W_{module} := 150\ ft$

Notation:

L: Length
W: Width
SW: Self Weight
s: spacing

$\rho_{steel} := 490\ \frac{lbf}{ft^3}$

$g := 386.09\ \frac{in}{s^2}$

$E_s := 29000\ ksi$

$F_y := 50\ ksi$

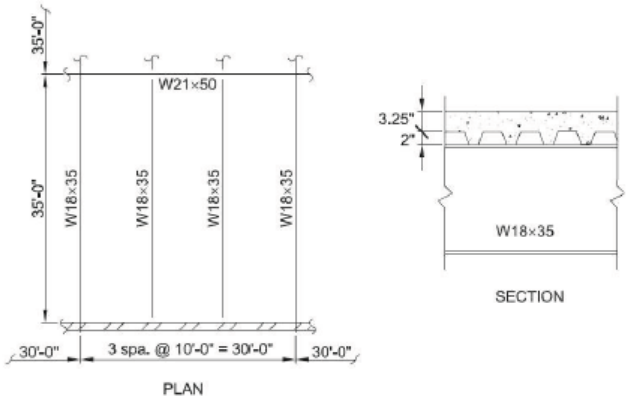

Fig. 4-5. Exterior bay floor framing details for Example 4.1.

2. INPUT: VIBRATION PARAMETERS

Electronic office

$\beta := 3\ \%$

$P_o := 65\ \text{lbf}$

3. INPUT: LOADS

Live Load

$LL := 11\ \text{psf}$

Dead Load

Members Self Weight

$$P_{slab} := \left(d_c + \frac{d_d}{2}\right) \cdot 110\ \frac{\text{lbf}}{\text{ft}^3} + 2\ \text{psf} = 40.96\ \text{psf}$$

$D_{beams} := SW_j = 35\ \frac{\text{lbf}}{\text{ft}}$

$D_{girder} := SW_g = 50\ \frac{\text{lbf}}{\text{ft}}$

Superimposed

$DL_s := 4\ \text{psf}$

4: CALCS: COMPOSITE PROPERTIES

$$n := \frac{E_s}{1.35 \cdot E_c} = 9.310$$

Deck-Slab Transformed Moment of Inertia

Composite moment of inertia neglecting shear studs, and assuming 100% composite action

$$b_{effc} := \min\left(\left[\ 2 \cdot \frac{L_j}{8}\ \ 2 \cdot \frac{W_{module}}{2}\ \right]\right) = 8.75\ \text{ft}$$

$$t_{eq} := d_c + \frac{d_d}{2} = 4.25\ \text{in}$$ Equivalent thickness

$$A_c := \frac{b_{effc}}{n} \cdot t_{eq} = 47.93\ \text{in}^2$$ Transformed area of concrete

$$I_{tr} := \frac{A_c \cdot t_{eq}^{\ 2}}{12} = 72.15\ \text{in}^4$$ Transformed moment of inertia, idealized as a rectangle.

Beam Transformed Moment of Inertia

$$W_{effj} := \min\left(\left[\ 0.4 \cdot L_j\ \ S_b\ \right]\right) = 10\ \text{ft}$$ Effective Concrete Slab Depth for beam panel

$$W_{teffj} := \frac{W_{effj}}{n} = 12.89\ \text{in}$$ Transformed Concrete Slab Width

$$A_{teffj} := d_c \cdot W_{teffj} = 41.89\ \text{in}^2$$ Transformed Concrete Slab Area

$$y_j := \frac{A_{teffj} \cdot \left(\frac{d_j}{2} + d_d + \frac{d_c}{2}\right)}{A_{teffj} + A_j} = 10.01\ \text{in}$$

$$I_j := \frac{W_{teffj} \cdot d_c^{\ 3}}{12} + A_{teffj} \cdot \left(\frac{d_j}{2} + d_d + \frac{d_c}{2} - y_j\right)^2 + I_{xj} + A_j \cdot y_j^{\ 2} = 1833\ \text{in}^4$$

Girder Transformed Moment of Inertia

$$W_{effg} := \min\left(\left[\ 0.2 \cdot L_g\ \ 0.5 \cdot L_j\ \right]\right) + \min\left(\left[\ 0.2 \cdot L_g\ \ 0.5 \cdot L_j\ \right]\right) = 12\ \text{ft}$$ Effective concrete slab width

$$W_{teffg} := \frac{W_{effg}}{n} = 15.47\ \text{in}$$ Transformed concrete slab width

$$W_{effdg} := \frac{\frac{W_{effg}}{2}}{n} = 7.734\ \text{in}$$ Effective width of the slab in the deck

$$A_{tcg} := d_c \cdot W_{teffg} = 50.27\ \text{in}^2$$ Transformed concrete slab area

$$A_{tdg} := d_d \cdot W_{effdg} = 15.47\ \text{in}^2$$ Transformed concrete slab area in the deck

$$y_g := \frac{A_{tcg} \cdot \left(\frac{d_g}{2} + d_d + \frac{d_c}{2}\right) + A_{tdg} \cdot \left(\frac{d_g}{2} + \frac{d_d}{2}\right)}{A_{tcg} + A_{tdg} + A_g} = 10.96\ \text{in}$$

$$I_g := \frac{W_{teffg} \cdot d_c^{\ 3}}{12} + A_{tcg} \cdot \left(\frac{d_g}{2} + d_d + \frac{d_c}{2} - y_g\right)^2 + \frac{W_{effdg} \cdot d_d^{\ 3}}{12} + A_{tdg} \cdot \left(\frac{d_g}{2} + \frac{d_c}{2} - y_g\right)^2 + I_{xg} + A_g \cdot y_g^{\ 2} = 3289\ \text{in}^4$$

5: CALCS: VIBRATION

Slab Panel Mode

$$w_p := P_{slab} \cdot b_{effc} + b_{effc} \cdot \left(DL_s + LL \right) = 489.6 \ \frac{lbf}{ft}$$

$$W_p := \frac{w_p}{b_{effc}} \cdot L_j \cdot S_b = 19590 \ lbf$$

Beam Panel Mode

$$w_j := D_{beams} + S_b \cdot \left(P_{slab} + DL_s + LL \right) = 594.6 \ \frac{lbf}{ft}$$ Supported weight on one beam

$$D_s := \frac{1 \ ft \cdot \left(d_c + \frac{d_d}{2} \right)^3}{12 \cdot n \cdot 1 \ ft} = 8.246 \ \frac{in^4}{ft}$$ Transformed plate moment of inertia per unit width in the slab span direction.

$$D_j := \frac{I_j}{S_b} = 183.3 \ \frac{in^4}{ft}$$ Transformed beam moment of inertia per unit width in the beam span direction, with beam spacing of 10 ft

Options for Cj $C_{j1} := 2.0$ $C_{j2} := 1.0$

$$C_j := C_{j1} = 2.0$$ Cj = 2.0. Typical bay without free edges (for most areas).
Cj = 1.0. Typical edge panel **(beams/joists parallel to a free edge)**.

$$B_j := C_j \cdot \left(\frac{D_s}{D_j} \right)^{\frac{1}{4}} \cdot L_j = 32.24 \ ft$$ Effective beam panel width

$$W_j := 1.5 \cdot \left(\frac{w_j}{S_b} \right) \cdot B_j \cdot L_j = 100600 \ lbf$$ Effective beam panel weight

Girder Panel Mode

Options for girder load: Interior girder, Wg1 and Exterior girder, Wg2

$$w_{g1} := L_j \cdot \frac{w_j}{S_b} + D_{girder} = 2131 \ \frac{lbf}{ft}$$ Supported weight interior girder

$$w_{g2} := \frac{w_{g1}}{2} = 1065.5208 \ \frac{lbf}{ft}$$ Supported weight exterior girder

$$w_g := w_{g1} = 2131 \ \frac{lbf}{ft}$$

$$D_g := \frac{I_g}{L_j} = 93.97 \ \frac{in^4}{ft}$$ Girder transformed moment of inertia per unit width

$$C_g := 1.8$$ Cg = 1.8. Girders supporting beams connected to the girder web

$$B_g := C_g \cdot \left(\frac{D_j}{D_g} \right)^{\frac{1}{4}} \cdot L_g = 63.82 \ ft \quad < \quad \frac{2}{3} \cdot \left(L_{module} \right) = 70 \ ft$$ Effective girder panel width for interior girders

$$W_g := 1.0 \cdot \left(\frac{w_g}{L_j} \cdot B_g \right) \cdot L_g = 116600 \ lbf$$ Effective girder panel weight (there is no 1.5 multiplier in front of it).

Slab Mode Properties

$$\Delta_p := \frac{5 \cdot w_p \cdot S_b^{\,4}}{384 \cdot E_s \cdot I_{tr}} = 0.05265\ \text{in}$$

$$f_{np} := 0.179 \cdot \sqrt{\frac{g}{\Delta_p}} = 15.33\ \text{Hz}$$

Beam Mode Properties

$$\Delta_j := \frac{5 \cdot w_j \cdot L_j^{\,4}}{384 \cdot E_s \cdot I_j} = 0.3776\ \text{in}$$

$$f_{nj} := 0.18 \cdot \sqrt{\frac{g}{\Delta_j}} = 5.76\ \text{Hz}$$

Girder Mode Properties

$$\Delta_g := \frac{5 \cdot w_g \cdot L_g^{\,4}}{384 \cdot E_s \cdot I_g} = 0.4072\ \text{in}$$

$$f_{ng} := 0.18 \cdot \sqrt{\frac{g}{\Delta_g}} = 5.543\ \text{Hz}$$

$$\Delta_{g'} := \frac{L_g}{B_j} \cdot \Delta_g = 0.3789\ \text{in}$$

Girder span is less than the joist panel, Bj, the girder deflection is reduced.

Combined mode

$$f_n := 0.18 \cdot \sqrt{\frac{g}{\Delta_p + \Delta_j + \Delta_g}} = 3.865\ \text{Hz}$$

$$f_{njg} := 0.18 \cdot \sqrt{\frac{g}{\Delta_j + \Delta_g}} = 3.99\ \text{Hz}$$

Floor fundamental frequency

Comparison between Equivalent Panel Mode Weight and the corresponding acceleration:

$$W_1 := \frac{\Delta_p}{\Delta_p + \Delta_j + \Delta_{g'}} \cdot W_p + \frac{\Delta_j}{\Delta_p + \Delta_j + \Delta_{g'}} \cdot W_j + \frac{\Delta_g}{\Delta_p + \Delta_j + \Delta_{g'}} \cdot W_g = 106900\ \text{lbf}$$

Equivalent panel mode weight

$$a_{p1} := \frac{P_o \cdot \exp\left(-0.35 \cdot \frac{f_n}{\text{Hz}}\right)}{\beta \cdot W_1} = 0.524\ \%\ g$$

> 0.5%g DG 11 Limit

$$W_2 := \left(\frac{\Delta_j}{\Delta_j + \Delta_{g'}} \cdot W_j + \frac{\Delta_g}{\Delta_j + \Delta_{g'}} \cdot W_g\right) = 112966.4\ \text{lbf}$$

Without plate panel contribution

$$a_{p2} := \frac{P_o \cdot \exp\left(-0.35 \cdot \frac{f_{njg}}{\text{Hz}}\right)}{\beta \cdot W_2} = 0.4742\ \%\ g$$

> 0.5%g DG 11 Limit

$$\frac{f_{np}}{f_{nj}} = 2.663 \qquad \frac{f_{np}}{f_{ng}} = 2.765$$

Ratio of Slab Mode to Beam Mode and Girder Mode, respectively

$$e := \left|\frac{a_{p2} - a_{p1}}{a_{p1}}\right| = 9.5104\ \%$$

Percentage of difference between accelerations including and neglecting the Slab Panel contribution

C. Analytical Calculations based on DG11

SM-68-3/8 – Worst Case

1. INPUT: GEOMETRIC PROPERTIES

Beam section: W24x68

$d_j := 23.7\ in$

$A_j := 20.1\ in^2$

$I_{xj} := 1830\ in^4$

$SW_j := 68\ \frac{lbf}{ft}$

$b_f := 8.97\ in$

Angles section: N/A

$d_L := 0\ in$

$A_L := 0\ in^2$

$I_{xL} := 0\ in^4$

$SW_L := 0\ \frac{lbf}{ft}$

$y_L := 0\ in$

$n_L := 0$

Girder section: W33x263

$d_g := 34.5\ in$

$A_g := 77.5\ in^2$

$I_{xg} := 15900\ in^4$

$SW_g := 263\ \frac{lbf}{ft}$

$L_g := 30\ ft$

Plate

$L_p := 40\ ft$

$t_p := \frac{3}{8}\ in$

Notation:

L: Length
W: Width
SW: Self Weight
s: spacing
d: depth
I: Inertia
n_a: number of angles

Subscripts:

j: Beam (Joist)
g: Girder
p: Plate
L: Angle

$\rho_{steel} := 490\ \frac{lbf}{ft^3}$

$g := 386.09\ \frac{in}{s^2}$

$E_s := 29000\ ksi$

$F_y := 50\ ksi$

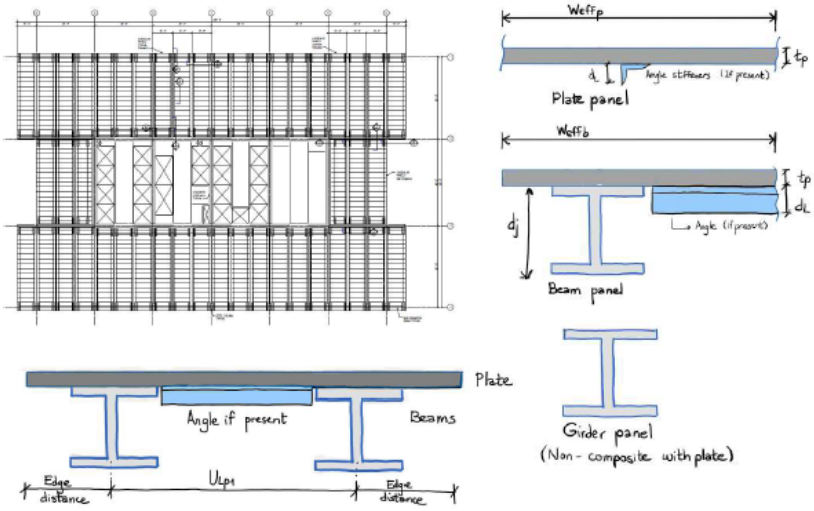

Module dimensions

$L_{module} := 40\ ft$

$W_{module} := 10\ ft$

$s_L := 1\ ft$ Angle spacing (1 ft : No angles, otherwise input angle spacing)

$d_{edge} := 2.5\ ft$ Edge distance

$U_{Lp1} := W_{module} - 2 \cdot \left(d_{edge}\right) = 5\ ft$ Center to center beam spacing

$U_{Lp2} := W_{module} - 2 \cdot \left(d_{edge}\right) - b_f = 4.253\ ft$ Clear distance between beam flanges

$U_{Lp} := U_{Lp2}$ Unsupported plate length to be used for the calculations

2. INPUT: VIBRATION PARAMETERS

Notation

$\beta_{fs} := 0.5\ \%$ — fs: Floor system Damping ratio

$\beta_{ss} := 1\ \%$ — ss: Structural System

$\beta_{a} := 1\ \%$ — a: additional (Ceiling and ductwork)

$\beta_{use} := 0.5\ \%$ — Use: Electronic office fit-out

$\beta := \beta_{fs} + \beta_{use} + \beta_{ss} + \beta_{a} = 3\ \%$ — Total damping

$P_o := 65\ lbf$

Variable: Floor system damping ratio $\left(\beta_{ss}\right)$

0.01: Structural system $\left(\beta_{fs}\right)$: Should be verified for this type of floor system.

0.01: Ceiling and ductwork $\left(\beta_{a}\right)$

0.5: Electronic office fit-out $\left(\beta_{use}\right)$

Additional damping associated with raised floors is neglected

Damping

The damping ratio, β, can be estimated using the component values shown in Table 4-2, noting that damping is cumulative. For example, a floor with ceiling and ductwork supporting an electronic office area has $\beta = \Sigma\beta_i = 0.01 + 0.01 + 0.005 = 0.025$, or 2.5% of critical damping.

Table 4-2. Recommended Component Damping Values for Use in Equation 4-1

Component	Ratio of Actual Damping-to-Critical Damping, β_i
Structural system	0.01
Ceiling and ductwork	0.01
Electronic office fit-out	0.005
Paper office fit-out	0.01
Churches, schools and malls	0.0
Full-height dry wall partitions in bay	0.02 to 0.05*

*Depending on the number of partitions in the bay and their location; nearer the center of the bay provides more damping.

3. INPUT: LOADS

Load assumptions

3.1. LL: 6 - 8 psf for electronic office (Worst case is 6 psf)

3.2. Assume superimposed load = 4 psf. Neglecting the weight of a raised floor.

From Tate, approx. weight of raised floor:

- ConCore Panels: 8 - 14 psf (Bare)
- All Steel Panels: 5 psf (Bare)
- Cavity Floor Panels/ StoneWork® Panels: 15 psf

Notation

P: Pressure (Loads in psf)
D: Distributed dead loads [lbf/ft]
DL: Superimposed dead loads per area [psf]

Live Load

$LL := 0\ psf$

Dead Load

Members Self Weight

$P_{plate} := t_p \cdot \rho_{steel} = 15.31\ psf$

$D_{angles} := n_L \cdot SW_L = 0\ \frac{lbf}{ft}$

$D_{beams} := SW_j = 68\ \frac{lbf}{ft}$

$D_{girder} := SW_g = 263\ \frac{lbf}{ft}$

Superimposed

$DL_{dg11} := 4\ psf$ Recommended sumperimposed load per DG11

$DL_{rf} := 5\ psf$ Raised floor superimposed dead load

$DL_s := DL_{dg11} + DL_{rf} = 9\ psf$ Total superimposed dead load

4: CALCS: COMPOSITE PROPERTIES

Effective slab width for plate panel

$B_{effL} := 25\ \%$ Effective width of plate for use with plate panel based on local buckling

$B_{effp} := \min\left(\left[\left(B_{effL} \cdot s_L\right)\left(0.4 \cdot U_{Lp2}\right)\right]\right) = 3\ in$

Notation

B: Widths

Plate Transformed Moment of Inertia

$d_p := d_L + t_p = 0.375\ in$

$A_p := B_{effp} \cdot t_p = 1.125\ in^2$

$y_p := \frac{A_L \cdot \left(d_L - y_L\right) + A_p \cdot \left(d_L + \frac{t_p}{2}\right)}{A_L + A_p} = 0.1875\ in$

Moment of inertia per angle spacing, s_L

$I_p := \frac{t_p^{\,3} \cdot B_{effp}}{12} + \left(A_p \cdot \left(d_p - y_p - \frac{t_p}{2}\right)^2\right) + \left(I_{xL} + A_L \cdot \left(y_p - y_L\right)^2\right) = 0.0132\ in^4$

Effective slab width for beam panel

$B_{effm} := 25\ \%$ Effective width of plate for use with beam panel based on local buckling

$B_{effb} := \min\left(\left[\left(B_{effm} \cdot W_{module}\right)\ 2 \cdot \left(0.2 \cdot \left(L_{module} + d_{edge}\right)\right)\right]\right) = 30\ in$

Beam Transformed Moment of Inertia (Calculations for entire width of module)

$A_{tpb} := \frac{B_{effb}}{2} \cdot t_p = 5.625\ in^2$ Effective Plate Area for beam panel

$D_t := d_j + t_p = 24.075\ in$

$y_j := \frac{A_j \cdot \frac{d_j}{2} + A_{tpb} \cdot \left(d_j + \frac{t_p}{2}\right)}{A_j + A_{tpb}} = 14.4821\ in$

$I_j := \frac{t_p^{\,3} \cdot B_{effb}}{24} + \left(A_{tpb} \cdot \left(D_t - y_j - \frac{t_p}{2}\right)^2\right) + I_{xj} + A_j \cdot \left(y_j - \frac{d_j}{2}\right)^2 = 2467\ in^4$

Girder Transformed Moment of Inertia

$I_g := I_{xg} = 15900\ in^4$ Girder is non composite, this number is directly taken from AISC manual.

5: CALCS: VIBRATION

Plate Panel Mode

$$w_p := \left(P_{plate} + \frac{D_{angles}}{L_{module}}\right) \cdot B_{effp} + B_{effp} \cdot \left(DL_s + LL\right) = 6.078\ \frac{lbf}{ft}$$ Supported weight

$$W_p := \frac{w_p}{B_{effp}} \cdot L_{module} \cdot U_{Lp1} = 4862\ lbf$$

Beam Panel Mode

$$w_j := D_{beams} + \left(\frac{D_{angles}}{L_{module}} \cdot \frac{U_{Lp1}}{2}\right) + \frac{W_{module}}{2} \cdot \left(P_{plate} + DL_s + LL\right) = 189.6\ \frac{lbf}{ft}$$ Supported weight

$$D_s := \frac{t_p^{\,3}}{12} = 0.0527\ \frac{in^4}{ft}$$ Transformed plate moment of inertia per unit width in the slab span direction.

$$D_j := \frac{I_j}{\frac{W_{module}}{2}} = 493.4\ \frac{in^4}{ft}$$ Transformed beam moment of inertia per unit width in the beam span direction, with beam spacing of 10 ft

Options for Cj

$C_{j1} := 2.0$ Cj = 2.0. Typical bay without free edges.

$C_{j2} := 1.0$ Cj = 1.0. Typical edge panel.

$C_j := C_{j1} = 2.0$

$$B_j := C_j \cdot \left(\frac{D_s}{D_j}\right)^{\frac{1}{4}} \cdot L_{module} = 8.134\ ft$$ Effective beam panel width

***The effective beam panel width, Bj, must be less than 2/3 of the floor width. Worst case floor width = 30 ft. And, two-thirds of 30ft is 20 ft.**

$$W_j := 1.5 \cdot \left(\frac{w_j}{W_{module}}\right) \cdot B_j \cdot L_{module} = 9252\ lbf$$ Effective beam panel weight

Girder Panel Mode

Options for girder load: Interior girder, Wg1 and Exterior girder, Wg2

$$w_{g1} := \frac{2 \cdot w_j}{W_{module}} \cdot L_{module} + D_{girder} = 1779\ \frac{lbf}{ft}$$ Supported weight interior girder

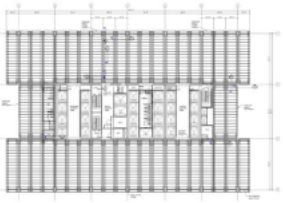

$$w_{g2} := \frac{2 \cdot w_j}{W_{module}} \cdot \frac{L_{module}}{2} + D_{girder} = 1021\ \frac{lbf}{ft}$$ Supported weight exterior girder

$w_g := w_{g1} = 1779\ \frac{lbf}{ft}$

$$D_g := \frac{I_g}{L_{module}} = 397.5\ \frac{in^4}{ft}$$ Girder transformed moment of inertia per unit width

$C_g := 1.8$ Cg = 1.8. Girders supporting beams connected to the girder web

$$B_g := C_g \cdot \left(\frac{D_j}{D_g}\right)^{\frac{1}{4}} \cdot L_g = 57.00\ ft$$ Effective girder panel width for interior girders

***The effective girder panel width, Bg, must be less than or equal to two-thirds of the floor length. Worst case floor length is 40ft per the floor plan we know so far. Two-thirds of 40ft is 26.7 ft. Using Bgmax of 26.7 ft is reasonable for this case.**

$B_{gmax} := 26.7\ ft$

$$W_g := 1.0 \cdot \left(\frac{w_g}{L_{module}} \cdot B_{gmax}\right) \cdot L_g = 35630\ lbf$$ Effective girder panel weight (there is no 1.5 multiplier in front of it).

Plate Mode Properties

$$\Delta_p := \frac{5 \cdot w_p \cdot U_{Lp}^{4}}{384 \cdot E_s \cdot I_p} = 0.2236 \text{ in}$$

$$f_{np} := 0.179 \cdot \sqrt{\frac{g}{\Delta_p}} = 7.44 \text{ Hz}$$

Beam Mode Properties

$$\Delta_j := \frac{5 \cdot w_j \cdot L_{module}^{4}}{384 \cdot E_s \cdot I_j} = 0.1526 \text{ in}$$

$$f_{nj} := 0.179 \cdot \sqrt{\frac{g}{\Delta_j}} = 9.00 \text{ Hz}$$

Girder panel

If Lg < Bj, the combined mode is restricted and system is effectively stiffened and deflection can be reduced. In this case, not true.

$$\Delta_g := \frac{5 \cdot w_g \cdot \left(3 \cdot W_{module}\right)^{4}}{384 \cdot E_s \cdot I_g} = 0.07033 \text{ in}$$

$$L_g = 360 \text{ in}$$

$$B_j = 97.61 \text{ in}$$

$$f_{ng} := 0.179 \cdot \sqrt{\frac{g}{\Delta_g}} = 13.26 \text{ Hz}$$

Combined mode

$$f_{n1} := 0.179 \cdot \sqrt{\frac{g}{\Delta_p + \Delta_j + \Delta_g}} = 5.264 \text{ Hz} \qquad f_{n2} := 0.179 \cdot \sqrt{\frac{g}{\Delta_j + \Delta_g}} = 7.45 \text{ Hz}$$

Floor fundamental frequency

Comparison between Equivalent Panel Mode Weight and the corresponding acceleration:

$$W_1 := \frac{\Delta_p}{\Delta_p + \Delta_j + \Delta_g} \cdot W_p + \frac{\Delta_j}{\Delta_p + \Delta_j + \Delta_g} \cdot W_j + \frac{\Delta_g}{\Delta_p + \Delta_j + \Delta_g} \cdot W_g = 11210 \text{ lbf}$$

Equivalent panel mode weight

$$a_{p1} := \frac{P_o \cdot \exp\left(-0.35 \cdot \frac{f_{n1}}{\text{Hz}}\right)}{\beta \cdot W_1} = 3.0628 \ g$$

< 0.5%g DG 11 Limit

$$W_2 := \left(\frac{\Delta_j}{\Delta_j + \Delta_g} \cdot W_j + \frac{\Delta_g}{\Delta_j + \Delta_g} \cdot W_g\right) = 17574.43 \text{ lbf}$$

Without plate panel contribution

$$a_{p2} := \frac{P_o \cdot \exp\left(-0.35 \cdot \frac{f_{n2}}{\text{Hz}}\right)}{\beta \cdot W_2} = 0.9092 \ g$$

< 0.5%g DG 11 Limit

SM-68-3/8 – Best Case

1. INPUT: GEOMETRIC PROPERTIES

Beam section: W24x68

$d_j := 23.7\ in$

$A_j := 20.1\ in^2$

$I_{xj} := 1830\ in^4$

$SW_j := 68\ \frac{lbf}{ft}$

$b_f := 8.97\ in$

Angles section: N/A

$d_L := 0\ in$

$A_L := 0\ in^2$

$I_{xL} := 0\ in^4$

$SW_L := 0\ \frac{lbf}{ft}$

$y_L := 0\ in$

$n_L := 0$

Girder section: W33x263

$d_g := 34.5\ in$

$A_g := 77.5\ in^2$

$I_{xg} := 15900\ in^4$

$SW_g := 263\ \frac{lbf}{ft}$

$L_g := 30\ ft$

Plate

$L_p := 40\ ft$

$t_p := \frac{3}{8}\ in$

Notation:

L: Length
W: Width
SW: Self Weight
s: spacing
d: depth
I: Inertia
n_a: number of angles

Subscripts:

j: Beam (Joist)
g: Girder
p: Plate
L: Angle

$\rho_{steel} := 490\ \frac{lbf}{ft^3}$

$g := 386.09\ \frac{in}{s^2}$

$E_s := 29000\ ksi$

$F_y := 50\ ksi$

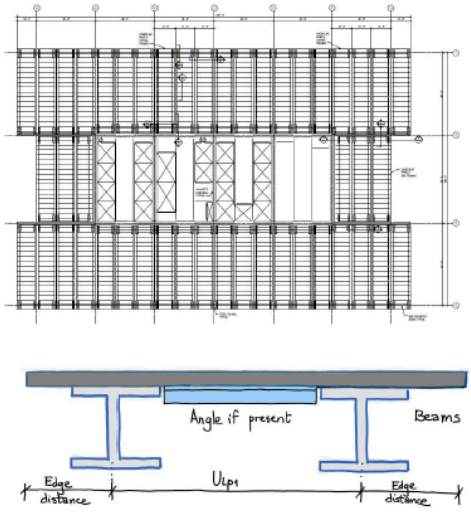

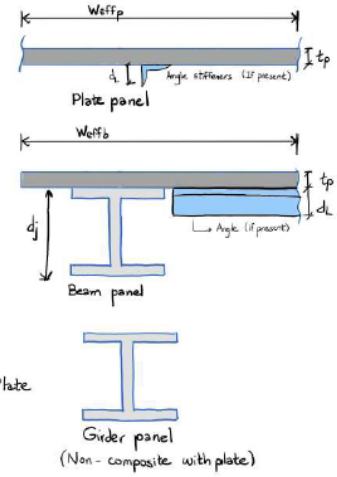

Module dimensions

$L_{module} := 40\ ft$

$W_{module} := 10\ ft$

$s_L := 1\ ft$ Angle spacing (1 ft : No angles, otherwise input angle spacing)

$d_{edge} := 2.5\ ft$ Edge distance

$U_{Lp1} := W_{module} - 2 \cdot \left(d_{edge}\right) = 5\ ft$ Center to center beam spacing

$U_{Lp2} := W_{module} - 2 \cdot \left(d_{edge}\right) - b_f = 4.253\ ft$ Clear distance between beam flanges

$U_{Lp} := U_{Lp2}$ Unsupported plate length to be used for the calculations

2. INPUT: VIBRATION PARAMETERS

Notation

$\beta_{fs} := 3.5\ \%$ — fs: Floor system Damping ratio

$\beta_{ss} := 1\ \%$ — ss: Structural System

$\beta_{a} := 1\ \%$ — a: additional (Ceiling and ductwork)

$\beta_{use} := 0.5\ \%$ — Use: Electronic office fit-out

$\beta := \beta_{fs} + \beta_{use} + \beta_{ss} + \beta_{a} = 6\ \%$ — Total damping

$P_o := 65\ lbf$

Variable: Floor system damping ratio $\left(\beta_{ss}\right)$

0.01: Structural system $\left(\beta_{fs}\right)$: Should be verified for this type of floor system.

0.01: Ceiling and ductwork $\left(\beta_{a}\right)$

0.5: Electronic office fit-out $\left(\beta_{use}\right)$

Additional damping associated with raised floors is neglected

Damping

The damping ratio, β, can be estimated using the component values shown in Table 4-2, noting that damping is cumulative. For example, a floor with ceiling and ductwork supporting an electronic office area has $\beta = \sum\beta_i = 0.01 + 0.01 + 0.005 = 0.025$, or 2.5% of critical damping.

Table 4-2. Recommended Component Damping Values for Use in Equation 4-1

Component	Ratio of Actual Damping-to-Critical Damping, β_i
Structural system	0.01
Ceiling and ductwork	0.01
Electronic office fit-out	0.005
Paper office fit-out	0.01
Churches, schools and malls	0.0
Full-height dry wall partitions in bay	0.02 to 0.05*

*Depending on the number of partitions in the bay and their location; nearer the center of the bay provides more damping.

3. INPUT: LOADS

Live Load

$LL := 8\ psf$

Dead Load

Members Self Weight

$P_{plate} := t_p \cdot \rho_{steel} = 15.31\ psf$

$D_{angles} := n_L \cdot SW_L = 0\ \frac{lbf}{ft}$

$D_{beams} := SW_j = 68\ \frac{lbf}{ft}$

$D_{girder} := SW_g = 263\ \frac{lbf}{ft}$

Superimposed

$DL_{dg11} := 4\ psf$ Recommended sumperimposed load per DG11

$DL_{rf} := 15\ psf$ Raised floor superimposed dead load

$DL_s := DL_{dg11} + DL_{rf} = 19\ psf$ Total superimposed dead load

Load assumptions

3.1. LL: 6 - 8 psf for electronic office (Worst case is 6 psf)

3.2. Assume superimposed load = 4 psf. Neglecting the weight of a raised floor.

From Tate, approx. weight of raised floor:

- ConCore Panels: 8 - 14 psf (Bare)
- All Steel Panels: 5 psf (Bare)
- Cavity Floor Panels/ StoneWork® Panels: 15 psf

Notation

P: Pressure (Loads in psf)
D: Distributed dead loads [lbf/ft]
DL: Superimposed dead loads per area [psf]

4: CALCS: COMPOSITE PROPERTIES

Effective slab width for plate panel

$B_{effL} := 100\ \%$ Effective width of plate for use with plate panel based on local buckling

$B_{effp} := \min\left(\left[\left(B_{effL} \cdot s_L\right)\left(0.4 \cdot U_{Lp2}\right)\right]\right) = 12\ in$

Notation

B: Widths

Plate Transformed Moment of Inertia

$d_p := d_L + t_p = 0.375\ in$

$A_p := B_{effp} \cdot t_p = 4.5\ in^2$

$y_p := \frac{A_L \cdot \left(d_L - y_L\right) + A_p \cdot \left(d_L + \frac{t_p}{2}\right)}{A_L + A_p} = 0.1875\ in$

Moment of inertia per angle spacing, s_L

$I_p := \frac{t_p^{\,3} \cdot B_{effp}}{12} + \left[A_p \cdot \left(d_p - y_p - \frac{t_p}{2}\right)^2\right] + \left(I_{xL} + A_L \cdot \left(y_p - y_L\right)^2\right) = 0.0527\ in^4$

Effective slab width for beam panel

$B_{effm} := 100\ \%$ Effective width of plate for use with beam panel based on local buckling

$B_{effb} := \min\left(\left[\left(B_{effm} \cdot W_{module}\right)\ 2 \cdot \left(0.2 \cdot \left(L_{module} + d_{edge}\right)\right)\right]\right) = 120\ in$

Beam Transformed Moment of Inertia (Calculations for entire width of module)

$A_{tpb} := \frac{B_{effb}}{2} \cdot t_p = 22.5\ in^2$ Effective Plate Area for beam panel

$D_t := d_j + t_p = 24.075\ in$

$y_j := \frac{A_j \cdot \frac{d_j}{2} + A_{tpb} \cdot \left(d_j + \frac{t_p}{2}\right)}{A_j + A_{tpb}} = 18.2078\ in$

$I_j := \frac{t_p^{\,3} \cdot B_{effb}}{24} + \left[A_{tpb} \cdot \left(D_t - y_j - \frac{t_p}{2}\right)^2\right] + I_{xj} + A_j \cdot \left(y_j - \frac{d_j}{2}\right)^2 = 3369\ in^4$

Girder Transformed Moment of Inertia

$I_g := I_{xg} = 15900\ in^4$ Girder is non composite, this number is directly taken from AISC manual.

5: CALCS: VIBRATION

Plate Panel Mode

$$w_p := \left(P_{plate} + \frac{D_{angles}}{L_{module}} \right) \cdot B_{effp} + B_{effp} \cdot \left(DL_s + LL \right) = 42.31 \ \frac{lbf}{ft}$$ Supported weight

$$W_p := \frac{w_p}{B_{effp}} \cdot L_{module} \cdot U_{Lp1} = 8462 \ lbf$$

Beam Panel Mode

$$w_j := D_{beams} + \left(\frac{D_{angles}}{L_{module}} \cdot \frac{U_{Lp1}}{2} \right) + \frac{W_{module}}{2} \cdot \left(P_{plate} + DL_s + LL \right) = 279.6 \ \frac{lbf}{ft}$$ Supported weight

$$D_s := \frac{t_p^{\,3}}{12} = 0.0527 \ \frac{in^4}{ft}$$ Transformed plate moment of inertia per unit width in the slab span direction.

$$D_j := \frac{I_j}{\frac{W_{module}}{2}} = 673.7 \ \frac{in^4}{ft}$$ Transformed beam moment of inertia per unit width in the beam span direction, with beam spacing of 10 ft

Options for Cj

$C_{j1} := 2.0$ Cj = 2.0. Typical bay without free edges.

$C_{j2} := 1.0$ Cj = 1.0. Typical edge panel.

$C_j := C_{j2} = 1.0$

$$B_j := C_j \cdot \left(\frac{D_s}{D_j} \right)^{\frac{1}{4}} \cdot L_{module} = 3.762 \ ft$$ Effective beam panel width

*The effective beam panel width, Bj, must be less than 2/3 of the floor width. Worst case floor width = 30 ft. And, two-thirds of 30ft is 20 ft.

$$W_j := 1.5 \cdot \left(\frac{w_j}{W_{module}} \right) \cdot B_j \cdot L_{module} = 6311 \ lbf$$ Effective beam panel weight

Girder Panel Mode

Options for girder load: Interior girder, Wg1 and Exterior girder, Wg2

$$w_{g1} := \frac{2 \cdot w_j}{W_{module}} \cdot L_{module} + D_{girder} = 2500 \ \frac{lbf}{ft}$$ Supported weight interior girder

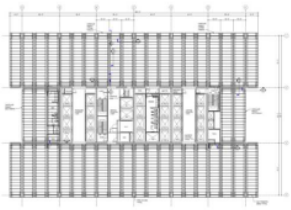

$$w_{g2} := \frac{2 \cdot w_j}{W_{module}} \cdot \frac{L_{module}}{2} + D_{girder} = 1381 \ \frac{lbf}{ft}$$ Supported weight exterior girder

$w_g := w_{g2} = 1381 \ \frac{lbf}{ft}$

$$D_g := \frac{I_g}{L_{module}} = 397.5 \ \frac{in^4}{ft}$$ Girder transformed moment of inertia per unit width

$C_g := 1.8$ Cg = 1.8. Girders supporting beams connected to the girder web

$$B_g := C_g \cdot \left(\frac{D_j}{D_g} \right)^{\frac{1}{4}} \cdot L_g = 61.61 \ ft$$ Effective girder panel width for interior girders

*The effective girder panel width, Bg, must be less than or equal to two-thirds of the floor length. Worst case floor length is 40ft per the floor plan we know so far. Two-thirds of 40ft is 26.7 ft. Using Bgmax of 26.7 ft is reasonable for this case.

$B_{gmax} := 26.7 \ ft$

$$W_g := 1.0 \cdot \left(\frac{w_g}{L_{module}} \cdot B_{gmax} \right) \cdot L_g = 27660 \ lbf$$ Effective girder panel weight (there is no 1.5 multiplier in front of it).

Plate Mode Properties

$$\Delta_p := \frac{1 \cdot w_p \cdot U_{Lp}^4}{384 \cdot E_s \cdot I_p} = 0.04072\ \text{in}$$

$$f_{np} := 0.179 \cdot \sqrt{\frac{g}{\Delta_p}} = 17.4\ \text{Hz}$$

Beam Mode Properties

$$\Delta_j := \frac{5 \cdot w_j \cdot L_{module}^4}{384 \cdot E_s \cdot I_j} = 0.1648\ \text{in}$$

$$f_{nj} := 0.179 \cdot \sqrt{\frac{g}{\Delta_j}} = 8.66\ \text{Hz}$$

Girder panel

If Lg < Bj, the combined mode is restricted and system is effectively stiffened and deflection can be reduced. In this case, not true.

$$\Delta_g := \frac{5 \cdot w_g \cdot \left(3 \cdot W_{module}\right)^4}{384 \cdot E_s \cdot I_g} = 0.05459\ \text{in}$$

$$L_g = 360\ \text{in}$$

$$B_j = 45.15\ \text{in}$$

$$f_{ng} := 0.179 \cdot \sqrt{\frac{g}{\Delta_g}} = 15.05\ \text{Hz}$$

Combined mode

$$f_{n1} := 0.179 \cdot \sqrt{\frac{g}{\Delta_p + \Delta_j + \Delta_g}} = 6.896\ \text{Hz} \qquad f_{n2} := 0.179 \cdot \sqrt{\frac{g}{\Delta_j + \Delta_g}} = 7.51\ \text{Hz}$$

Floor fundamental frequency

Comparison between Equivalent Panel Mode Weight and the corresponding acceleration:

$$W_1 := \frac{\Delta_p}{\Delta_p + \Delta_j + \Delta_g} \cdot W_p + \frac{\Delta_j}{\Delta_p + \Delta_j + \Delta_g} \cdot W_j + \frac{\Delta_g}{\Delta_p + \Delta_j + \Delta_g} \cdot W_g = 11130\ \text{lbf}$$

Equivalent panel mode weight

$$a_{p1} := \frac{P_o \cdot \exp\left(-0.35 \cdot \frac{f_{n1}}{\text{Hz}}\right)}{\beta \cdot W_1} = 0.8713\ g$$

< 0.5%g DG 11 Limit

$$W_2 := \left(\frac{\Delta_j}{\Delta_j + \Delta_g} \cdot W_j + \frac{\Delta_g}{\Delta_j + \Delta_g} \cdot W_g\right) = 11622.40\ \text{lbf}$$

Without plate panel contribution

$$a_{p2} := \frac{P_o \cdot \exp\left(-0.35 \cdot \frac{f_{n2}}{\text{Hz}}\right)}{\beta \cdot W_2} = 0.6732\ \%\ g$$

< 0.5%g DG 11 Limit

SM-68-3/8 – Best Guess

1. INPUT: GEOMETRIC PROPERTIES

Beam section: W24x68

$d_j := 23.7\ in$

$A_j := 20.1\ in^2$

$I_{xj} := 1830\ in^4$

$SW_j := 68\ \frac{lbf}{ft}$

$b_f := 8.97\ in$

Angles section: N/A

$d_L := 0\ in$

$A_L := 0\ in^2$

$I_{xL} := 0\ in^4$

$SW_L := 0\ \frac{lbf}{ft}$

$Y_L := 0\ in$

$n_L := 0$

Girder section: W33x263

$d_g := 34.5\ in$

$A_g := 77.5\ in^2$

$I_{xg} := 15900\ in^4$

$SW_g := 263\ \frac{lbf}{ft}$

$L_g := 30\ ft$

Plate

$L_p := 40\ ft$

$t_p := \frac{3}{8}\ in$

Notation:

L: Length
W: Width
SW: Self Weight
s: spacing
d: depth
I: Inertia
n_a: number of angles

Subscripts:

j: Beam (Joist)
g: Girder
p: Plate
L: Angle

$\rho_{steel} := 490\ \frac{lbf}{ft^3}$

$g := 386.09\ \frac{in}{s^2}$

$E_s := 29000\ ksi$

$F_y := 50\ ksi$

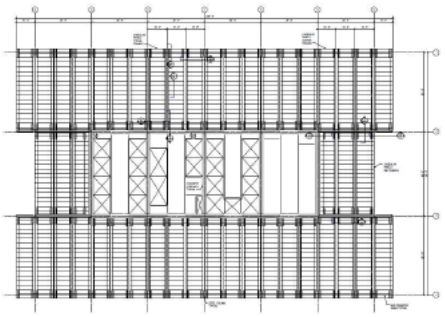

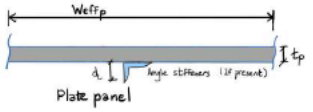

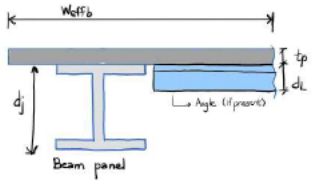

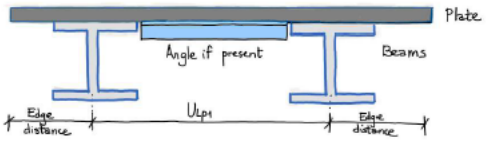

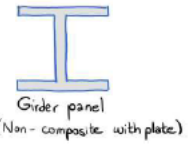

Module dimensions

$L_{module} := 40\ ft$

$W_{module} := 10\ ft$

$s_L := 1\ ft$ Angle spacing (1 ft : No angles, otherwise input angle spacing)

$d_{edge} := 2.5\ ft$ Edge distance

$U_{Lp1} := W_{module} - 2 \cdot \left(d_{edge} \right) = 5\ ft$ Center to center beam spacing

$U_{Lp2} := W_{module} - 2 \cdot \left(d_{edge} \right) - b_f = 4.253\ ft$ Clear distance between beam flanges

$U_{Lp} := U_{Lp2}$ Unsupported plate length to be used for the calculations

2. INPUT: VIBRATION PARAMETERS

Notation

$\beta_{fs} := 1.5\ \%$ — fs: Floor system Damping ratio

$\beta_{ss} := 1\ \%$ — ss: Structural System

$\beta_{a} := 1\ \%$ — a: additional (Ceiling and ductwork)

$\beta_{use} := 0.5\ \%$ — Use: Electronic office fit-out

$\beta := \beta_{fs} + \beta_{use} + \beta_{ss} + \beta_{a} = 4\ \%$ — Total damping

$P_o := 65\ \text{lbf}$

Variable: Floor system damping ratio $\left(\beta_{ss}\right)$

0.01: Structural system $\left(\beta_{fs}\right)$: Should be verified for this type of floor system.

0.01: Ceiling and ductwork $\left(\beta_{a}\right)$

0.5: Electronic office fit-out $\left(\beta_{use}\right)$

Additional damping associated with raised floors is neglected

Damping

The damping ratio, β, can be estimated using the component values shown in Table 4-2, noting that damping is cumulative. For example, a floor with ceiling and ductwork supporting an electronic office area has $\beta = \Sigma\beta_i = 0.01 + 0.01 + 0.005 = 0.025$, or 2.5% of critical damping.

Table 4-2. Recommended Component Damping Values for Use in Equation 4-1

Component	Ratio of Actual Damping-to-Critical Damping, β_i
Structural system	0.01
Ceiling and ductwork	0.01
Electronic office fit-out	0.005
Paper office fit-out	0.01
Churches, schools and malls	0.0
Full-height dry wall partitions in bay	0.02 to 0.05*

*Depending on the number of partitions in the bay and their location; nearer the center of the bay provides more damping.

3. INPUT: LOADS

Load assumptions

Live Load

$LL := 8\ psf$

3.1. LL: 6 - 8 psf for electronic office (Worst case is 6 psf)

3.2. Assume superimposed load = 4 psf. Neglecting the weight of a raised floor.

From Tate, approx. weight of raised floor:

- ConCore Panels: 8 - 14 psf (Bare)
- All Steel Panels: 5 psf (Bare)
- Cavity Floor Panels/ StoneWork® Panels: 15 psf

Dead Load

Members Self Weight

$P_{plate} := t_p \cdot \rho_{steel} = 15.31\ psf$

$D_{angles} := n_L \cdot SW_L = 0\ \frac{lbf}{ft}$

$D_{beams} := SW_j = 68\ \frac{lbf}{ft}$

$D_{girder} := SW_g = 263\ \frac{lbf}{ft}$

Notation

P: Pressure (Loads in psf)
D: Distributed dead loads [lbf/ft]
DL: Superimposed dead loads per area [psf]

Superimposed

$DL_{dg11} := 4\ psf$ Recommended sumperimposed load per DG11

$DL_{rf} := 9\ psf$ Raised floor superimposed dead load

$DL_s := DL_{dg11} + DL_{rf} = 13\ psf$ Total superimposed dead load

4: CALCS: COMPOSITE PROPERTIES

Effective slab width for plate panel

$B_{effL} := 100\ \%$ Effective width of plate for use with plate panel based on local buckling

$B_{effp} := \min\left(\left[\left(B_{effL} \cdot s_L\right)\left(0.4 \cdot U_{Lp2}\right)\right]\right) = 12\ in$

Notation

B: Widths

Plate Transformed Moment of Inertia

$d_p := d_L + t_p = 0.375\ in$

$A_p := B_{effp} \cdot t_p = 4.5\ in^2$

$y_p := \dfrac{A_L \cdot \left(d_L - y_L\right) + A_p \cdot \left(d_L + \frac{t_p}{2}\right)}{A_L + A_p} = 0.1875\ in$

Moment of inertia per angle spacing, s_L

$I_p := \dfrac{t_p^{\,3} \cdot B_{effp}}{12} + \left(A_p \cdot \left(d_p - y_p - \frac{t_p}{2}\right)^2\right) + \left(I_{xL} + A_L \cdot \left(y_p - y_L\right)^2\right) = 0.0527\ in^4$

Effective slab width for beam panel

$B_{effm} := 100\ \%$ Effective width of plate for use with beam panel based on local buckling

$B_{effb} := \min\left(\left[\left(B_{effm} \cdot W_{module}\right)\ 2 \cdot \left(0.2 \cdot \left(L_{module} + d_{edge}\right)\right)\right]\right) = 120\ in$

Beam Transformed Moment of Inertia (Calculations for entire width of module)

$A_{tpb} := \dfrac{B_{effb}}{2} \cdot t_p = 22.5\ in^2$ Effective Plate Area for beam panel

$D_t := d_j + t_p = 24.075\ in$

$y_j := \dfrac{A_j \cdot \frac{d_j}{2} + A_{tpb} \cdot \left(d_j + \frac{t_p}{2}\right)}{A_j + A_{tpb}} = 18.2078\ in$

$I_j := \dfrac{t_p^{\,3} \cdot B_{effb}}{24} + \left(A_{tpb} \cdot \left(D_t - y_j - \frac{t_p}{2}\right)^2\right) + I_{xj} + A_j \cdot \left(y_j - \frac{d_j}{2}\right)^2 = 3369\ in^4$

Girder Transformed Moment of Inertia

$I_g := I_{xg} = 15900\ in^4$ Girder is non composite, this number is directly taken from AISC manual.

5: CALCS: VIBRATION

Plate Panel Mode

$$w_p := \left(P_{plate} + \frac{D_{angles}}{L_{module}} \right) \cdot B_{effp} + B_{effp} \cdot \left(DL_s + LL \right) = 36.31 \ \frac{lbf}{ft}$$ Supported weight

$$W_p := \frac{w_p}{B_{effp}} \cdot L_{module} \cdot U_{Lp1} = 7262 \ lbf$$

Beam Panel Mode

$$w_j := D_{beams} + \left(\frac{D_{angles}}{L_{module}} \cdot \frac{U_{Lp1}}{2} \right) + \frac{W_{module}}{2} \cdot \left(P_{plate} + DL_s + LL \right) = 249.6 \ \frac{lbf}{ft}$$ Supported weight

$$D_s := \frac{t_p^{\,3}}{12} = 0.0527 \ \frac{in^4}{ft}$$ Transformed plate moment of inertia per unit width in the slab span direction.

$$D_j := \frac{I_j}{\frac{W_{module}}{2}} = 673.7 \ \frac{in^4}{ft}$$ Transformed beam moment of inertia per unit width in the beam span direction, with beam spacing of 10 ft

Options for Cj

$C_{j1} := 2.0$ Cj = 2.0. Typical bay without free edges.

$C_{j2} := 1.0$ Cj = 1.0. Typical edge panel.

$C_j := C_{j2} = 1.0$

$$B_j := C_j \cdot \left(\frac{D_s}{D_j} \right)^{\frac{1}{4}} \cdot L_{module} = 3.762 \ ft$$ Effective beam panel width

***The effective beam panel width, Bj, must be less than 2/3 of the floor width. Worst case floor width = 30 ft. And, two-thirds of 30ft is 20 ft.**

$$W_j := 1.5 \cdot \left(\frac{w_j}{W_{module}} \right) \cdot B_j \cdot L_{module} = 5634 \ lbf$$ Effective beam panel weight

Girder Panel Mode

Options for girder load: Interior girder, Wg1 and Exterior girder, Wg2

$$w_{g1} := \frac{2 \cdot w_j}{W_{module}} \cdot L_{module} + D_{girder} = 2259 \ \frac{lbf}{ft}$$ Supported weight interior girder

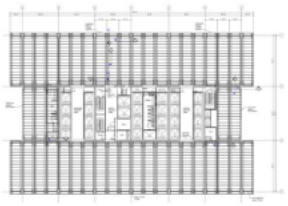

$$w_{g2} := \frac{2 \cdot w_j}{W_{module}} \cdot \frac{L_{module}}{2} + D_{girder} = 1261 \ \frac{lbf}{ft}$$ Supported weight exterior girder

$w_g := w_{g2} = 1261 \ \frac{lbf}{ft}$

$$D_g := \frac{I_g}{L_{module}} = 397.5 \ \frac{in^4}{ft}$$ Girder transformed moment of inertia per unit width

$C_g := 1.8$ Cg = 1.8. Girders supporting beams connected to the girder web

$$B_g := C_g \cdot \left(\frac{D_j}{D_g} \right)^{\frac{1}{4}} \cdot L_g = 61.61 \ ft$$ Effective girder panel width for interior girders

***The effective girder panel width, Bg, must be less than or equal to two-thirds of the floor length. Worst case floor length is 40ft per the floor plan we know so far. Two-thirds of 40ft is 26.7 ft. Using Bgmax of 26.7 ft is reasonable for this case.**

$B_{gmax} := 26.7 \ ft$

$$W_g := 1.0 \cdot \left(\frac{w_g}{L_{module}} \cdot B_{gmax} \right) \cdot L_g = 25260 \ lbf$$ Effective girder panel weight (there is no 1.5 multiplier in front of it).

Plate Mode Properties

$$\Delta_p := \frac{5 \cdot w_p \cdot U_{lp}^4}{384 \cdot E_s \cdot I_p} = 0.1747 \text{ in}$$

$$f_{np} := 0.179 \cdot \sqrt{\frac{g}{\Delta_p}} = 8.41 \text{ Hz}$$

Beam Mode Properties

$$\Delta_j := \frac{5 \cdot w_j \cdot L_{module}^4}{384 \cdot E_s \cdot I_j} = 0.1471 \text{ in}$$

$$f_{nj} := 0.179 \cdot \sqrt{\frac{g}{\Delta_j}} = 9.17 \text{ Hz}$$

Girder panel

If Lg < Bj, the combined mode is restricted and system is effectively stiffened and deflection can be reduced. In this case, not true.

$$\Delta_g := \frac{5 \cdot w_g \cdot \left(3 \cdot W_{module}\right)^4}{384 \cdot E_s \cdot I_g} = 0.04985 \text{ in}$$

$$L_g = 360 \text{ in}$$

$$B_j = 45.15 \text{ in}$$

$$f_{ng} := 0.179 \cdot \sqrt{\frac{g}{\Delta_g}} = 15.75 \text{ Hz}$$

Combined mode

$$f_{n1} := 0.179 \cdot \sqrt{\frac{g}{\Delta_p + \Delta_j + \Delta_g}} = 5.769 \text{ Hz} \qquad f_{n2} := 0.179 \cdot \sqrt{\frac{g}{\Delta_j + \Delta_g}} = 7.92 \text{ Hz}$$

Floor fundamental frequency

Comparison between Equivalent Panel Mode Weight and the corresponding acceleration:

$$W_1 := \frac{\Delta_p}{\Delta_p + \Delta_j + \Delta_g} \cdot W_p + \frac{\Delta_j}{\Delta_p + \Delta_j + \Delta_g} \cdot W_j + \frac{\Delta_g}{\Delta_p + \Delta_j + \Delta_g} \cdot W_g = 9031 \text{ lbf}$$

Equivalent panel mode weight

$$a_{p1} := \frac{P_o \cdot \exp\left(-0.35 \cdot \frac{f_{n1}}{\text{Hz}}\right)}{\beta \cdot W_1} = 2.3891 \ g$$

< 0.5%g DG 11 Limit

$$W_2 := \left(\frac{\Delta_j}{\Delta_j + \Delta_g} \cdot W_j + \frac{\Delta_g}{\Delta_j + \Delta_g} \cdot W_g\right) = 10599.27 \text{ lbf}$$

Without plate panel contribution

$$a_{p2} := \frac{P_o \cdot \exp\left(-0.35 \cdot \frac{f_{n2}}{\text{Hz}}\right)}{\beta \cdot W_2} = 0.9573 \% \ g$$

< 0.5%g DG 11 Limit

SM-94-1/2 – Worst Case

1. INPUT: GEOMETRIC PROPERTIES

Beam section: W24x94

$d_j := 24.3\ in$

$A_j := 27.7\ in^2$

$I_{xj} := 2700\ in^4$

$SW_j := 94\ \frac{lbf}{ft}$

$b_f := 9.07\ in$

Angles section: N/A

$d_L := 0\ in$

$A_L := 0\ in^2$

$I_{xL} := 0\ in^4$

$SW_L := 0\ \frac{lbf}{ft}$

$y_L := 0\ in$

$n_L := 0$

Girder section: W33x263

$d_g := 34.5\ in$

$A_g := 77.5\ in^2$

$I_{xg} := 15900\ in^4$

$SW_g := 263\ \frac{lbf}{ft}$

$L_g := 30\ ft$

Plate

$L_p := 40\ ft$

$t_p := \frac{1}{2}\ in$

Module dimensions

$L_{module} := 40\ ft$

$W_{module} := 10\ ft$

$s_L := 1\ ft$ Angle spacing (1 ft : No angles, otherwise input angle spacing)

$d_{edge} := 2.5\ ft$ Edge distance

$U_{Lp1} := W_{module} - 2 \cdot \left(d_{edge}\right) = 5\ ft$ Center to center beam spacing

$U_{Lp2} := W_{module} - 2 \cdot \left(d_{edge}\right) - b_f = 4.244\ ft$ Clear distance between beam flanges

$U_{Lp} := U_{Lp1}$ Unsupported plate length to be used for the calculations

Notation:

L: Length
W: Width
SW: Self Weight
s: spacing
d: depth
I: Inertia
n_a: number of angles

Subscripts:

j: Beam (Joist)
g: Girder
p: Plate
L: Angle

$\rho_{steel} := 490\ \frac{lbf}{ft^3}$

$g := 386.09\ \frac{in}{s^2}$

$E_s := 29000\ ksi$

$F_y := 50\ ksi$

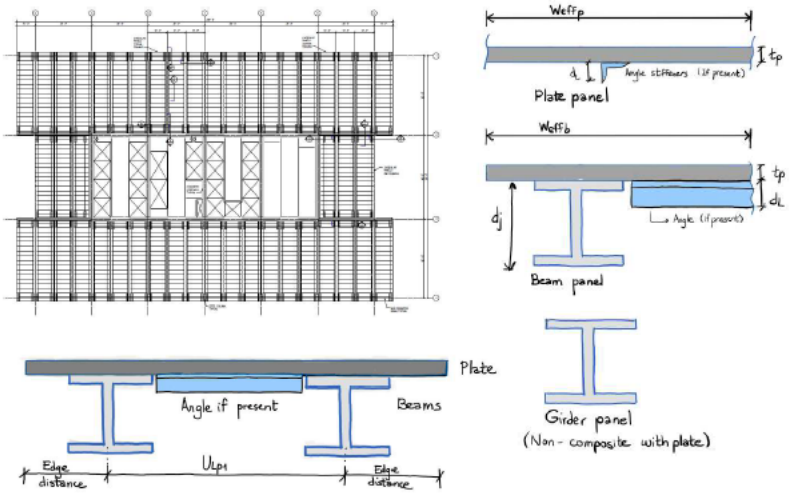

2. INPUT: VIBRATION PARAMETERS

Notation

$\beta_{fs} := 0.5\ \%$ — fs: Floor system Damping ratio

$\beta_{ss} := 1\ \%$ — ss: Structural System

$\beta_a := 1\ \%$ — a: additional (Ceiling and ductwork)

$\beta_{use} := 0.5\ \%$ — Use: Electronic office fit-out

$\beta := \beta_{fs} + \beta_{use} + \beta_{ss} + \beta_a = 3\ \%$ — Total damping

$P_o := 65\ lbf$

Variable: Floor system damping ratio $\left(\beta_{ss}\right)$

0.01: Structural system $\left(\beta_{fs}\right)$: Should be verified for this type of floor system.

0.01: Ceiling and ductwork $\left(\beta_a\right)$

0.5: Electronic office fit-out $\left(\beta_{use}\right)$

Additional damping associated with raised floors is neglected

Damping

The damping ratio, β, can be estimated using the component values shown in Table 4-2, noting that damping is cumulative. For example, a floor with ceiling and ductwork supporting an electronic office area has $\beta = \Sigma\beta_i = 0.01 + 0.01 + 0.005 = 0.025$, or 2.5% of critical damping.

Table 4-2. Recommended Component Damping Values for Use in Equation 4-1

Component	Ratio of Actual Damping-to-Critical Damping, β_i
Structural system	0.01
Ceiling and ductwork	0.01
Electronic office fit-out	0.005
Paper office fit-out	0.01
Churches, schools and malls	0.0
Full-height dry wall partitions in bay	0.02 to 0.05*

*Depending on the number of partitions in the bay and their location; nearer the center of the bay provides more damping.

3. INPUT: LOADS

Load assumptions

Live Load

$LL := 0\ psf$

3.1. LL: 6 - 8 psf for electronic office (Worst case is 6 psf)

3.2. Assume superimposed load = 4 psf. Neglecting the weight of a raised floor.

From Tate, approx. weight of raised floor:

- ConCore Panels: 8 - 14 psf (Bare)
- All Steel Panels: 5 psf (Bare)
- Cavity Floor Panels/ StoneWork® Panels: 15 psf

Dead Load

Members Self Weight

$P_{plate} := t_p \cdot \rho_{steel} = 20.42\ psf$

$D_{angles} := n_L \cdot SW_L = 0\ \frac{lbf}{ft}$

$D_{beams} := SW_j = 94\ \frac{lbf}{ft}$

$D_{girder} := SW_g = 263\ \frac{lbf}{ft}$

Notation

P: Pressure (Loads in psf)
D: Distributed dead loads [lbf/ft]
DL: Superimposed dead loads per area [psf]

Superimposed

$DL_{dg11} := 4\ psf$ Recommended sumperimposed load per DG11

$DL_{rf} := 5\ psf$ Raised floor superimposed dead load

$DL_s := DL_{dg11} + DL_{rf} = 9\ psf$ Total superimposed dead load

4: CALCS: COMPOSITE PROPERTIES

Effective slab width for plate panel

$B_{effL} := 25\ \%$ Effective width of plate for use with plate panel based on local buckling

$B_{effp} := \min\left(\left[\left(B_{effL} \cdot s_L\right)\left(0.4 \cdot U_{Lp2}\right)\right]\right) = 3\ in$

Notation

B: Widths

Plate Transformed Moment of Inertia

$d_p := d_L + t_p = 0.5\ in$

$A_p := B_{effp} \cdot t_p = 1.5\ in^2$

$y_p := \frac{A_L \cdot \left(d_L - y_L\right) + A_p \cdot \left(d_L + \frac{t_p}{2}\right)}{A_L + A_p} = 0.25\ in$

Moment of inertia per angle spacing, s_L

$I_p := \frac{t_p^{\,3} \cdot B_{effp}}{12} + \left(A_p \cdot \left(d_p - y_p - \frac{t_p}{2}\right)^2\right) + \left(I_{xL} + A_L \cdot \left(y_p - \left(d_L - y_L\right)\right)^2\right) = 0.0312\ in^4$

Effective slab width for beam panel

$B_{effm} := 25\ \%$ Effective width of plate for use with beam panel based on local buckling

$B_{effb} := \min\left(\left[\left(B_{effm} \cdot W_{module}\right)\ 2 \cdot \left(0.2 \cdot \left(L_{module} + d_{edge}\right)\right)\right]\right) = 30\ in$

Beam Transformed Moment of Inertia (Calculations for entire width of module)

$A_{tpb} := \frac{B_{effb}}{2} \cdot t_p = 7.5\ in^2$ Effective Plate Area for beam panel

$D_t := d_j + t_p = 24.8\ in$

$y_j := \frac{A_j \cdot \frac{d_j}{2} + A_{tpb} \cdot \left(d_j + \frac{t_p}{2}\right)}{A_j + A_{tpb}} = 14.792\ in$

$I_j := \frac{t_p^{\,3} \cdot B_{effb}}{24} + \left(A_{tpb} \cdot \left(D_t - y_j - \frac{t_p}{2}\right)^2\right) + I_{xj} + A_j \cdot \left(y_j - \frac{d_j}{2}\right)^2 = 3608\ in^4$

Girder Transformed Moment of Inertia

$I_g := I_{xg} = 15900\ in^4$ Girder is non composite, this number is directly taken from AISC manual.

5: CALCS: VIBRATION

Plate Panel Mode

$$w_p := \left(P_{plate} + \frac{D_{angles}}{L_{module}} \right) \cdot B_{effp} + B_{effp} \cdot \left(DL_s + LL \right) = 7.354 \ \frac{lbf}{ft}$$ Supported weight

$$W_p := \frac{w_p}{B_{effp}} \cdot L_{module} \cdot U_{Lp1} = 5883 \ lbf$$

Beam Panel Mode

$$w_j := D_{beams} + \left(\frac{D_{angles}}{L_{module}} \cdot \frac{U_{Lp1}}{2} \right) + \frac{W_{module}}{2} \cdot \left(P_{plate} + DL_s + LL \right) = 241.1 \ \frac{lbf}{ft}$$ Supported weight

$$D_s := \frac{t_p^{\,3}}{12} = 0.125 \ \frac{in^4}{ft}$$ Transformed plate moment of inertia per unit width in the slab span direction.

$$D_j := \frac{I_j}{\frac{W_{module}}{2}} = 721.5 \ \frac{in^4}{ft}$$ Transformed beam moment of inertia per unit width in the beam span direction, with beam spacing of 10 ft

Options for Cj

$C_{j1} := 2.0$ Cj = 2.0. Typical bay without free edges.

$C_{j2} := 1.0$ Cj = 1.0. Typical edge panel.

$C_j := C_{j1} = 2.0$

$$B_j := C_j \cdot \left(\frac{D_s}{D_j} \right)^{\frac{1}{4}} \cdot L_{module} = 9.178 \ ft$$ Effective beam panel width

***The effective beam panel width, Bj, must be less than 2/3 of the floor width. Worst case floor width = 30 ft. And, two-thirds of 30ft is 20 ft.**

$$W_j := 1.5 \cdot \left(\frac{w_j}{W_{module}} \right) \cdot B_j \cdot L_{module} = 13280 \ lbf$$ Effective beam panel weight

Girder Panel Mode

Options for girder load: Interior girder, Wg1 and Exterior girder, Wg2

$$w_{g1} := \frac{2 \cdot w_j}{W_{module}} \cdot L_{module} + D_{girder} = 2192 \ \frac{lbf}{ft}$$ Supported weight interior girder

$$w_{g2} := \frac{2 \cdot w_j}{W_{module}} \cdot \frac{L_{module}}{2} + D_{girder} = 1227 \ \frac{lbf}{ft}$$ Supported weight exterior girder

$w_g := w_{g1} = 2192 \ \frac{lbf}{ft}$

$$D_g := \frac{I_g}{L_{module}} = 397.5 \ \frac{in^4}{ft}$$ Girder transformed moment of inertia per unit width

$C_g := 1.8$ Cg = 1.8. Girders supporting beams connected to the girder web

$$B_g := C_g \cdot \left(\frac{D_j}{D_g} \right)^{\frac{1}{4}} \cdot L_g = 62.68 \ ft$$ Effective girder panel width for interior girders

***The effective girder panel width, Bg, must be less than or equal to two-thirds of the floor length. Worst case floor length is 40ft per the floor plan we know so far. Two-thirds of 40ft is 26.7 ft. Using Bgmax of 26.7 ft is reasonable for this case.**

$B_{gmax} := 26.7 \ ft$

$$W_g := 1.0 \cdot \left(\frac{w_g}{L_{module}} \cdot B_{gmax} \right) \cdot L_g = 43890 \ lbf$$ Effective girder panel weight (there is no 1.5 multiplier in front of it).

Plate Mode Properties

$$\Delta_p := \frac{5 \cdot w_p \cdot U_{Lp}^{4}}{384 \cdot E_s \cdot I_p} = 0.1141 \text{ in}$$

$$f_{np} := 0.179 \cdot \sqrt{\frac{g}{\Delta_p}} = 10.4 \text{ Hz}$$

Beam Mode Properties

$$\Delta_j := \frac{5 \cdot w_j \cdot L_{module}^{4}}{384 \cdot E_s \cdot I_j} = 0.1327 \text{ in}$$

$$f_{nj} := 0.179 \cdot \sqrt{\frac{g}{\Delta_j}} = 9.65 \text{ Hz}$$

Girder panel

If Lg < Bj, the combined mode is restricted and system is effectively stiffened and deflection can be reduced. In this case, not true.

$$\Delta_g := \frac{5 \cdot w_g \cdot \left(3 \cdot W_{module}\right)^{4}}{384 \cdot E_s \cdot I_g} = 0.08663 \text{ in}$$

$$L_g = 360 \text{ in}$$

$$B_j = 110.1 \text{ in}$$

$$f_{ng} := 0.179 \cdot \sqrt{\frac{g}{\Delta_g}} = 11.95 \text{ Hz}$$

Combined mode

$$f_{n1} := 0.179 \cdot \sqrt{\frac{g}{\Delta_p + \Delta_j + \Delta_g}} = 6.091 \text{ Hz} \qquad f_{n2} := 0.179 \cdot \sqrt{\frac{g}{\Delta_j + \Delta_g}} = 7.51 \text{ Hz}$$

Floor fundamental frequency

Comparison between Equivalent Panel Mode Weight and the corresponding acceleration:

$$W_1 := \frac{\Delta_p}{\Delta_p + \Delta_j + \Delta_g} \cdot W_p + \frac{\Delta_j}{\Delta_p + \Delta_j + \Delta_g} \cdot W_j + \frac{\Delta_g}{\Delta_p + \Delta_j + \Delta_g} \cdot W_g = 18700 \text{ lbf}$$

Equivalent panel mode weight

$$a_{p1} := \frac{P_o \cdot \exp\left(-0.35 \cdot \frac{f_{n1}}{\text{Hz}}\right)}{\beta \cdot W_1} = 1.3746 \text{ g}$$

< 0.5%g DG 11 Limit

$$W_2 := \left(\frac{\Delta_j}{\Delta_j + \Delta_g} \cdot W_j + \frac{\Delta_g}{\Delta_j + \Delta_g} \cdot W_g\right) = 25365.15 \text{ lbf}$$

Without plate panel contribution

$$a_{p2} := \frac{P_o \cdot \exp\left(-0.35 \cdot \frac{f_{n2}}{\text{Hz}}\right)}{\beta \cdot W_2} = 0.6167 \text{ \%g}$$

< 0.5%g DG 11 Limit

SM-94-1/2 – Best Case

1. INPUT: GEOMETRIC PROPERTIES

Beam section: W24x94

$d_j := 24.3\ in$

$A_j := 27.7\ in^2$

$I_{xj} := 2700\ in^4$

$SW_j := 94\ \frac{lbf}{ft}$

$b_f := 9.07\ in$

Angles section: N/A

$d_L := 0\ in$

$A_L := 0\ in^2$

$I_{xL} := 0\ in^4$

$SW_L := 0\ \frac{lbf}{ft}$

$Y_L := 0\ in$

$n_L := 0$

Girder section: W33x263

$d_g := 34.5\ in$

$A_g := 77.5\ in^2$

$I_{xg} := 15900\ in^4$

$SW_g := 263\ \frac{lbf}{ft}$

$L_g := 30\ ft$

Plate

$L_p := 40\ ft$

$t_p := \frac{1}{2}\ in$

Notation:

L: Length
W: Width
SW: Self Weight
s: spacing
d: depth
I: Inertia
n_a: number of angles

Subscripts:

j: Beam (Joist)
g: Girder
p: Plate
L: Angle

$\rho_{steel} := 490\ \frac{lbf}{ft^3}$

$g := 386.09\ \frac{in}{s^2}$

$E_s := 29000\ ksi$

$F_y := 50\ ksi$

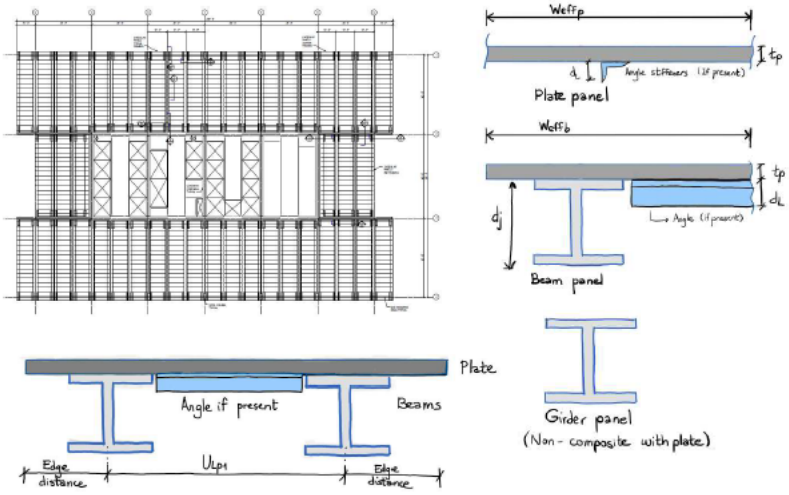

Module dimensions

$L_{module} := 40\ ft$

$W_{module} := 10\ ft$

$s_L := 1\ ft$ Angle spacing (1 ft : No angles, otherwise input angle spacing)

$d_{edge} := 2.5\ ft$ Edge distance

$L_{Lp1} := W_{module} - 2 \cdot \left(d_{edge}\right) = 5\ ft$ Center to center beam spacing

$L_{Lp2} := W_{module} - 2 \cdot \left(d_{edge}\right) - b_f = 4.244\ ft$ Clear distance between beam flanges

$L_{Lp} := L_{Lp2}$ Unsupported plate length to be used for the calculations

2. INPUT: VIBRATION PARAMETERS

Notation

$\beta_{fs} := 3.5\ \%$ — fs: Floor system Damping ratio

$\beta_{ss} := 1\ \%$ — ss: Structural System

$\beta_{a} := 1\ \%$ — a: additional (Ceiling and ductwork)

$\beta_{use} := 0.5\ \%$ — Use: Electronic office fit-out

$\beta := \beta_{fs} + \beta_{use} + \beta_{ss} + \beta_{a} = 6\ \%$ — Total damping

$P_o := 65\ lbf$

Variable: Floor system damping ratio $\left(\beta_{ss}\right)$

0.01: Structural system $\left(\beta_{fs}\right)$: Should be verified for this type of floor system.

0.01: Ceiling and ductwork $\left(\beta_{a}\right)$

0.5: Electronic office fit-out $\left(\beta_{use}\right)$

Additional damping associated with raised floors is neglected

Damping

The damping ratio, β, can be estimated using the component values shown in Table 4-2, noting that damping is cumulative. For example, a floor with ceiling and ductwork supporting an electronic office area has $\beta = \sum\beta_i = 0.01 + 0.01 + 0.005 = 0.025$, or 2.5% of critical damping.

Table 4-2. Recommended Component Damping Values for Use in Equation 4-1

Component	Ratio of Actual Damping-to-Critical Damping, β_i
Structural system	0.01
Ceiling and ductwork	0.01
Electronic office fit-out	0.005
Paper office fit-out	0.01
Churches, schools and malls	0.0
Full-height dry wall partitions in bay	0.02 to 0.05*

*Depending on the number of partitions in the bay and their location; nearer the center of the bay provides more damping.

3. INPUT: LOADS

Live Load

$LL := 8\ psf$

Dead Load

Members Self Weight

$P_{plate} := t_p \cdot \rho_{steel} = 20.42\ psf$

$D_{angles} := n_L \cdot SW_L = 0\ \frac{lbf}{ft}$

$D_{beams} := SW_j = 94\ \frac{lbf}{ft}$

$D_{girder} := SW_g = 263\ \frac{lbf}{ft}$

Superimposed

$DL_{dg11} := 4\ psf$ Recommended sumperimposed load per DG11

$DL_{rf} := 15\ psf$ Raised floor superimposed dead load

$DL_s := DL_{dg11} + DL_{rf} = 19\ psf$ Total superimposed dead load

Load assumptions

3.1. LL: 6 - 8 psf for electronic office (Worst case is 6 psf)

3.2. Assume superimposed load = 4 psf. Neglecting the weight of a raised floor.

From Tate, approx. weight of raised floor:

- ConCore Panels: 8 - 14 psf (Bare)
- All Steel Panels: 5 psf (Bare)
- Cavity Floor Panels/ StoneWork® Panels: 15 psf

Notation

P: Pressure (Loads in psf)
D: Distributed dead loads [lbf/ft]
DL: Superimposed dead loads per area [psf]

4: CALCS: COMPOSITE PROPERTIES

Effective slab width for plate panel

$B_{effL} := 100\ \%$ Effective width of plate for use with plate panel based on local buckling

$B_{effp} := \min\left(\left[\left(B_{effL} \cdot s_L\right)\left(0.4 \cdot U_{Lp2}\right)\right]\right) = 12\ in$

Notation

B: Widths

Plate Transformed Moment of Inertia

$d_p := d_L + t_p = 0.5\ in$

$A_p := B_{effp} \cdot t_p = 6\ in^2$

$y_p := \frac{A_L \cdot \left(d_L - y_L\right) + A_p \cdot \left(d_L + \frac{t_p}{2}\right)}{A_L + A_p} = 0.25\ in$

Moment of inertia per angle spacing, s_L

$I_p := \frac{t_p^{\,3} \cdot B_{effp}}{12} + \left(A_p \cdot \left(d_p - y_p - \frac{t_p}{2}\right)^2\right) + \left(I_{xL} + A_L \cdot \left(y_p - \left(d_L - y_L\right)\right)^2\right) = 0.125\ in^4$

Effective slab width for beam panel

$B_{effm} := 100\ \%$ Effective width of plate for use with beam panel based on local buckling

$B_{effb} := \min\left(\left[\left(B_{effm} \cdot W_{module}\right)\ 2 \cdot \left(0.2 \cdot \left(L_{module} + d_{edge}\right)\right)\right]\right) = 120\ in$

Beam Transformed Moment of Inertia (Calculations for entire width of module)

$A_{tpb} := \frac{B_{effb}}{2} \cdot t_p = 30\ in^2$ Effective Plate Area for beam panel

$D_t := d_j + t_p = 24.8\ in$

$y_j := \frac{A_j \cdot \frac{d_j}{2} + A_{tpb} \cdot \left(d_j + \frac{t_p}{2}\right)}{A_j + A_{tpb}} = 18.5971\ in$

$I_j := \frac{t_p^{\,3} \cdot B_{effb}}{24} + \left(A_{tpb} \cdot \left(D_t - y_j - \frac{t_p}{2}\right)^2\right) + I_{xj} + A_j \cdot \left(y_j - \frac{d_j}{2}\right)^2 = 4915\ in^4$

Girder Transformed Moment of Inertia

$I_g := I_{xg} = 15900\ in^4$ Girder is non composite, this number is directly taken from AISC manual

5: CALCS: VIBRATION

Plate Panel Mode

$$w_p := \left(P_{plate} + \frac{D_{angles}}{L_{module}} \right) \cdot B_{effp} + B_{effp} \cdot \left(DL_s + LL \right) = 47.42 \ \frac{lbf}{ft}$$ Supported weight

$$W_p := \frac{w_p}{B_{effp}} \cdot L_{module} \cdot U_{Lp1} = 9483 \ lbf$$

Beam Panel Mode

$$w_j := D_{beams} + \left(\frac{D_{angles}}{L_{module}} \cdot \frac{U_{Lp1}}{2} \right) + \frac{W_{module}}{2} \cdot \left(P_{plate} + DL_s + LL \right) = 331.1 \ \frac{lbf}{ft}$$ Supported weight

$$D_s := \frac{t_p^{\,3}}{12} = 0.125 \ \frac{in^4}{ft}$$ Transformed plate moment of inertia per unit width in the slab span direction.

$$D_j := \frac{I_j}{\frac{W_{module}}{2}} = 983.0 \ \frac{in^4}{ft}$$ Transformed beam moment of inertia per unit width in the beam span direction, with beam spacing of 10 ft

Options for Cj

$C_{j1} := 2.0$ Cj = 2.0. Typical bay without free edges.

$C_{j2} := 1.0$ Cj = 1.0. Typical edge panel.

$C_j := C_{j2} = 1.0$

$$B_j := C_j \cdot \left(\frac{D_s}{D_j} \right)^{\frac{1}{4}} \cdot L_{module} = 4.248 \ ft$$ Effective beam panel width

***The effective beam panel width, Bj, must be less than 2/3 of the floor width. Worst case floor width = 30 ft. And, two-thirds of 30ft is 20 ft.**

$$W_j := 1.5 \cdot \left(\frac{w_j}{W_{module}} \right) \cdot B_j \cdot L_{module} = 8438 \ lbf$$ Effective beam panel weight

Girder Panel Mode

Options for girder load: Interior girder, Wg1 and Exterior girder, Wg2

$$w_{g1} := \frac{2 \cdot w_j}{W_{module}} \cdot L_{module} + D_{girder} = 2912 \ \frac{lbf}{ft}$$ Supported weight interior girder

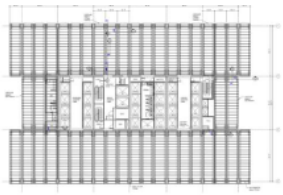

$$w_{g2} := \frac{2 \cdot w_j}{W_{module}} \cdot \frac{L_{module}}{2} + D_{girder} = 1587 \ \frac{lbf}{ft}$$ Supported weight exterior girder

$w_g := w_{g2} = 1587 \ \frac{lbf}{ft}$

$$D_g := \frac{I_g}{L_{module}} = 397.5 \ \frac{in^4}{ft}$$ Girder transformed moment of inertia per unit width

$C_g := 1.8$ Cg = 1.8. Girders supporting beams connected to the girder web

$$B_g := C_g \cdot \left(\frac{D_j}{D_g} \right)^{\frac{1}{4}} \cdot L_g = 67.72 \ ft$$ Effective girder panel width for interior girders

***The effective girder panel width, Bg, must be less than or equal to two-thirds of the floor length. Worst case floor length is 40ft per the floor plan we know so far. Two-thirds of 40ft is 26.7 ft. Using Bgmax of 26.7 ft is reasonable for this case.**

$B_{gmax} := 26.7 \ ft$

$$W_g := 1.0 \cdot \left(\frac{w_g}{L_{module}} \cdot B_{gmax} \right) \cdot L_g = 31790 \ lbf$$ Effective girder panel weight (there is no 1.5 multiplier in front of it).

Plate Mode Properties

$$\Delta_p := \frac{1 \cdot w_p \cdot U_{Lp}^4}{384 \cdot E_s \cdot I_p} = 0.01910 \text{ in}$$

$$f_{np} := 0.179 \cdot \sqrt{\frac{g}{\Delta_p}} = 25.5 \text{ Hz}$$

Beam Mode Properties

$$\Delta_j := \frac{5 \cdot w_j \cdot L_{module}^4}{384 \cdot E_s \cdot I_j} = 0.1338 \text{ in}$$

$$f_{nj} := 0.179 \cdot \sqrt{\frac{g}{\Delta_j}} = 9.62 \text{ Hz}$$

Girder panel

If Lg < Bj, the combined mode is restricted and system is effectively stiffened and deflection can be reduced. In this case, not true.

$$\Delta_g := \frac{5 \cdot w_g \cdot \left(3 \cdot W_{module}\right)^4}{384 \cdot E_s \cdot I_g} = 0.06274 \text{ in}$$

$$L_g = 360 \text{ in}$$

$$B_j = 50.97 \text{ in}$$

$$f_{ng} := 0.179 \cdot \sqrt{\frac{g}{\Delta_g}} = 14.04 \text{ Hz}$$

Combined mode

$$f_{n1} := 0.179 \cdot \sqrt{\frac{g}{\Delta_p + \Delta_j + \Delta_g}} = 7.574 \text{ Hz}$$

$$f_{n2} := 0.179 \cdot \sqrt{\frac{g}{\Delta_j + \Delta_g}} = 7.93 \text{ Hz}$$

Floor fundamental frequency

Comparison between Equivalent Panel Mode Weight and the corresponding acceleration:

$$W_1 := \frac{\Delta_p}{\Delta_p + \Delta_j + \Delta_g} \cdot W_p + \frac{\Delta_j}{\Delta_p + \Delta_j + \Delta_g} \cdot W_j + \frac{\Delta_g}{\Delta_p + \Delta_j + \Delta_g} \cdot W_g = 15320 \text{ lbf}$$

Equivalent panel mode weight

$$a_{p1} := \frac{P_o \cdot \exp\left(-0.35 \cdot \frac{f_{n1}}{\text{Hz}}\right)}{\beta \cdot W_1} = 0.499 \% \, g$$

< 0.5%g DG 11 Limit

$$W_2 := \left(\frac{\Delta_j}{\Delta_j + \Delta_g} \cdot W_j + \frac{\Delta_g}{\Delta_j + \Delta_g} \cdot W_g\right) = 15891.52 \text{ lbf}$$

Without plate panel contribution

$$a_{p2} := \frac{P_o \cdot \exp\left(-0.35 \cdot \frac{f_{n2}}{\text{Hz}}\right)}{\beta \cdot W_2} = 0.4243 \% \, g$$

< 0.5%g DG 11 Limit

1. INPUT: GEOMETRIC PROPERTIES

Beam section: W24x94

$d_j := 24.3\ in$

$A_j := 27.7\ in^2$

$I_{xj} := 2700\ in^4$

$SW_j := 94\ \frac{lbf}{ft}$

$b_f := 9.07\ in$

Angles section: N/A

$d_L := 0\ in$

$A_L := 0\ in^2$

$I_{xL} := 0\ in^4$

$SW_L := 0\ \frac{lbf}{ft}$

$y_L := 0\ in$

$n_L := 0$

Girder section: W33x263

$d_g := 34.5\ in$

$A_g := 77.5\ in^2$

$I_{xg} := 15900\ in^4$

$SW_g := 263\ \frac{lbf}{ft}$

$L_g := 30\ ft$

Plate

$L_p := 40\ ft$

$t_p := \frac{1}{2}\ in$

Notation:

L: Length
W: Width
SW: Self Weight
s: spacing
d: depth
I: Inertia
n_a: number of angles

Subscripts:

j: Beam (Joist)
g: Girder
p: Plate
L: Angle

$\rho_{steel} := 490\ \frac{lbf}{ft^3}$

$g := 386.09\ \frac{in}{s^2}$

$E_s := 29000\ ksi$

$F_y := 50\ ksi$

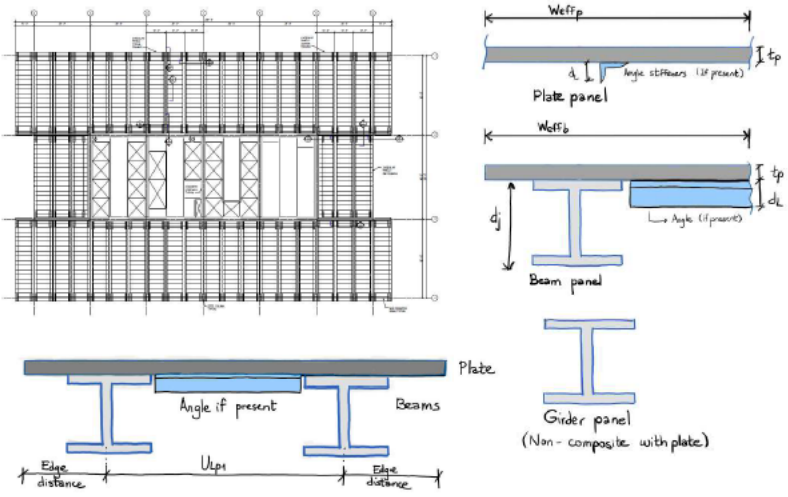

Module dimensions

$L_{module} := 40\ ft$

$W_{module} := 10\ ft$

$s_L := 1\ ft$ Angle spacing (1 ft : No angles, otherwise input angle spacing)

$d_{edge} := 2.5\ ft$ Edge distance

$U_{Lp1} := W_{module} - 2 \cdot \left(d_{edge} \right) = 5\ ft$ Center to center beam spacing

$U_{Lp2} := W_{module} - 2 \cdot \left(d_{edge} \right) - b_f = 4.244\ ft$ Clear distance between beam flanges

$U_{Lp} := U_{Lp2}$ Unsupported plate length to be used for the calculations

2. INPUT: VIBRATION PARAMETERS

Notation

$\beta_{fs} := 1.5\ \%$ — fs: Floor system Damping ratio

$\beta_{ss} := 1\ \%$ — ss: Structural System

$\beta_{a} := 1\ \%$ — a: additional (Ceiling and ductwork)

$\beta_{use} := 0.5\ \%$ — Use: Electronic office fit-out

$\beta := \beta_{fs} + \beta_{use} + \beta_{ss} + \beta_{a} = 4\ \%$ — Total damping

$P_o := 65\ lbf$

Variable: Floor system damping ratio $\left(\beta_{ss}\right)$

0.01: Structural system $\left(\beta_{fs}\right)$: Should be verified for this type of floor system.

0.01: Ceiling and ductwork $\left(\beta_{a}\right)$

0.5: Electronic office fit-out $\left(\beta_{use}\right)$

Additional damping associated with raised floors is neglected

Damping

The damping ratio, β, can be estimated using the component values shown in Table 4-2, noting that damping is cumulative. For example, a floor with ceiling and ductwork supporting an electronic office area has $\beta = \Sigma\beta_i = 0.01 + 0.01 + 0.005 = 0.025$, or 2.5% of critical damping.

Table 4-2. Recommended Component Damping Values for Use in Equation 4-1

Component	Ratio of Actual Damping-to-Critical Damping, β_i
Structural system	0.01
Ceiling and ductwork	0.01
Electronic office fit-out	0.005
Paper office fit-out	0.01
Churches, schools and malls	0.0
Full-height dry wall partitions in bay	0.02 to 0.05*

*Depending on the number of partitions in the bay and their location; nearer the center of the bay provides more damping.

3. INPUT: LOADS

Live Load

$LL := 8\ psf$

Dead Load

Members Self Weight

$P_{plate} := t_p \cdot \rho_{steel} = 20.42\ psf$

$D_{angles} := n_L \cdot SW_L = 0\ \frac{lbf}{ft}$

$D_{beams} := SW_j = 94\ \frac{lbf}{ft}$

$D_{girder} := SW_g = 263\ \frac{lbf}{ft}$

Superimposed

$DL_{dg11} := 4\ psf$ Recommended sumperimposed load per DG11

$DL_{rf} := 9\ psf$ Raised floor superimposed dead load

$DL_s := DL_{dg11} + DL_{rf} = 13\ psf$ Total superimposed dead load

Load assumptions

3.1. LL: 6 - 8 psf for electronic office (Worst case is 6 psf)

3.2. Assume superimposed load = 4 psf. Neglecting the weight of a raised floor.

From Tate, approx. weight of raised floor:

- ConCore Panels: 8 - 14 psf (Bare)
- All Steel Panels: 5 psf (Bare)
- Cavity Floor Panels/ StoneWork® Panels: 15 psf

Notation

P: Pressure (Loads in psf)
D: Distributed dead loads [lbf/ft]
DL: Superimposed dead loads per area [psf]

4: CALCS: COMPOSITE PROPERTIES

Effective slab width for plate panel

$B_{effL} := 100\ \%$ Effective width of plate for use with plate panel based on local buckling

$B_{effp} := \min\left(\left[\left(B_{effL} \cdot s_L\right)\left(0.4 \cdot U_{Lp2}\right)\right]\right) = 12\ in$

Notation

B: Widths

Plate Transformed Moment of Inertia

$d_p := d_L + t_p = 0.5\ in$

$A_p := B_{effp} \cdot t_p = 6\ in^2$

$y_p := \frac{A_L \cdot \left(d_L - y_L\right) + A_p \cdot \left(d_L + \frac{t_p}{2}\right)}{A_L + A_p} = 0.25\ in$

Moment of inertia per angle spacing, s_L

$I_p := \frac{t_p^{\,3} \cdot B_{effp}}{12} + \left(A_p \cdot \left(d_p - y_p - \frac{t_p}{2}\right)^2\right) + \left(I_{xL} + A_L \cdot \left(y_p - \left(d_L - y_L\right)\right)^2\right) = 0.125\ in^4$

Effective slab width for beam panel

$B_{effm} := 100\ \%$ Effective width of plate for use with beam panel based on local buckling

$B_{effb} := \min\left(\left[\left(B_{effm} \cdot W_{module}\right)\ 2 \cdot \left(0.2 \cdot \left(L_{module} + d_{edge}\right)\right)\right]\right) = 120\ in$

Beam Transformed Moment of Inertia (Calculations for entire width of module)

$A_{tpb} := \frac{B_{effb}}{2} \cdot t_p = 30\ in^2$ Effective Plate Area for beam panel

$D_t := d_j + t_p = 24.8\ in$

$y_j := \frac{A_j \cdot \frac{d_j}{2} + A_{tpb} \cdot \left(d_j + \frac{t_p}{2}\right)}{A_j + A_{tpb}} = 18.5971\ in$

$I_j := \frac{t_p^{\,3} \cdot B_{effb}}{24} + \left(A_{tpb} \cdot \left(D_t - y_j - \frac{t_p}{2}\right)^2\right) + I_{xj} + A_j \cdot \left(y_j - \frac{d_j}{2}\right)^2 = 4915\ in^4$

Girder Transformed Moment of Inertia

$I_g := I_{xg} = 15900\ in^4$ Girder is non composite, this number is directly taken from AISC manual.

5: CALCS: VIBRATION

Plate Panel Mode

$$w_p := \left(P_{plate} + \frac{D_{angles}}{L_{module}} \right) \cdot B_{effp} + B_{effp} \cdot \left(DL_s + LL \right) = 41.42 \ \frac{lbf}{ft}$$ Supported weight

$$W_p := \frac{w_p}{B_{effp}} \cdot L_{module} \cdot U_{Lp1} = 8283 \ lbf$$

Beam Panel Mode

$$w_j := D_{beams} + \left(\frac{D_{angles}}{L_{module}} \cdot \frac{U_{Lp1}}{2} \right) + \frac{W_{module}}{2} \cdot \left(P_{plate} + DL_s + LL \right) = 301.1 \ \frac{lbf}{ft}$$ Supported weight

$$D_s := \frac{t_p^3}{12} = 0.125 \ \frac{in^4}{ft}$$ Transformed plate moment of inertia per unit width in the slab span direction.

$$D_j := \frac{I_j}{\frac{W_{module}}{2}} = 983.0 \ \frac{in^4}{ft}$$ Transformed beam moment of inertia per unit width in the beam span direction, with beam spacing of 10 ft

Options for Cj

$C_{j1} := 2.0$ Cj = 2.0. Typical bay without free edges.

$C_{j2} := 1.0$ Cj = 1.0. Typical edge panel.

$C_j := C_{j2} = 1.0$

$$B_j := C_j \cdot \left(\frac{D_s}{D_j} \right)^{\frac{1}{4}} \cdot L_{module} = 4.248 \ ft$$ Effective beam panel width

*The effective beam panel width, Bj, must be less than 2/3 of the floor width. Worst case floor width = 30 ft. And, two-thirds of 30ft is 20 ft.

$$W_j := 1.5 \cdot \left(\frac{w_j}{W_{module}} \right) \cdot B_j \cdot L_{module} = 7673 \ lbf$$ Effective beam panel weight

$$B_g := C_g \cdot \left(\frac{D_j}{D_g} \right)^{\frac{1}{4}} \cdot L_g = 67.72 \ ft$$ Effective girder panel width for interior girders

*The effective girder panel width, Bg, must be less than or equal to two-thirds of the floor length. Worst case floor length is 40ft per the floor plan we know so far. Two-thirds of 40ft is 26.7 ft. Using Bgmax of 26.7 ft is reasonable for this case.

$B_{gmax} := 26.7 \ ft$

$$W_g := 1.0 \cdot \left(\frac{w_g}{L_{module}} \cdot B_{gmax} \right) \cdot L_g = 29380 \ lbf$$ Effective girder panel weight (there is no 1.5 multiplier in front of it).

Girder Panel Mode

Options for girder load: Interior girder, Wg1 and Exterior girder, Wg2

$$w_{g1} := \frac{2 \cdot w_j}{W_{module}} \cdot L_{module} + D_{girder} = 2672 \ \frac{lbf}{ft}$$ Supported weight interior girder

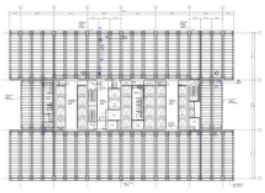

$$w_{g2} := \frac{2 \cdot w_j}{W_{module}} \cdot \frac{L_{module}}{2} + D_{girder} = 1467 \ \frac{lbf}{ft}$$ Supported weight exterior girder

$w_g := w_{g2} = 1467 \ \frac{lbf}{ft}$

$$D_g := \frac{I_g}{L_{module}} = 397.5 \ \frac{in^4}{ft}$$ Girder transformed moment of inertia per unit width

$C_g := 1.8$ Cg = 1.8. Girders supporting beams connected to the girder web

Plate Mode Properties

$$\Delta_p := \frac{5 \cdot w_p \cdot U_{Lp}^4}{384 \cdot E_s \cdot I_p} = 0.08341\ \text{in}$$

$$f_{np} := 0.179 \cdot \sqrt{\frac{g}{\Delta_p}} = 12.2\ \text{Hz}$$

Beam Mode Properties

$$\Delta_j := \frac{5 \cdot w_j \cdot L_{module}^4}{384 \cdot E_s \cdot I_j} = 0.1217\ \text{in}$$

$$f_{nj} := 0.179 \cdot \sqrt{\frac{g}{\Delta_j}} = 10.1\ \text{Hz}$$

Girder panel

If Lg < Bj, the combined mode is restricted and system is effectively stiffened and deflection can be reduced. In this case, not true.

$$\Delta_g := \frac{5 \cdot w_g \cdot \left(3 \cdot W_{module}\right)^4}{384 \cdot E_s \cdot I_g} = 0.05800\ \text{in}$$

$L_g = 360\ \text{in}$

$B_j = 50.97\ \text{in}$

$$f_{ng} := 0.179 \cdot \sqrt{\frac{g}{\Delta_g}} = 14.60\ \text{Hz}$$

Combined mode

$$f_{n1} := 0.179 \cdot \sqrt{\frac{g}{\Delta_p + \Delta_j + \Delta_g}} = 6.857\ \text{Hz}$$

$$f_{n2} := 0.179 \cdot \sqrt{\frac{g}{\Delta_j + \Delta_g}} = 8.3\ \text{Hz}$$

Floor fundamental frequency

Comparison between Equivalent Panel Mode Weight and the corresponding acceleration:

$$W_1 := \frac{\Delta_p}{\Delta_p + \Delta_j + \Delta_g} \cdot W_p + \frac{\Delta_j}{\Delta_p + \Delta_j + \Delta_g} \cdot W_j + \frac{\Delta_g}{\Delta_p + \Delta_j + \Delta_g} \cdot W_g = 12650\ \text{lbf}$$

Equivalent panel mode weight

$$a_{p1} := \frac{P_o \cdot \exp\left(-0.35 \cdot \frac{f_{n1}}{\text{Hz}}\right)}{\beta \cdot W_1} = 1.165\ \%\ g$$

< 0.5%g DG 11 Limit

$$W_2 := \left(\frac{\Delta_j}{\Delta_j + \Delta_g} \cdot W_j + \frac{\Delta_g}{\Delta_j + \Delta_g} \cdot W_g\right) = 14681.39\ \text{lbf}$$

Without plate panel contribution

$$a_{p2} := \frac{P_o \cdot \exp\left(-0.35 \cdot \frac{f_{n2}}{\text{Hz}}\right)}{\beta \cdot W_2} = 0.6064\ \%\ g$$

< 0.5%g DG 11 Limit

D. Analytical Calculations Based on SCI-P354 – Light Steel Floors

SM-68-3/8

1. INPUT: GEOMETRIC PROPERTIES

Beam section: W24x68

$d_j := 23.7\ in$

$A_j := 20.1\ in^2$

$I_{xj} := 1830\ in^4 = 76170\ cm^4$

$SW_j := 68\ \frac{lbf}{ft}$

$b_f := 8.97\ in$

Angles section (N/A)

$d_L := 0\ in$

$A_L := 0\ in^2$

$I_{xL} := 0\ in^4$

$SW_L := 0\ \frac{lbf}{ft}$

$y_L := 0\ in$

$n_a := 0$

Plate

$L_p := 40\ ft$

$t_p := \frac{3}{8}\ in$

Notation:

L: Length
W: Width
SW: Self Weight
s: spacing
d: depth
I: Inertia

$\rho_{steel} := 490\ \frac{lbf}{ft^3}$

$g := 386.09\ \frac{in}{s^2}$

$E_s := 29000\ ksi$

$F_y := 50\ ksi$

Subscripts:

j: Beam (Joist)
g: Girder
p: Plate

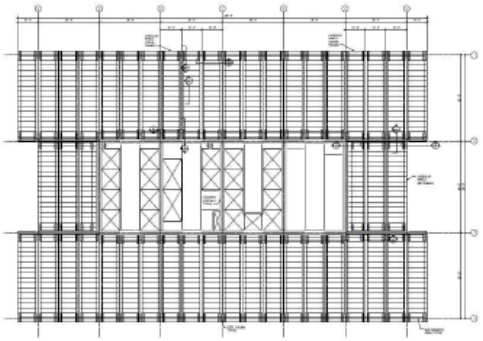

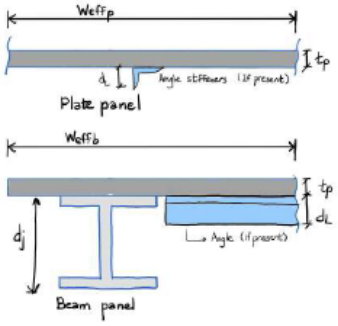

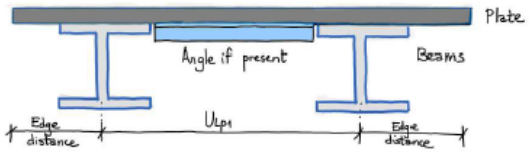

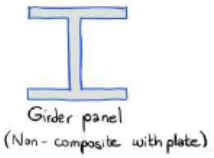

Module dimensions

$L_y := 40\ ft$

$L_x := 10\ ft$

$d_{edge} := 2.5\ ft$ Edge distance

$U_{Lp1} := L_x - 2 \cdot \left(d_{edge}\right) = 5\ ft$ Center to center beam spacing

$U_{Lp2} := L_x - 2 \cdot \left(d_{edge}\right) - b_f = 4.2525\ ft$ Clear distance between beam flanges

$U_{Lp} := U_{Lp2}$ Unsupported plate length to be used for the calculations

Floor loading

$D_{imposed} := 2.5 \frac{kN}{m^2} = 52.21\ psf$ Service sumperimposed load pe SCI P354

$P_{plate} := t_p \cdot \rho_{steel} = 15.31\ psf$ Slab (Steel plate)

$P_{beams} := \frac{\frac{SW_j}{U_{Lp}}}{2} = 31.9812\ psf$ Beams

$P_{angles} := \frac{SW_L}{s_L} = 0\ psf$ Angles

$P_{cs} := \frac{SW_L}{s_L} = 0\ psf$ Ceiling and services

$P_{rf} := 9\ psf$ Raised floor superimposed dead load

$P_{SCI} := 0.1 \cdot D_{imposed} = 5.221\ psf$ Recommended imposed load per SCI P354

$P_{total} := P_{plate} + P_{beams} + P_{angles} + P_{cs} + P_{rf} + P_{SCI} = 61.52\ psf$

$m := \frac{P_{total}}{g} = 61.51 \frac{lb}{ft^2}$ Distributed mass

Assume beam and plate act compositely.

Composite Properties

$b_e := \min\left(\left[\frac{L_y}{4}\ U_{Lp}\right]\right) = 4.2525\ ft$ Effective plate width

$A_{tpb} := b_e \cdot t_p = 19.14\ in^2$ Effective Plate Area for beam panel

$D_t := d_j + t_p = 24.08\ in$

$y := \frac{A_j \cdot \frac{d_j}{2} + A_{tpb} \cdot \left(d_j + \frac{t_p}{2}\right)}{A_j + A_{tpb}} = 17.72\ in$ Position of elastic neutral axis

$I := \left(\frac{t_p^3 \cdot b_e}{12} + \left(A_{tpb} \cdot \left(D_t - y - \frac{t_p}{2}\right)^2\right) + I_{xj} + A_j \cdot \left(y - \frac{d_j}{2}\right)^2\right) \cdot \frac{1}{U_{Lp}} = 764.4 \frac{in^4}{ft}$ Composite moment of inertia

$I = 104388.89 \frac{cm^4}{m}$

2. NATURAL FREQUENCY

$$W := P_{total} \cdot L_y = 2461 \ \frac{lbf}{ft}$$

Assume simply supported end condition

$$\delta := \frac{5 \cdot W \cdot L_y^{\ 3}}{384 \cdot E_s \cdot I} = 0.1598 \ in$$

$$f_o := \frac{18 \cdot 1 \ mm}{\sqrt{\delta \cdot 1 \ mm}} \cdot 1 \ Hz = 8.933 \ Hz$$

3. MODAL MASS

$n_y := 1$ Number of consecutive floor spans in the direction of the floor joists (where ny ≤ 4)

$n_x := 1$ Number of consecutive floor spans in the direction of the floor joists (where ny ≤ 4)

$$L_{eff1} := n_y \cdot \left(0.2 \cdot \frac{L_y^{\ 2}}{1 \ m} - 2.1 \cdot L_y + 7.5 \ m \right) \cdot \sqrt{\frac{I}{5.3 \cdot 10^{-6} \ m^3}} = 535.3 \ ft$$

$$L_{eff} := \min\left(\left[\left(L_{eff1} \right) \left(n_y \cdot L_y \right) \right] \right) = 40 \ ft$$

$$S_1 := 0.75 \cdot \left(L_x + 1 \ m \right) \cdot \sqrt{\frac{I}{5.3 \cdot 10^{-6} \ m^3}} + 5.9 \cdot \left(0.6 \ m - \frac{U_{Lp1}}{2} \right) = 136.7 \ ft$$

$$S := \min\left(\left[S_1 \ \ n_x \cdot L_x \right] \right) = 10 \ ft$$

$$M := m \cdot L_{eff} \cdot S = 11160 \ kg$$

4. FLOOR RESPONSE

$\mu_e := 1$

$\mu_r := 1$

$Q := 746 \ N$

$$W := \frac{8}{f_o} = 0.8955 \ s$$

$$a_{wrms} := 2 \cdot \pi \cdot \mu_e \cdot \mu_r \cdot \frac{185 \ Hz^{0.3}}{M \cdot f_o^{\ 0.3}} \cdot \frac{Q}{700} \cdot \frac{1}{\sqrt{2}} \cdot \frac{W}{s} = 1.4345 \cdot \frac{1}{s^2} \ in$$

Response Factor

$$R := \frac{a_{wrms}}{0.005 \frac{m}{s^2}} = 7.2873$$

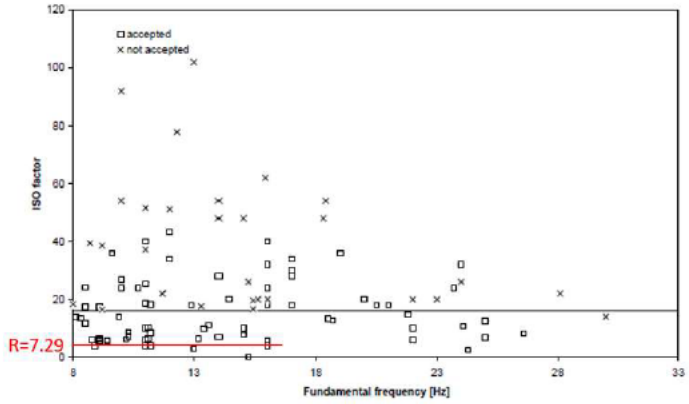

The floor is acceptable for continuous vibrations. No need to consider the effect of intermittent vibrations.

1. INPUT: GEOMETRIC PROPERTIES

Beam section: W24x94

$d_j := 24.3\ in$

$A_j := 27.7\ in^2$

$I_{xj} := 2700\ in^4 = 112382\ cm^4$

$SW_j := 94\ \frac{lbf}{ft}$

$b_f := 9.07\ in$

Angles section (N/A)

$d_L := 0\ in$

$A_L := 0\ in^2$

$I_{xL} := 0\ in^4$

$SW_L := 0\ \frac{lbf}{ft}$

$y_L := 0\ in$

$n_a := 0$

Plate

$L_p := 40\ ft$

$t_p := \frac{1}{2}\ in$

Notation:

L: Length
W: Width
SW: Self Weight
s: spacing
d: depth
I: Inertia

Subscripts:

j: Beam (Joist)
g: Girder
p: Plate

$\rho_{steel} := 490\ \frac{lbf}{ft^3}$

$g := 386.09\ \frac{in}{s^2}$

$E_s := 29000\ ksi$

$F_y := 50\ ksi$

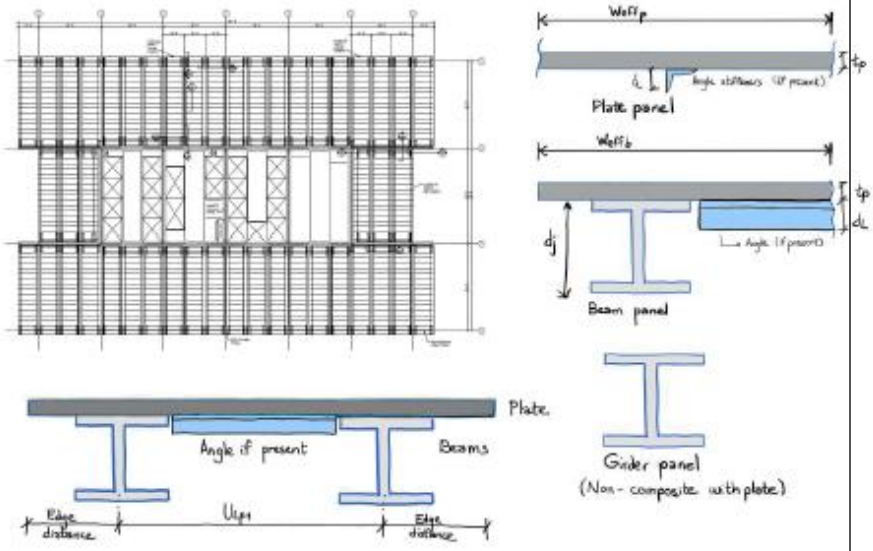

Module dimensions

$L_y := 40\ ft$

$L_x := 10\ ft$

$d_{edge} := 2.5\ ft$ Edge distance

$U_{Lp1} := L_x - 2 \cdot \left(d_{edge}\right) = 5\ ft$ Center to center beam spacing

$U_{Lp2} := L_x - 2 \cdot \left(d_{edge}\right) - b_f = 4.2442\ ft$ Clear distance between beam flanges

$U_{Lp} := U_{Lp2}$ Unsupported plate length to be used for the calculations

Floor loading

$D_{imposed} := 2.5 \frac{kN}{m^2} = 52.21\ psf$ Service sumperimposed load pe SCI P354

$P_{plate} := t_p \cdot \rho_{steel} = 20.42\ psf$ Slab (Steel plate)

$P_{beams} := \frac{\frac{SW_j}{U_{Lp}}}{2} = 44.2961\ psf$ Beams

$P_{angles} := \frac{SW_L}{s_L} = 0\ psf$ Angles

$P_{cs} := \frac{SW_L}{s_L} = 0\ psf$ Ceiling and services

$P_{rf} := 9\ psf$ Raised floor superimposed dead load

$P_{SCI} := 0.1 \cdot D_{imposed} = 5.221\ psf$ Recommended imposed load per SCI P354

$P_{total} := P_{plate} + P_{beams} + P_{angles} + P_{cs} + P_{rf} + P_{SCI} = 78.93\ psf$

$m := \frac{P_{total}}{g} = 78.93 \frac{lb}{ft^2}$ Distributed mass

Assume beam and plate act compositely.

Composite Properties

$b_e := \min\left(\left[\frac{L_y}{4}\ U_{Lp}\right]\right) = 4.2442\ ft$ Effective plate width

$A_{tpb} := \frac{b_e}{2} \cdot t_p = 12.73\ in^2$ Effective Plate Area for beam panel

$D_t := d_j + t_p = 24.80\ in$

$y := \frac{A_j \cdot \frac{d_j}{2} + A_{tpb} \cdot \left(d_j + \frac{t_p}{2}\right)}{A_j + A_{tpb}} = 16.05\ in$ Position of elastic neutral axis

$I := \left(\frac{t_p^3 \cdot b_e}{2 \cdot 12} + \left(A_{tpb} \cdot \left(D_t - y - \frac{t_p}{2}\right)^2\right) + I_{xj} + A_j \cdot \left(y - \frac{d_j}{2}\right)^2\right) \cdot \frac{1}{U_{Lp}} = 952.2 \frac{in^4}{ft}$ Composite moment of inertia

$I = 130038.08 \frac{cm^4}{m}$

2. NATURAL FREQUENCY

$W := P_{total} \cdot L_y = 3157 \frac{lbf}{ft}$

Assume simply supported end condition

$\delta := \frac{5 \cdot W \cdot L_y^{\,3}}{384 \cdot E_s \cdot I} = 0.1646\ in$

$f_o := \frac{18 \cdot 1\ mm}{\sqrt{\delta \cdot 1\ mm}} \cdot 1\ Hz = 8.802\ Hz$

3. MODAL MASS

$n_y := 1$ Number of consecutive floor spans in the direction of the floor joists (where ny ≤ 4)

$n_x := 1$ Number of consecutive floor spans in the direction of the floor joists (where ny ≤ 4)

$L_{effi} := n_y \cdot \left(0.2 \cdot \frac{L_y^{\,2}}{1\ m} - 2.1 \cdot L_y + 7.5\ m \right) \cdot \sqrt{\frac{I}{5.3 \cdot 10^{-6}\ m^3}} = 597.5\ ft$

$L_{eff} := \min\left(\left[\left(L_{effi} \right) \left(n_y \cdot L_y \right) \right] \right) = 40\ ft$

$S_i := 0.75 \cdot \left(L_x + 1\ m \right) \cdot \sqrt{\frac{I}{5.3 \cdot 10^{-6}\ m^3}} + 5.9 \cdot \left(0.6\ m - \frac{U_{Lp1}}{2} \right) = 152.9\ ft$

$S := \min\left(\left[S_i \ \ n_x \cdot L_x \right] \right) = 10\ ft$

$M := m \cdot L_{eff} \cdot S = 14320\ kg$

4. FLOOR RESPONSE

$\mu_e := 1$

$\mu_r := 1$

$Q := 746\ N$

$W := \frac{8}{f_o} = 0.9089\ s$

$a_{wrms} := 2 \cdot \pi \cdot \mu_e \cdot \mu_r \cdot \frac{185\ Hz^{0.3}}{M \cdot f_o^{\,0.3}} \cdot \frac{Q}{700} \cdot \frac{1}{\sqrt{2}} \cdot \frac{W}{s} = 1.1397 \cdot \frac{1}{s^2}\ in$

Response Factor

$$R := \frac{a_{wrms}}{0.005 \frac{m}{s^2}} = 5.7896$$

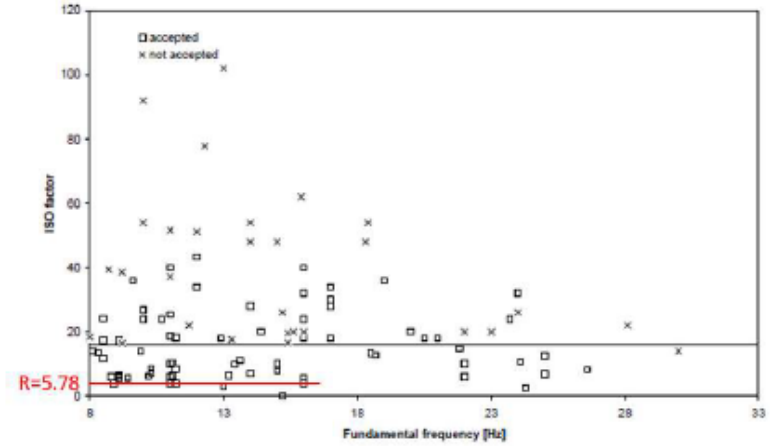

The floor is acceptable for continuous vibrations. No need to consider the effect of intermittent vibrations.

E. Calculations for FE Modeling based on DG11 - Calibration Example

Deck Slab

$d_e := 3.25\ in$

$d_r := 2\ in$

$d_s := d_e + d_r = 5.25\ in$

$w := 12\ in$

$w_r := 5\ in$

$w_d := 1\ in$

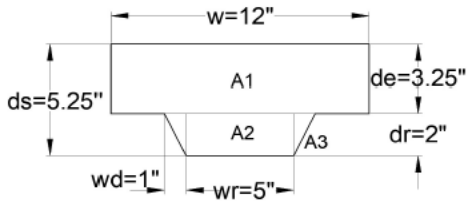

Slab Cross-Section

$f_c := 3\ ksi$

$E_c := 110^{1.5} \cdot \sqrt{f_c\ ksi} = 1998\ ksi$

$E_s := 29000\ ksi$

$n := \frac{E_s}{1.35 \cdot E_c} = 10.75$ Dynamic Modulus of Concrete (DG11)

Beam section: W16x26

$d_j := 15.7\ in$

$A_j := 7.68\ in^2$

$I_{xj} := 301\ in^4$

$SW_j := 26\ \frac{lbf}{ft}$

$S_b := 8\ ft$

$L_j := 30\ ft$

Girder section: W24x55

$d_g := 23.6\ in$

$A_g := 16.2\ in^2$

$I_{xg} := 1350\ in^4$

$SW_g := 55\ \frac{lbf}{ft}$

$L_g := 24\ ft$ Interior girders length

$L_{gc} := 16\ ft$ Cantilevered girders length

Orthotropic Deck Moment of Inertia and Orthotropic Property Modifier Calculations:

Slab

Direction perpendicular to ribs

$$I_{perp} := \frac{w \cdot d_e^{\,3}}{12} = 34.33\ in^4$$

Direction parallel to ribs

$$A_1 := w \cdot d_e = 39\ in^2$$

$$A_2 := w_r \cdot d_r = 10\ in^2$$

$$A_3 := 2 \cdot \left(w_d \cdot \frac{d_r}{2} \right) = 2\ in^2$$

$$y_{slab} := \frac{A_1 \cdot \left(d_r + \frac{d_e}{2} \right) + A_2 \cdot \frac{d_r}{2} + A_3 \cdot \left(\frac{2}{3} \cdot d_r \right)}{A_1 + A_2 + A_3} = 3.020\ in$$ From bottom of section

$$I_1 := \frac{w \cdot d_e^{\,3}}{12} = 34.33\ in^4$$

$$I_2 := \frac{w_r \cdot d_r^{\,3}}{12} = 3.333\ in^4$$

$$I_3 := 2 \cdot \frac{w_d \cdot d_r^{\,3}}{36} = 0.4444\ in^4$$

$$I_{par} := I_1 + A_1 \cdot \left(d_s - \frac{d_e}{2} - y_{slab} \right)^2 + I_2 + A_2 \cdot \left(y_{slab} - \frac{d_r}{2} \right)^2 + I_3 + A_3 \cdot \left(y_{slab} - \frac{2 \cdot d_r}{3} \right)^2 = 98.87\ in^4$$

SAP2000 - Slab Bending Modifier:

$$PM_{slab} := \frac{I_{par}}{I_{perp}} = 2.88$$

Transformed Moment of Inertia and FE Property Modifier Calculations:

Interior Beam Transformed Moment of Inertia

$W_{effj} := \min\left(\left[\begin{array}{cc} 0.4 \cdot L_j & S_b \end{array}\right]\right) = 8\ ft$ Effective Concrete Slab Depth for beam panel

$W_{teffj} := \frac{W_{effj}}{n} = 8.930\ in$ Transformed Concrete Slab Width

$A_{teffj} := d_e \cdot W_{teffj} = 29.02\ in^2$ Transformed Concrete Slab Area

$$y_j := \frac{A_{teffj} \cdot \left(\frac{d_j}{2} + d_r + \frac{d_e}{2}\right)}{A_{teffj} + A_j} = 9.074\ in$$

$$I_{j.t} := \frac{W_{teffj} \cdot d_e^{\,3}}{12} + A_{teffj} \cdot \left(\frac{d_j}{2} + d_r + \frac{d_e}{2} - y_j\right)^2 + I_{xj} + A_j \cdot y_j^{\,2} = 1126\ in^4$$

Beam Transformed moment of inertia

The moment of inertia of the transformed 3.25 in. slab area element about its own neutral axis must be subtracted so that it is not accounted for twice.

$I_{perp.t} := \frac{W_{teffj} \cdot d_e^{\,3}}{12} = 25.55\ in^4$ Transformed moment of inertia of slab in the perpendicular direction to ribs

SAP2000 - Strong Axis Moment of Inertia Property Modifier for INTERIOR beams

$$PM_{beam} := \frac{I_{j.t} - I_{perp.t}}{I_{xj}} = 3.66$$

Spandrel Beam Transformed Moment of Inertia

$W_{effj} := \min\left(\left[\begin{array}{cc} 0.2 \cdot L_j & \frac{S_b}{2} \end{array}\right]\right) = 4\ ft$ Effective Concrete Slab Depth for beam panel

$W_{teffj} := \frac{W_{effj}}{n} = 4.465\ in$ Transformed Concrete Slab Width

$A_{teffj} := d_e \cdot W_{teffj} = 14.51\ in^2$ Transformed Concrete Slab Area

$$y_j := \frac{A_{teffj} \cdot \left(\frac{d_j}{2} + d_r + \frac{d_e}{2}\right)}{A_{teffj} + A_j} = 7.504\ in$$

$$I_{j.t} := \frac{W_{teffj} \cdot d_e^{\,3}}{12} + A_{teffj} \cdot \left(\frac{d_j}{2} + d_r + \frac{d_e}{2} - y_j\right)^2 + I_{xj} + A_j \cdot y_j^{\,2} = 975.1\ in^4$$

The moment of inertia of the transformed 3.25 in. slab area element about its own neutral axis must be subtracted so that it is not accounted for twice.

$I_{perp.t} := \frac{W_{teffj} \cdot d_e^{\,3}}{12} = 12.77\ in^4$ Transformed moment of inertia of slab in the perpendicular direction to ribs

SAP2000 - Strong Axis Moment of Inertia Property Modifier for EXTERIOR beams

$$PM_{beam} := \frac{I_{j.t} - I_{perp.t}}{I_{xj}} = 3.197$$

$PM_{beam} \cdot 2.5 = 7.99$

Interior Girder Transformed Moment of Inertia

$W_{effg} := \min\left(\left[\begin{array}{cc} 0.2 \cdot L_g & 0.5 \cdot L_j \end{array}\right]\right) + \min\left(\left[\begin{array}{cc} 0.2 \cdot L_g & 0.5 \cdot L_j \end{array}\right]\right) = 9.6\ \text{ft}$ Effective concrete slab width

$W_{teffg} := \frac{W_{effg}}{n} = 10.72\ \text{in}$ Transformed concrete slab width

$W_{effdg} := \frac{\frac{W_{effg}}{2}}{n} = 5.358\ \text{in}$ Effective width of the slab in the deck

$A_{tcg} := d_e \cdot W_{teffg} = 34.83\ \text{in}^2$ Transformed concrete slab area

$A_{tdg} := d_r \cdot W_{effdg} = 10.72\ \text{in}^2$ Transformed concrete slab area in the deck

$y_g := \frac{A_{tcg} \cdot \left(\frac{d_g}{2} + d_r + \frac{d_e}{2}\right) + A_{tdg} \cdot \left(\frac{d_g}{2} + \frac{d_r}{2}\right)}{A_{tcg} + A_{tdg} + A_g} = 10.92\ \text{in}$ From centroid of steel section

$$I_{g.t} := \frac{W_{teffg} \cdot d_e^{\,3}}{12} + A_{tcg} \cdot \left(\frac{d_g}{2} + d_r + \frac{d_e}{2} - y_g\right)^2 + \frac{W_{effdg} \cdot d_r^{\,3}}{12} + A_{tdg} \cdot \left(\frac{d_g}{2} + \frac{d_r}{2} - y_g\right)^2 + I_{xg} + A_g \cdot y_g^{\,2} = 4061\ \text{in}^4$$

The moment of inertia of the transformed 3.25 in. slab area element about its own neutral axis must be subtracted so that it is not accounted for twice.

$I_{par.t} := PM_{slab} \cdot \frac{W_{teffg} \cdot d_e^{\,3}}{12} = 88.30\ \text{in}^4$ Transformed moment of inertia of slab in the parallel direction to ribs

SAP2000 - Strong Axis Moment of Inertia Property Modifier for INTERIOR beams

$PM_{girder} := \frac{I_{g.t} - I_{par.t}}{I_{xg}} = 2.94$

Cantilevered Girder Transformed Moment of Inertia

$W_{effg} := \min\left(\left[\begin{array}{cc} 0.2 \cdot L_{gc} & 0.5 \cdot L_j \end{array}\right]\right) + \min\left(\left[\begin{array}{cc} 0.2 \cdot L_{gc} & 0.5 \cdot L_j \end{array}\right]\right) = 6.4\ \text{ft}$ Effective concrete slab width

$W_{teffg} := \frac{W_{effg}}{n} = 7.144\ \text{in}$ Transformed concrete slab width

$W_{effdg} := \frac{\frac{W_{effg}}{2}}{n} = 3.572\ \text{in}$ Effective width of the slab in the deck

$A_{tcg} := d_e \cdot W_{teffg} = 23.22\ \text{in}^2$ Transformed concrete slab area

$A_{tdg} := d_r \cdot W_{effdg} = 7.144\ \text{in}^2$ Transformed concrete slab area in the deck

$$y_g := \frac{A_{tcg} \cdot \left(\frac{d_g}{2} + d_r + \frac{d_e}{2}\right) + A_{tdg} \cdot \left(\frac{d_g}{2} + \frac{d_r}{2}\right)}{A_{tcg} + A_{tdg} + A_g} = 9.656\ \text{in}$$ From centroid of steel section

$$I_{g.t} := \frac{W_{teffg} \cdot d_e^{\,3}}{12} + A_{tcg} \cdot \left(\frac{d_g}{2} + d_r + \frac{d_e}{2} - y_g\right)^2 + \frac{W_{effdg} \cdot d_r^{\,3}}{12} + A_{tdg} \cdot \left(\frac{d_g}{2} + \frac{d_r}{2} - y_g\right)^2 + I_{xg} + A_g \cdot y_g^{\,2} = 3727\ \text{in}^4$$

The moment of inertia of the transformed 3.25 in. slab area element about its own neutral axis must be subtracted so that it is not accounted for twice.

$I_{par.t} := PM_{slab} \cdot \frac{W_{teffg} \cdot d_e^{\,3}}{12} = 58.86\ \text{in}^4$ Transformed moment of inertia of slab in the parallel direction to ribs

SAP2000 - Strong Axis Moment of Inertia Property Modifier for Cantilevered beams

$$PM_{girder} := \frac{I_{g.t} - I_{par.t}}{I_{xg}} = 2.72$$

F. Single Module Vibration Specimens – Fabrication Drawing

Test Matrix		
Specimen	**Beams**	**Plate thickness (in.)**
SM-68-3/8	W24x68	3/8
SM-94-1/2	W24x94	1/2

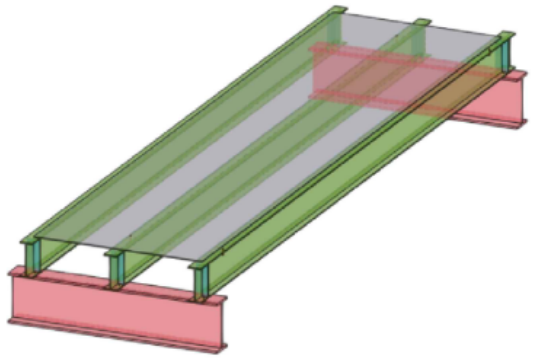

Notes:

1. All material of the same thickness or section shall be from the same heat.

2. Provide a 4 ft x 4 ft piece of each plate thickness, for every heat, and a 4 ft long beam section, for every beam size and heat, for material testing purposes.

FAST FLOOR	TITLE: Test Matrix for Single Module Tests		DRAWN BY: MAMC
DRAWING SET: Single Module Vibration Specimens	01/13/2023	SCALE: VARIABLE	SHEET SM1

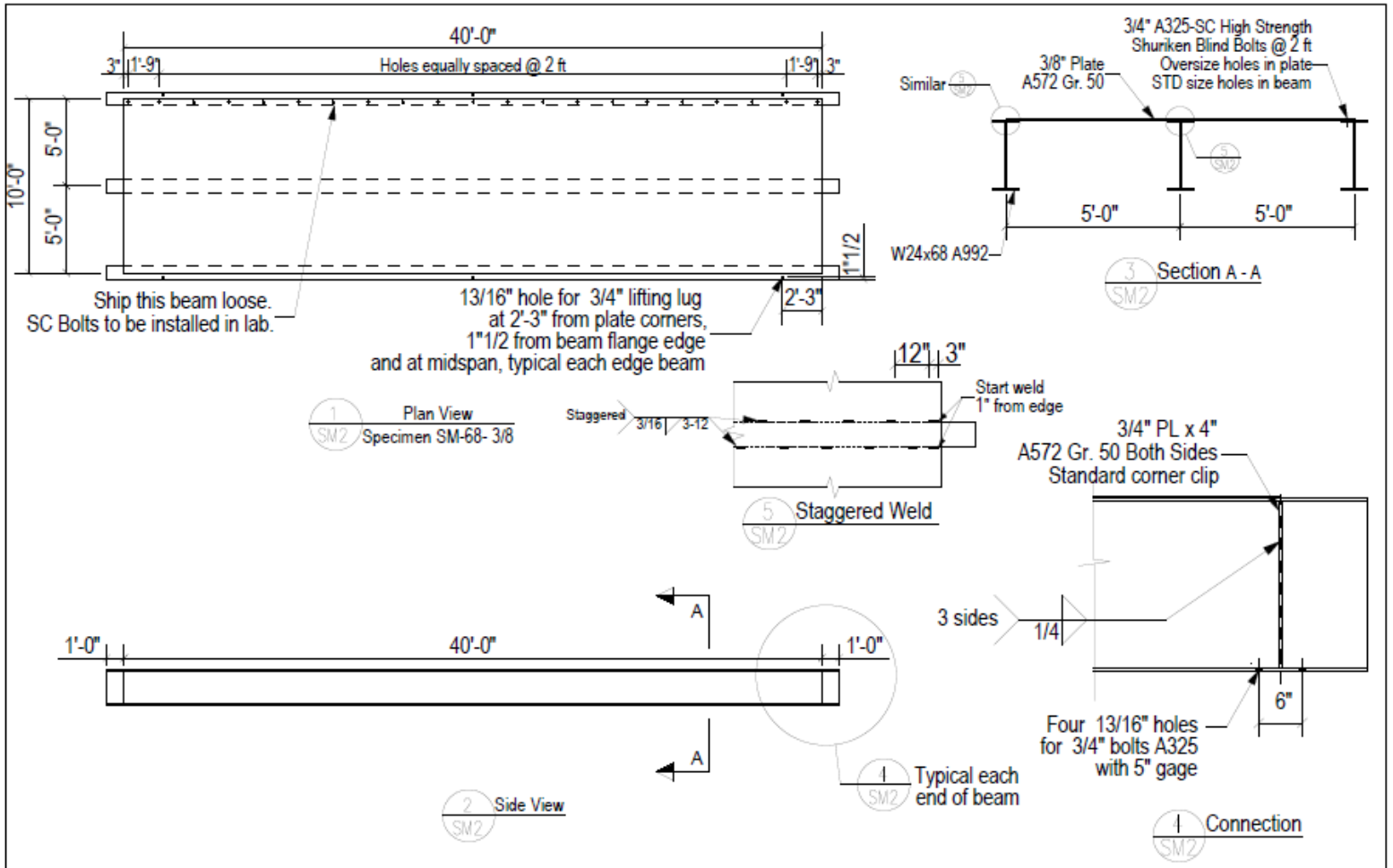

FAST FLOOR	TITLE: Specimen SM-68-3/8		DRAWN BY: MAMC
DRAWING SET: Single Module Vibration Specimens	01/13/2023	SCALE: VARIABLE	SHEET SM2

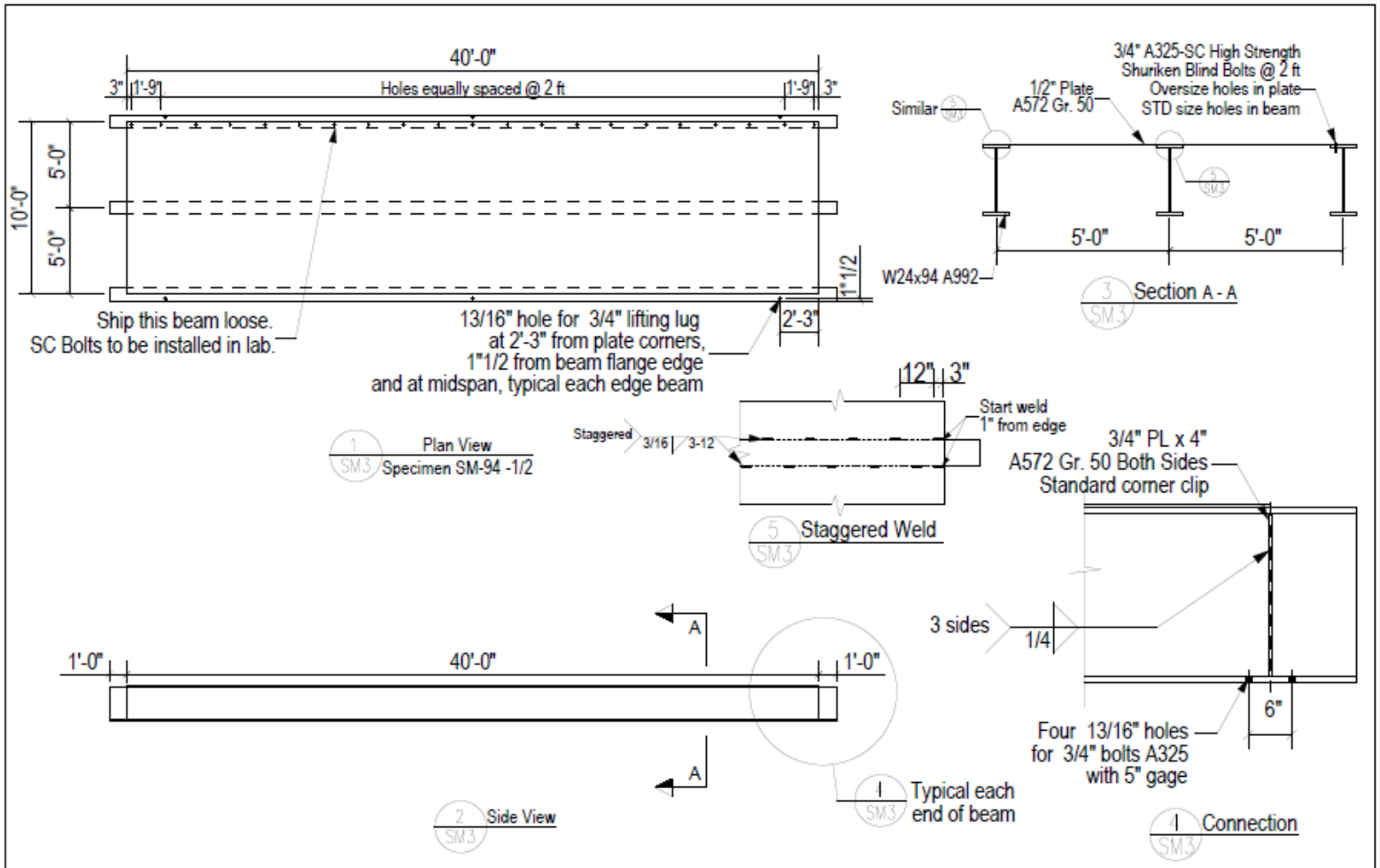

FAST FLOOR	TITLE: Specimen SM-94-1/2	DRAWN BY: MAMC
DRAWING SET: Single Module Vibration Specimens	01/13/2023	SCALE: VARIABLE	SHEET SM3

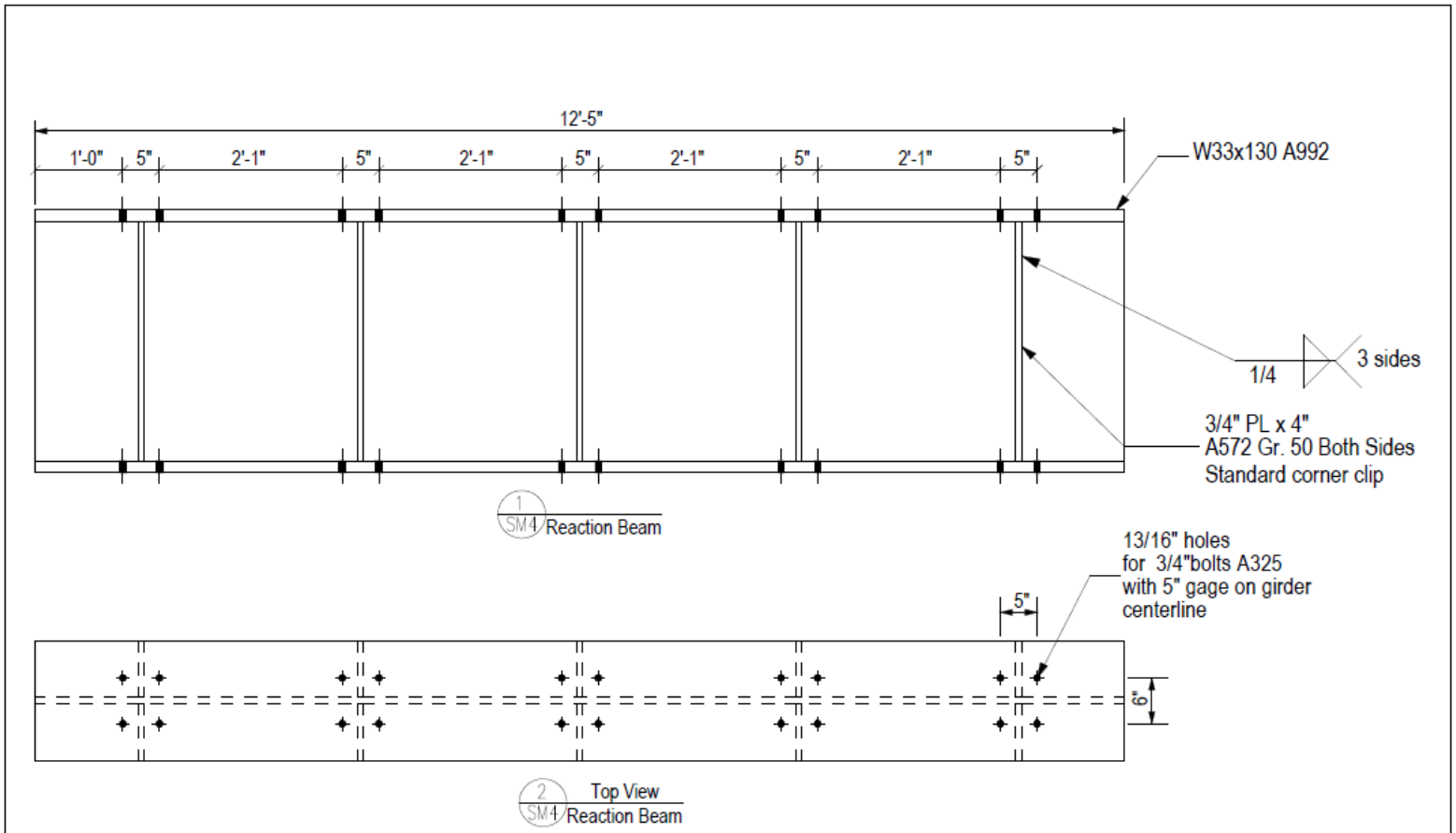

FAST FLOOR	TITLE: Reaction Girders			DRAWN BY: MAMC
DRAWING SET: Single Module Vibration Specimens		01/13/2023	SCALE: VARIABLE	SHEET SM4